2023

Sense and Sensitivity: Spatial Structure of conspecific signals during social interaction

Keshav Ramachandra
klr0019@mix.wvu.edu

Sense and Sensitivity: Spatial Structure of conspecific signals during social interaction

Keshav Ramachandra

A dissertation submitted
To the Eberly College of Arts and Sciences
at West Virginia University
in partial fulfillment of the requirements for the degree of
Doctor of Philosophy
in Biology

Gary Marsat, PhD., Chair
Kevin Daly, PhD
Andrew Dacks, Ph.D.
Sadie Bergeron, Ph.D.
Charles Anderson, Ph.D.

Department of Biology

Morgantown, West Virginia
2023

Keywords: Neuroethology, weakly electric fish, detection, resolution

Abstract:

Sense and Sensitivity: Spatial Structure of conspecific signals during social interaction

Keshav Ramachandra

Organisms rely on sensory systems to gather information about their environment. Localizing the source of a signal is key in guiding the behavior of the animal successfully. Localization mechanisms must cope with the challenges of representing the spatial information of weak, noisy signals. In this dissertation, I investigate the spatial dynamics of natural stimuli and explore how the electrosensory system of weakly electric fish encodes these realistic spatial signals. To do so In Chapter 2, I develop a model that examines the strength of the signal as it reaches the sensory array and simulates the responses of the receptors. The results demonstrate that beyond distances of 20 cm, the signal strength is only a fraction of the self-generated signal, often measuring less than a few percent. Chapter 2 also focuses on modeling a heterogeneous population of receptors to gain insights into the encoding of the spatial signal perceived by the fish. The findings reveal a significant decrease in signal detection beyond 40 cm, with a corresponding decrease in localization accuracy at 30 cm. Additionally, I investigate the impact of receptor density differences between the front and back on both signal detection and resolution accuracy. In Chapter 3, I analyze distinct movement patterns observed during agonistic encounters and their correlation with the estimated range of receptor sensitivity. Furthermore, I uncover that these agonistic interactions follow a classical pattern of cumulative assessment of competitors' abilities. The outcome of this research is a comprehensive understanding of the spatial dynamics of social interactions and how this information is captured by the sensory system. Moreover, the research contributed to the development of a range of tools and models that will play crucial roles in future investigations of sensory processing within this system

Acknowledgments

The list of people to thank is long and the space is limited to do it properly. I hope you understand.

I am here today because of all the amazing teachers I had over the years. Each one of you were patient to teach me the joys of research. Dr. Assisi Collins, you helped me learn to code and gave me my first proper research experience thank you. Dr. Randolf Menzel thank you for mentoring me and letting me work in your lab and help me fall in love with coding.

Thank you, Dad and Mom, for teaching me joy in hard work, and curiosity, and for installing in me a love for science, literature, poetry, art, and chess.

Thank you, Christal Hanson, for your constant support and understanding during the long hours of writing and analysis.

Thank you to all of the friends I made along the way for your constant support. Dr. Lexie Schmidt, Katie Boone, Dr. Becca Coltogirone, Pooja Joshi, Brandon Baker, Adam Polio, Alicia Mayle, Dr. Federico Pedraja, Valerie Lucks, Dr. Lucia Ruiz, Marryn Bennett, Dionysis and Farzaan Salman, Cameron Corbett, Mathilda Santee. I couldn't have done it without you.

Special thanks to TDT for keeping me sane and Sam, Brent, John and Henry thank you for all the soccer weekends.

To my lab mates in the Marsat Lab, Kate Allen, Danielle Dillion, Ian McCoy, Robin Oliverio, Elora Shinn and Dakota Miller thank you for all the extra help on this journey. To Oak Milam thank you for the best lab partner to go through PhD from start to finish.

To my committee members, Drs. Kevin Daly, Andrew Dacks, Sadie Bergeron, and Charles Anderson, thank you for all the help, comments, and advice you have given me. Thank you for everything.

And to Dr. Gary Marsat, thank you the most. Thank you letting me pursue a PhD in your lab on a topic I enjoy. Thank you for your patience especially editing my writing over and over, thank you for your advice, teaching, friendship and sharing with us all the nice moments. I couldn't have asked for a better mentor

Table of Contents

Chapter 1: Introduction

Abstract

Localizing the source of a signal is often as important as deciphering the signal's message. Localization mechanisms must cope with the challenges of representing the spatial information of weak, noisy signals. Comparing these strategies across modalities and model systems allows a broader understanding of the general principles shaping spatial processing. In this chapter, I describe the current knowledge and gaps in the knowledge on how sensory systems localize signals in space. I focus on the electrosensory system of knifefish and provide an overview of our current understanding of spatial processing in this system, in particular, localization of conspecific signals.

Note: Parts of this chapter is taken directly from my publication:

"Ramachandra, K. L., Milam, O. E., & Marsat, G. (2019). Behavioral and neural aspects of the spatial processing of conspecifics signals in the electrosensory system. Behavioral Neuroscience, 133(3), 282."

General Context

The primary function of an animal's brain is to generate appropriate behavior in response to a constantly changing environment. This involves analyzing complex sensory information provided by the senses, extracting important information, and making decisions based on the animal's internal state. Neuroscience aims to understand this process in order to gain a better understanding of ourselves. Animals have evolved sensory systems such as vision, hearing, and smell, each presenting its own challenges (Smith, 2008). Receptor cells in these sensory organs convert relevant parts of the physical stimulus into electrical signals that can be processed by the nervous system, creating a neural representation of the stimulus. The information obtained from each sense can be used for various purposes, such as navigation, finding food, and communication, and different aspects of the sensory input are relevant depending on the specific purpose (Arikawa et al., 2005; Bee, 2000; Singh & Theunissen, 2003). Therefore, a sensory system must analyze the sensory input for a wide range of features that may be important to the animal.

While the quality and quantity of a signal contain much of the relevant information for behavior, its spatial structure also plays a crucial role (Bradbury & Vehrencamp, 2011; McGregor, 1993). Spectral and temporal modulations, such as amplitude and frequency changes in bird songs (Konishi, 1985; Lohr et al., 2003; Reid et al., 2005), color variations in body ornaments (Doucet et al., 2007; Guilford & Dawkins, 1993; Keyser & Hill, 2000), or chirping patterns in weakly electric fish (Dunlap et al., 2010; Engler et al., 2000), carry significant meaning in communication and conspecific signals. Even for olfactory signals, the message lies in the odor's identity and concentration (Aragón, 2009; Daly et al., 2016; de

Bruyne & Baker, 2008). In addition to understanding the content of the signal, receivers often need to determine its source location. This spatial aspect is essential for tasks like finding a signaling mate (Arikawa et al., 2005; Byrne & Keogh, 2007; Mathis, 1990), localizing threats and alarm calls (Cäsar et al., 2013), or avoiding competitors marking their territory (Bee, 2000; Behr et al., 2009). However, localizing the source of a signal poses challenges as the directionality and intensity of the signal is weakened as the signal propagates through the environment(Bradbury & Vehrencamp, 2011). The neural circuitry of sensory systems provides solutions for the challenges faced during feature extraction and scene analysis. To understand the mechanisms and functions of higher sensory processing stages, it is crucial to comprehend an animal's natural environment, the stimuli it encounters, and the problems the sensory system successfully solves in that environment.

To understand fully the neural mechanisms of how the sensory system of the animal decodes a signal it is important to understand what the signal is, and the problems the sensory system successfully solves in that environment (Lewicki et al., 2014). Knowing which stimulus features are important allows researchers to create appropriate artificial stimuli for investigating sensory processing. This has been demonstrated in studies of early processing in the retina. As processing moves to higher stages, natural stimuli become even more critical as neurons become selective for specific aspects, such as faces and sounds (Hromádka et al., 2008). Moreover, neurons exhibit different responses to natural stimuli compared to simplified stimuli (Vinje & Gallant, 2002). For example, auditory neurons in birds and blowfly horizontal cells show distinct responses when stimulated with naturalistic stimuli (Kern et al., 2005; Theunissen et al., 2000). Also , scene analysis problems in sensory systems are often ill-posed,

meaning there is insufficient information for a unique solution. These ambiguities can be resolved by incorporating prior knowledge about scene structure (Kersten et al., 2004; McDermott, 2009). Additionally, sensory processing involves detecting weak signals in a noisy background, and understanding the neural mechanisms for solving such problems requires appropriate and challenging naturalistic stimuli.

The encoding of the signal's temporal and spatial content by sensory systems has been explored widely in various modalities and model systems. However, the general mechanisms of spatial localization are not well understood. Comparing across modalities and species can help reveal the core principles and key adaptations involved in localization. The electrosensory system offers an excellent model to provide additional perspective on the mechanisms involved in spatial localization and help us gain a general understanding of how spatial signals are processed. The electric sense possesses characteristics and faces challenges similar to both the visual and auditory systems. Topographic mapping during localizing of a small object/prey can be compared to the way the visual system processes spatial information. However, conspecific signals are spatially diffuse for electric fish and activate all the electroreceptors (Kelly et al., 2008). Localization would thus require comparisons across inputs similar to the auditory localization process. Spatial coding of objects and temporal coding have been thoroughly investigated in weakly electric fish (Maler, 2007; Nelson & MacIver, 1999). However, when it comes to spatial processing of conspecific signals there is little known.

Based on the information above using weakly electric fish is ideal for investigating how the sensory system localizes spatial signals. This dissertation will focus on understanding the

spatiotemporal structure of the sensory input to the nervous system during conspecific interactions.

The electrosensory system

The ability to sense electric fields is thought to have evolved early in the vertebrate lineage (Bodznick & Northcutt, 1981) and is developmentally derived from lateral line placodes (Modrell et al., 2011). Electroreception was lost in teleost fish but regained at least twice (in Osteoglossomorpha and Ostariophysi) thereby explaining the presence of electroreceptors in a variety of species, including catfish, elephantnose fish, and knifefish (see Baker, Modrell, & Gillis, 2013 for a recent review on the topic). In teleost, electroreceptors are thought to have evolved as a modification of neuromast (Baker et al., 2013). Beyond their detailed evolutionary trajectory, electroreceptor origin is clearly linked to the lateral line and mechanosensory system, similar to the origin of vertebrate auditory receptors (Duncan & Fritzsch, 2012). As a reflection of their similar evolutionary origin, both electroreceptors and auditory receptors travel along the VIIIth cranial nerve (Carr et. al, 1982). Ampullary receptors are the most common type of electroreceptors across species, but in two orders of teleost (Gymnotiformes and Mormyriformes) a second type of electroreceptor evolved - tuberous receptors (Szabo, 1974). Where ampullary receptors are sensitive to low-frequency electric signals, such as the ones produced by contracting muscles, tuberous receptors are sensitive to high frequencies (Bennett et al., 1989; Maler, 2009a; Maler, 2009b; Hopkins, 1976) and their evolution accompanies the evolution of electric organs (EO) that generate high-frequency weak electric fields. Derived from a modified muscle or a modified nerve terminal, EO produces pulsatile or continuously oscillating electric fields (Kramer, 1996). Weakly electric fish (Gymnotiformes and

Mormyriformes) thereby possess an active electrosense where the electric organ discharges (EOD) (Lissmann, 1958) are perceived by electroreceptors on the skin. Anything in their environment that is more or less resistive than water will cause a distortion of this electric field that will cast an “electric shadow” (Rasnow, 1996) on the sensory surface (we refer to the electrosensory sensorium as the “sensory surface” throughout the review). They rely heavily on this active sense to navigate, and localize prey, but also to communicate and interact with conspecifics (Bullock et al.,1986; Lissmann, 1963). Although Gymnotiformes and Mormyriformes have many similarities in the way they use and process electric signals, the fact that they evolved this active electric sense independently also leads to significant differences, in particular at the neural level. For the purposes of the thesis, I will be focusing on the South American Gymnotiformes in particular Apteronotid fish which I will refer to as simply weakly electric fish throughout the thesis.

Knifefish are typically nocturnal species and thus rely heavily on this active electrosense to perceive their environment. The sensory image caused by objects close to them is quite accurate thanks to a relatively high density of receptors over the entire surface of the skin (Carr et al., 1982); allowing them to be efficient hunters of invertebrate prey (Nelson & MacIver, 1999). Similarly, they can locate and identify a conspecific based on the EOD it produces or mediate social interactions via electrocommunication signals such as chirps (Engler & Zupanc, 2001). The sensitivity of their ability to locate each other based on this sense is easily observable both in the field and in the lab. For example, they will chase each other at high speed in a noisy environment with multiple other signal sources or locate each other at such distances that they must base this detection on extremely weak signals.

Localization of conspecifics

The localization of conspecific signals is a different sensory problem to the localization of small objects such as prey items. An object close to the body will cause a local disturbance in the EOD which will be picked up by a limited number of receptors on the corresponding portion of the skin (Rasnow, 1996). The localization strategy in this case is likely to be closer to visual localization or localization in the somatosensory system where exclusive activation of a subset of receptors encodes location in a labeled line code (Cichy & Teng, 2017; Hartmann & Bower, 2001; Krekelberg et al., 2003; Okada & Toh, 2006). Localizing a conspecific based on the EOD it produces cannot rely on this strategy since the sender's EOD will impact the majority of electroreceptors over the entire skin surface (Kelly et al., 2008). Therefore, localization of conspecifics probably relies on comparison of the input at the various receptors and location would be computed by the nervous system based on the differences. This task shares similarities with localization in the auditory system, which relies on comparisons of binaural input(Brand et al., 2002; Carr & Konishi, 1990; Jeffress, 1948). Localization in the electrosensory system might therefore be described as a hybrid mechanism that relies on a labeled line strategy for passive objects (e.g., small prey) that cause a local electrical disturbance, but needs to compute the spatial information about active electro-generating sources (e.g., conspecifics). As such, the electrosensory system is faced with many of the same challenges faced by the auditory or the visual system when localizing signal sources in complex environments. Whether it is a question of localization accuracy (e.g. auditory system), localizing in a noisy environment (cocktail party problem in the auditory system; Cherry, 1953; Liberman et al., 1957) or foreground-background separation (visual system; Ölveczky et al., 2003), there is a rich

literature documenting the various neural and behavioral mechanisms in place to face these challenges.

The electrosensory system has a long history of contribution to our understanding of sensory processing(Bastian & Heiligenberg, 1980). Issues of temporal coding have been particularly well explored in this system (Gabbiani et al., 1996; Krahe et al., 2008). Understanding localization in the electrosensory system has focused heavily on the spatial aspect of prey capture or the localization of small objects (Babineau er al., 2007; Caputi & Budelli, 2006; Nelson & MacIver, 1999; Rasnow, 1996). Less is known about the spatial processing of conspecific signals, but there are several new studies and a growing interest in the topic (Kelly et al., 2008).

Behavior and signal properties

This electrosense is advantageous for navigating at night or in murky waters. Their ability to navigate and locate prey based on this sense is well documented (Nelson & MacIver, 1999; Postlethwaite et al., 2009; Stamper et. al, 2012; Von Der Emde et al., 1998). Similarly, they also rely heavily on this electrosense when interacting with conspecifics to identify, communicate and locate each other. Identity can be determined from the EOD pattern depending on the species, EOD frequency, shape or pulse pattern can be used to identify conspecifics from individuals of another species (Zupanc et al., 2006) or even differentiate amongst conspecifics (Zakon et al., 2002). In wave type species, the EOD frequency (and possibly shape; Kolodziejski, et al., 2007; Petzold, Marsat, & Smith, 2016) is perceived indirectly.

Indeed, when two or more individuals come into close proximity, the electric fields of each fish summate, and the resulting field contains amplitude and phase modulations, collectively known as a "beat" (Heiligenberg, 1991). The beat frequency is equal to the frequency difference between the EOD of the sender and receiver (note that both fish send and both fish receive but we use this terminology throughout this article to describe the perspective we use (Stamper et al., 2012). Furthermore, phase modulations can indicate whether the other fish has an EOD frequency higher or lower than its own (see Carlson & Kawasaki, 2007; Metzner, 1999; Stamper et al., 2012 for more information). Determining beat frequency is important since each fish has a baseline EOD frequency and thus individual discrimination can be based on this signal. In some species, EOD frequency is sexually dimorphic leading beat frequencies to be lower during same-sex interactions and higher for male-female pairs (Engler & Zupanc, 2001). Since beat frequency can indicate species, sex, maturity and even individual identity, many species react differently when exposed to beat signals of various frequencies. For example, the rate of production of certain communication signals in black ghost or brown ghost knifefish depends on the beat frequency (Hupé et al., 2008). The most common type of communication signal produced by these fish -chirps- are brief increases in EOD frequency (see Kolodziejski et al., 2007 for more info).

Sensitivity of conspecific detection and localization

In wave type fish, the beat signal results from the presence of a conspecific, and, therefore, carries information about a conspecific's location. The beat signal will strengthen as the conspecific gets closer and the strength of the signal across the sensory surface (i.e., the body's surface) correlates with its relative position. Both lab and field studies clearly show that they monitor this information to detect the presence and position of a conspecific. In an insightful field study, Henninger et al (Henninger et al., 2018) used grids of electrodes placed in river streams and creeks to triangulate and follow individuals in their natural environment during long periods of time. Besides revealing the behavioral and communication dynamic happening during various types of interactions -including courtship or aggression- this study showed the range of detection of conspecifics via this electrosense. Although their data suggests that fish routinely communicate with each other over distances of up to 30 cm, it also shows that two fish can detect and assess a conspecific at distances of 1 meter or more. For example, they showed that a resident fish-initiated attacks on an intruder located as far as 1.7 m away. To emphasize how challenging this task is, they estimated the strength of the sender's signal and showed that a fish 30 cm away creates a signal of 10 µV/cm and that a fish 1.7 m away causes a signal smaller than 1 µV/cm. Note also that this data suggests that these weak signals were not only detected, but also localized since it guided the resident to launch an attack directed at the intruder.

Laboratory studies confirm the sensitivity of this system in detecting and locating a conspecific. Fish adjusted their EOD output (i.e. the response called "envelope tracking") when presented with beats of 10-15% contrast (Metzen et al., 2018) which would correspond to a

conspecific 20-30 cm away (Fotowat et al., 2013). In another study, fish exposed to a conspecific signal presented from various distances regularly produced chirps only in response to the stimuli located fairly closely (10 cm; Zupanc et al., 2006). However, conditioned responses to weak signals demonstrated that fish could detect signals weaker than 1 µV/cm corresponding to a distance of up to 1.6 m (Knudsen, 1974; Knudsen, 1975). Therefore, despite coming to their conclusion through very different methods, the field and laboratory studies provide very similar estimates and identify a certain range within which fish actively interact with each other (e.g., chirp or envelope tracking) and a wider range delineating the limits of their detection and localization ability.

Conspecific localization and EOD temporal modulation

Information about conspecific location is present in two aspects of the signal: its temporal modulations and its spatial structure. Temporal modulations are indeed imparted by the relative movement of two fish. As a sender moves closer and further from the receiver, the beat will proportionally increase and decrease in strength. The strength of the beat is also called its “contrast” and contrast modulations are called the “envelope signal”. The characteristics of these envelope signals have been determined experimentally by recording the signals received by a fish exposed to one or several other moving conspecifics (Fotowat et al., 2013; Yu et al., 2012). Since movement is relatively slow, envelope signals are typically low frequency (<10 Hz). The data also confirmed that the beat elicited by a conspecific nearby can be strong (often above 50% contrast at <10 cm), but decreases quickly with distance (a few % at 30 cm; Fotowat et al., 2013) since these electric fields decrease in strength as a function of the cube of the distance (Caputi, Aguilera, Pereira, & Rodríguez-Cattáneo, 2013). Furthermore,

these recordings illustrate another important principle that influences the properties of electric signals. The strength of the signal is not simply related to the distance but also to the relative orientation of the receiver and sender “dipoles” (Rasnow, Assad, & Bower, 1993). To simplify, the EO can be thought of as a stimulus dipole and electroreceptors are sensing dipoles detecting the potential difference across the skin. Electric fields are characterized by isopotential lines and a sensing dipole positioned parallel to an isopotential line would not pick up the signal even if it is close to the stimulus dipole (Assad & Bower, 1997; Rasnow et al., 1993). Consequently, the strength of the envelope can decrease to zero as the fish moves away or as it rotates 90° making the envelope signal picked up by a given receptor ambiguously related to the location of the sender.

Envelope signals are common in various modalities. In the visual system they are linked to the ability to distinguish contrast based visual contours (Grosof et al., 1993). They are also used by the auditory system for speech perception and sound localization (Lohuis & Fuzessery, 2000; Smith et al., 2002). The electrosensory system has provided important insight into how these signals are processed by the nervous system, but we do not yet know how they are used to gauge the distance of the sender. Furthermore, azimuth and elevation of the sender relative to the receiver is not encoded in this temporal signal, it can only be estimated by comparing the strength of the signal across the sensory surface.

Electrosensory image

The sensory surface is well suited to capture the spatial aspect of the sensory environment. Most of the body surface of knifefish contains a high density of electroreceptors each capturing the electrical potential within its vicinity (Carr et al., 1982). Distortion of the

fish's own EOD caused by its environment can thus be mapped on this spatially organized sensory array. Distortions experienced by these fish can be categorized as either a passive electric image or an active electric image. The active electric image arises when an object or animal that is more or less conductive than the surrounding water locally influences the strength of the electric field generated by the fish. For example, a conductive prey item near the head will locally increase the strength of the electric field and cast an "electrical shadow" (or a bright spot in this case) on the skin. A series of seminal studies using modeling, physiological and behavioral approaches have detailed the characterization of the electrosensory image of prey items during hunting behaviors (Nelson & MacIver, 1999; Nelson, MacIver, & Coombs, 2002). The authors measured the 3D relative position of the fish and its prey, modeled the electrosensory image that would result, estimated the activation strength of the various receptors and reconstructed a 3D activation map of the sensory surface. They determined that black ghost knifefish typically detect prey when they are 1-2 cm away that elicit a signal of 1-3 μV and can potentially detect a signal as weak as 0.2 μV. These studies point out once again the extreme sensitivity of this system and provide a clear understanding of how these signals are represented at the periphery. The neural mechanisms underlying prey localization and detection are also a good example of sophisticated neural processing strategies used to accomplish challenging tasks (see next section; Chacron & Bastian, 2008; Clarke et al., 2014; Jung et al., 2016).

A conspecific in close proximity to the receiver will also cast such an active electrosensory image -albeit a bigger one- but few studies have characterized this sensory image. In a recent study combining behavioral recordings and modelling of the electric field and

sensory image, Pedraja et al (2016) showed that this active image could guide behavior during aggressive encounters. However, they showed that the passive electrosensory image (see below), rather than the active one, was better correlated with the initiation of attack behavior at close range. This study also indicates that the image of the conspecific is fairly sharp at close range (a small portion of receptors are strongly activated and the others much weaklier) thereby giving a clear labeled-line representation of conspecific location. In contrast, the image elicited by a conspecific further away (>10 cm) is uniformly weak, thus detection most likely involves pooling all the responses together to average out the noise and localization must rely on comparing the weak responses to determine the even-weaker differences among them. This analysis highlights once again the challenging task that this system must perform. Although it is still not clear to what degree they rely on the passive image versus a combination of passive and active images in close range interactions, the active image cannot underlie the ability to detect and localize conspecifics far away (Knudsen, 1975).

They must thus rely on the passive electrosensory image to detect and localize distant conspecifics. The passive image consists of the spatial pattern of distortion of the receiver EOD caused by the sender EOD. It is important to point out that this terminology, although well-defined for prey and for pulse species, is more ambiguous for wave-type species since this passive image is the result of both sender and receiver's active signals (EODs and the resulting beat). Furthermore, the passive and active components will both be perceived through modulations of the receiver's own EOD and thus, are not truly different images but different components of the electrosensory image. We nevertheless use this terminology for consistency with previous studies (e.g. Pedraja et al., 2016).

The strength of the beat signal at different points on the receiver's skin will vary with position and orientation of the sender. A sender located in front, for example, would cause stronger beats on the rostral than caudal end of the receiver. The detailed activation pattern of the sensory surface also depends on receptor orientation (e.g., dorsal receptors are nearly orthogonal to the nearby receptors on the side of the body). For this reason, the activation pattern of areas like the head will be more complex that for relatively flat area like the side of the mid-body. Several researchers have modelled the electrosensory image caused by a conspecific either fixed (Kelly et al., 2008) or approaching (Castelló et al., 2016; Gómez-Sena et al., 2014) the focal fish. Despite being extremely valuable data, the studies typically have simplifications that make evaluating the strength of the input for all electroreceptors more difficult. For example, the models looking at conspecific signals were either limited to 2D or considered receptors only along a line on the side of the fish or did not take into account the various orientation of receptors. This complexity will be most obvious for regions like the head where receptors very close to one another will have very different orientation and thus very different activation levels. Considering how receptor activation will depend on the relative orientation, in 3D, of the receptor relative to the stimulus, further studies are required to obtain a detailed characterization of the sensory image of conspecifics. An incomplete understanding of the spatial structure of these sensory signals limits our ability to understand how the sensory system extracts this spatial information.

Electroreceptors and Processing

In Weakly electric fish the sensory image activates the electroreceptors that are distributed across the surface the body (Bennett, 1971; Carr et al., 1982). There are two types of electroreceptors found on the surface of the skin of the fish. Ampullary receptors which are the most common type of receptors across the species but in two orders of teleost (Gymnotiformes and Mormyriformes) a second type of electroreceptor evolved - tuberous receptors (Szabo, 1974). Where ampullary receptors are sensitive to low-frequency electric signals, such as the ones produced by contracting muscles, tuberous receptors are sensitive to high frequencies (Bennett et al., 1989; Hopkins, 1976; Leonard Maler, 2009a). Ampullary receptors (mediating low-frequency passive electrosensation; see Introduction) are less numerous (~700 total in brown ghost knifefish) compared to tuberous receptors (~13,000-17,000 total; (Carr et al., 1982)). The density of ampullary and tuberous receptors varies across the body surface. Regions of the mouth, face, and head are higher in receptor density, resulting in the formation of an electrosensory fovea. Similar to other sensory systems, this foveal arrangement of receptors permits a higher resolution of sensory input and its location near the mouth is well suited to guide the final stages of prey capture.

There are two kinds of tuberous receptors involved in active electrosensation: T-units and P-units. Time coding units (T-units) are few in number and form a separate channel early in the sensory pathway through spherical cells of the electrosensory lateral line lobe (ELL) and onto a dedicated layer of the Torus semicircularis (Ts) (Maler et al., 1981). Most tuberous

receptors are amplitude coding (or probability coding units: P-units), providing direct input to ELL pyramidal cells. P-units are solely responsible for encoding the amplitude of the fish's own EOD and the amplitude modulations (AMs) arising from electrolocation and electrocommunication (Xu et al., 1996).

All the receptors project onto the pyramidal cells in the electrosensory lateral line lobe (ELL), the primary electrosensory area in the hindbrain. The ELL is divided into four distinct topographical maps. The ampullary receptors synapse onto the medial segment, on the other hand the tuberous receptors synapse onto the centromedial segment (CMS), centrolateral segment (CLS) and the lateral segment (LS) (Heiligenberg & Dye, 1982). Each map consists of six classes of pyramidal cells that vary in their spatiotemporal properties and the feedback they receive, resulting in multiple topographical representations of electrosensory activity across the body surface (Krahe & Maler, 2014). The Electrosensory Lateral Line lobe (ELL) can be considered as a preprocessing stage: while electroreceptors encode stimuli using a dense code, the encoding by ELL pyramidal cells is already more selective and sparser (Vonderschen & Chacron, 2011). These maps have been shown to have distinct functional roles (Metzner & Juranek, 1997). The pyramidal cells, which are the main output neurons of the ELL, can be classified into two major classes: On and Off center-like cells, referred to as E- and I-cells (Krahe & Gabbiani, 2004; Saunders & Bastian, 1984). Some pyramidal neurons, known as deep cells, project to the nucleus praeeminentialis (nP), which mediates feedback, while all pyramidal cells project to the midbrain torus semicircularis (TS). The nP is involved in both direct and indirect feedback pathways, with the indirect pathway involving cerebellar granule cells (EGp) and influencing the spatiotemporal processing properties of the pyramidal cells. The direct feedback

is implicated in a 'sensory searchlight' mechanism, whereas one function of the indirect pathway is to remove redundant global low-frequency input caused by self-movement (Bastian et al., 2004). The TS contains both dense coding and sparse coding neurons that selectively respond to specific beat frequencies, different types of chirps, movement direction, and higher-order signal envelopes (Fortune & Rose, 2000,Vonderschen & Chacron, 2011). However, the mechanisms underlying the transformation from dense to a selective and sparse response remain unclear.

Conclusions

The existing research and literature have revealed the difficult task of detecting and localizing conspecifics. Many of the challenges resemble those seen in other modalities but the uniqueness of the electrosense allows us to understand the generality across sensory systems. In order to understand the neural mechanisms that underlie conspecific interaction, it is important to understand the signal that the fish is receiving, in that spirit my thesis aims to provide an in dept analysis of the spatiotemporal structure of the sensory input to the nervous system during conspecific interactions. I first show the strength of the signal reaching the fish from a conspecific and then, model the responses of the heterogenous population of receptors to get a conservative estimate of the accuracy of detection and localization **(Chapter 2).** I then characterize and quantify the sensory task faced by the fish while localizing conspecifics during social interactions **(Chapter 3).** Taken together these findings provide a characterization of the sensory input that must be processed by the higher brain regions in order to localize a conspecific. The tools I developed and the data gathered allow a quantitative understanding of

this system from behavior to sensory input and thus serve as foundational work for all future studies on spatial coding in this system.

References

Aragón, P. (2009). Conspecific male chemical cues influence courtship behaviour in the male newt Lissotriton boscai. *Behaviour*, *146*(8), 1137–1151. https://doi.org/10.1163/156853909X413097

Arikawa, K, Wakakuwa, M., Qiu, X. D., Kurasawa, M., & Stavenga, D. G. (2005). Sexual dimorphism of short-wavelength photoreceptors in the small white butterfly, Pieris rapae crucivora. *Journal of Neuroscience*, *25*(25), 5935–5942. https://doi.org/Doi 10.1523/Jneurosci.1364-05.2005

Assad, C., & Bower, J. M. (1997). Electric field maps and boundary element simulations of electrolocation in weakly electric fish. In *Engineering and Applied Science: Vol. PhD*. https://doi.org/10.1080/01639374.2011.545343

Babineau, D., Lewis, J. E., & Longtin, A. (2007). Spatial Acuity and Prey Detection in Weakly Electric Fish. *PLoS Computational Biology*, *3*(3), e38. https://doi.org/10.1371/journal.pcbi.0030038

Baker, C. V. H., Modrell, M. S., & Gillis, J. A. (2013). The evolution and development of vertebrate lateral line electroreceptors. *Journal of Experimental Biology*, *216*(13), 2515–2522. https://doi.org/10.1242/jeb.082362

Bastian, J., & Heiligenberg, W. (1980). Neural correlates of the jamming avoidance response ofEigenmannia. *Journal of Comparative Physiology A*, *136*(2), 135–152. https://doi.org/10.1007/BF00656908

Bee, M. A. (2000). Male green frogs lower the pitch of acoustic signals in defense of territories: a possible dishonest signal of size? *Behavioral Ecology*, *11*(2), 169–177. https://doi.org/10.1093/beheco/11.2.169

Behr, O., Knörnschild, M., & Von Helversen, O. (2009). Territorial counter-singing in male sac-winged bats saccopteryx bilineata: Low-frequency songs trigger a stronger response. *Behavioral Ecology and Sociobiology*, *63*(3), 433–442. https://doi.org/10.1007/s00265-008-0677-2

Bennett, M. V. L. (1971). Electroreception. *Fish Physiology*, *5*, 493–574. https://doi.org/10.1016/S1546-5098(08)60052-7

Bennett, M. V. L., Sandri, C., & Akert, K. (1989). Fine structure of the tuberous electroreceptor of the high-frequency electric fish, Sternarchus albifrons (gymnotiformes). *Journal of Neurocytology*, *18*(2), 265–283. https://doi.org/10.1007/BF01206667

Bodznick, D., & Northcutt, R. G. (1981). Electroreception in lampreys: evidence that the earliest vertebrates were electroreceptive. *Science*, *212*(4493), 465–467. https://doi.org/10.1126/science.7209544

Bradbury, J. W., & Vehrencamp, S. L. (2011). *Principles of animal communication* (2nd ed.). Sinauer Associates.

Brand, A., Behrend, O., Marquardt, T., McAlpine, D., & Grothe, B. (2002). Precise inhibition is essential for microsecond interaural time difference coding. *Nature*, *417*(6888), 543–547. https://doi.org/10.1038/417543a

Bullock, Theodore H, Hopkins, C. D., Popper, A. N., & Fay, R. R. (2005). Electroreception. In Theodore H. Bullock, C. D. Hopkins, A. N. Popper, & R. R. Fay (Eds.), *Eletroreception* (Vol. 21). Springer New York. https://doi.org/10.1007/0-387-28275-0

Byrne, P. G., & Keogh, J. S. (2007). Terrestrial toadlets use chemosignals to recognize conspecifics, locate mates and strategically adjust calling behaviour. *Animal Behaviour*, *74*(5), 1155–1162. https://doi.org/https://doi.org/10.1016/j.anbehav.2006.10.033

Caputi, A. A., & Budelli, R. (2006). Peripheral electrosensory imaging by weakly electric fish. *Journal of Comparative Physiology A*, *192*(6), 587–600. https://doi.org/10.1007/s00359-006-0100-2

Caputi, Angel A., Aguilera, P. A., Carolina Pereira, A., & Rodríguez-Cattáneo, A. (2013). On the haptic nature of the active electric sense of fish. *Brain Research*, *1536*, 27–43. https://doi.org/10.1016/J.BRAINRES.2013.05.028

Carlson, B. A., & Kawasaki, M. (2007). Behavioral responses to jamming and "phantom" jamming stimuli in the weakly electric fish Eigenmannia. *Journal of Comparative Physiology A: Neuroethology, Sensory, Neural, and Behavioral Physiology*, *193*(9), 927–941. https://doi.org/10.1007/s00359-007-0246-6

Carr, C., & Konishi, M. (1990). A circuit for detection of interaural time differences in the brain stem of the barn owl. *The Journal of Neuroscience*, *10*(10), 3227–3246. https://doi.org/10.1523/JNEUROSCI.10-10-03227.1990

Carr, C E, Maler, L., & Sas, E. (1982). Peripheral organization and central projections of the

electrosensory nerves in gymnotiform fish. *Journal of Comparative Neurology*, *211*(2), 139–153. https://doi.org/10.1002/cne.902110204

Cäsar, C., Zuberbühler, K., Young, R. J., & Byrne, R. W. (2013). Titi monkey call sequences vary with predator location and type. *Biology Letters*, *9*(5). https://doi.org/10.1098/rsbl.2013.0535

Castelló, M. E., Aguilera, P. A., Trujillo-Cenóz, O., & Caputi, A. A. (2016). Electroreception in Gymnotus carapo: pre-receptor processing and the distribution of electroreceptor types. *The Journal of Experimental Biology*, *21*(Pt 21), 3279–3287. https://doi.org/10.3109/14659891.2015.1122101

Chacron, M. J., & Bastian, J. (2008). Population coding by electrosensory neurons. *Journal of Neurophysiology*, *99*(4), 1825–1835. https://doi.org/DOI 10.1152/jn.01266.2007

Cherry, E. C. (1953). Some Experiments on the Recognition of Speech, with One and with Two Ears. *The Journal of the Acoustical Society of America*, *25*(5), 975–979. https://doi.org/10.1121/1.1907229

Cichy, R. M., & Teng, S. (2017). Resolving the neural dynamics of visual and auditory scene processing in the human brain: A methodological approach. *Philosophical Transactions of the Royal Society B: Biological Sciences*, *372*(1714). https://doi.org/10.1098/rstb.2016.0108

Clarke, S. E., Longtin, A., & Maler, L. (2014). A Neural Code for Looming and Receding Motion Is Distributed over a Population of Electrosensory ON and OFF Contrast Cells. *Journal of*

Neuroscience, *34*(16), 5583–5594. https://doi.org/10.1523/JNEUROSCI.4988-13.2014

Daly, K. C., Bradley, S., Chapman, P. D., Staudacher, E. M., Tiede, R., & Schachtner, J. (2016). Space Takes Time: Concentration Dependent Output Codes from Primary Olfactory Networks Rapidly Provide Additional Information at Defined Discrimination Thresholds. *Frontiers in Cellular Neuroscience*, *9*, 515. https://doi.org/10.3389/fncel.2015.00515

de Bruyne, M., & Baker, T. C. (2008). Odor detection in insects: Volatile codes. *Journal of Chemical Ecology*, *34*(7), 882–897. https://doi.org/DOI 10.1007/s10886-008-9485-4

Doucet, S. M., Mennill, D. J., & Hill, G. E. (2007). The Evolution of Signal Design in Manakin Plumage Ornaments. *The American Naturalist*, *169*(S1), S62–S80. https://doi.org/10.1086/510162

Duncan, J. S., & Fritzsch, B. (2012). Evolution of sound and balance perception: Innovations that aggregate single hair cells into the ear and transform a gravistatic sensor into the organ of corti. *Anatomical Record*, *295*(11), 1760–1774. https://doi.org/10.1002/ar.22573

Dunlap, K. D., DiBenedictis, B. T., & Banever, S. R. (2010). Chirping response of weakly electric knife fish (Apteronotus leptorhynchus) to low-frequency electric signals and to heterospecific electric fish. *The Journal of Experimental Biology*. https://doi.org/10.1242/jeb.038653

Engler, G., Fogarty, C. M., Banks, J. R., & Zupanc, G. K. H. (2000). Spontaneous modulations of the electric organ discharge in the weakly electric fish, Apteronotus leptorhynchus: a biophysical and behavioral analysis. *Journal of Comparative Physiology A*, *186*(7–8), 645–

660. https://doi.org/10.1007/s003590000118

Engler, G., & Zupanc, G. (2001). Differential production of chirping behavior evoked by electrical stimulation of the weakly electric fish, Apteronotus leptorhynchus. *Journal of Comparative Physiology - A Sensory, Neural, and Behavioral Physiology*, *187*(9), 747–756. https://doi.org/10.1007/s00359-001-0248-8

Fortune, E. S., & Rose, G. J. (2000). Short-term synaptic plasticity contributes to the temporal filtering of electrosensory information. *Journal of Neuroscience*, *20*(18), 7122–7130.

Fotowat, H., Harrison, R. R., & Krahe, R. (2013). Statistics of the Electrosensory Input in the Freely Swimming Weakly Electric Fish Apteronotus leptorhynchus. *Journal of Neuroscience*, *33*(34), 13758–13772. https://doi.org/10.1523/JNEUROSCI.0998-13.2013

Gabbiani, F., Metzner, W., Wessel, R., & Koch, C. (1996). From stimulus encoding to feature extraction in weakly electric fish. *Letters to Nature*, *384*, 564–567.

Gómez-Sena, L., Pedraja, F., Sanguinetti-Scheck, J. I., & Budelli, R. (2014). Computational modeling of electric imaging in weakly electric fish: Insights for physiology, behavior and evolution. In *Journal of Physiology Paris* (Vol. 108, Issues 2–3, pp. 112–128). Elsevier. https://doi.org/10.1016/j.jphysparis.2014.08.009

Grosof, D. H., Shapley, R. M., & Hawken, M. J. (1993). Macaque V1 neurons can signal "illusory" contours. *Nature*, *365*(6446), 550–552. https://doi.org/10.1038/365550a0

Guilford, T., & Dawkins, M. S. (1993). Receiver Psychology and the Design of Animal Signals. *Trends in Neurosciences*, *16*(11), 430–436. https://doi.org/Doi 10.1016/0166-

2236(93)90068-W

Hartmann, M. J., & Bower, J. M. (2001). Tactile responses in the granule cell layer of cerebellar folium crus IIa of freely behaving rats. *The Journal of Neuroscience*, *21*(10), 3549–3563. https://doi.org/21/10/3549 [pii]

Heiligenberg, W. (1991). Sensory control of behavior in electric fish. *Current Opinion in Neurobiology*, *1*(4), 633–637. https://doi.org/10.1016/S0959-4388(05)80041-8

Heiligenberg, W., & Dye, J. (1982). Labeling of electroreceptive afferents in a Gymnotoid fish by intracellular injection of HRP - the mystery of multiple maps. *Journal of Comparative Physiology. A*, *148*(3), 287–296. https://doi.org/10.1007/BF00679013

Henninger, J., Krahe, R., Kirschbaum, F., Grewe, J., & Benda, J. (2018). Statistics of natural communication signals observed in the wild identify important yet neglected stimulus regimes in weakly electric fish. *The Journal of Neuroscience*. https://doi.org/10.1523/JNEUROSCI.0350-18.2018

Hopkins, C. D. (1976). Stimulus filtering and electroreception: Tuberous electroreceptors in three species of Gymnotoid fish. *Journal of Comparative Physiology A*, *111*(2), 171–207. https://doi.org/10.1007/BF00605531

Hromádka, T., Deweese, M. R., & Zador, A. M. (2008). Sparse representation of sounds in the unanesthetized auditory cortex. *PLoS Biology*, *6*(1), e16. https://doi.org/10.1371/journal.pbio.0060016

Hupé, G. J., Lewis, J. E., & Benda, J. (2008). The effect of difference frequency on

electrocommunication: Chirp production and encoding in a species of weakly electric fish, Apteronotus leptorhynchus. *Journal of Physiology Paris*, *102*(4–6), 164–172. https://doi.org/DOI 10.1016/j.jphysparis.2008.10.013

Jeffress, L. A. (1948). A place theory of sound localization. In *Journal of Comparative and Physiological Psychology* (Vol. 41, Issue 1, pp. 35–39). American Psychological Association. https://doi.org/10.1037/h0061495

Jung, S. N., Longtin, A., & Maler, L. (2016). Weak signal amplification and detection by higher-order sensory neurons. *Journal of Neurophysiology*, *115*(4), 2158–2175. https://doi.org/10.1152/jn.00811.2015

Kelly, M., Babineau, D., Longtin, A., & Lewis, J. E. (2008). Electric field interactions in pairs of electric fish: Modeling and mimicking naturalistic inputs. *Biological Cybernetics*. https://doi.org/10.1007/s00422-008-0218-0

Kern, R., van Hateren, J. H., Michaelis, C., Lindemann, J. P., & Egelhaaf, M. (2005). Function of a fly motion-sensitive neuron matches eye movements during free flight. *PLoS Biology*, *3*(6), e171. https://doi.org/10.1371/journal.pbio.0030171

Kersten, D., Mamassian, P., & Yuille, A. (2004). Object perception as Bayesian inference. *Annual Review of Psychology*, *55*, 271–304. https://doi.org/10.1146/annurev.psych.55.090902.142005

Keyser, A. J., & Hill, G. E. (2000). Structurally based plumage coloration is an honest signal of quality in male blue grosbeaks. *Behavioral Ecology*, *11*(2), 202–209. https://doi.org/DOI

10.1093/beheco/11.2.202

Knudsen, E. (1974). Behavioral thresholds to electric signals in high frequency electric fish. *Journal of Comparative Physiology*, *91*(4), 333–353. https://doi.org/10.1007/bf00694465

Knudsen, E. I. (1975). Spatial aspects of the electric fields generated by weakly electric fish. *Journal of Comparative Physiology A*, *99*(2), 103–118. https://doi.org/10.1007/BF00618178

Kolodziejski, J. a, Sanford, S. E., & Smith, G. T. (2007). Stimulus frequency differentially affects chirping in two species of weakly electric fish: implications for the evolution of signal structure and function. *The Journal of Experimental Biology*, *210*(Pt 14), 2501–2509. https://doi.org/10.1242/jeb.005272

Konishi, M. (1985). Birdsong: From Behavior to Neuron. *Annual Review of Neuroscience*, *8*(1), 125–170. https://doi.org/10.1146/annurev.ne.08.030185.001013

Krahe, R., Bastian, J., & Chacron, M. J. (2008). Temporal processing across multiple topographic maps in the electrosensory system. *Journal of Neurophysiology*, *100*(2), 852–867. https://doi.org/10.1152/jn.90300.2008

Krahe, R., & Gabbiani, F. (2004). Burst firing in sensory systems. *Nature Reviews Neuroscience*, *5*(1), 13–23. https://doi.org/10.1038/nrn1296

Krahe, R., & Maler, L. (2014). Neural maps in the electrosensory system of weakly electric fish. *Current Opinion in Neurobiology*, *24*(1), 13–21. https://doi.org/10.1016/j.conb.2013.08.013

Kramer, B. (1996). Electroreception and communication in fishes. In *Progress in Zoology* (Vol. 42). Gustav Fischer. https://epub.uni-regensburg.de/2108/

Krekelberg, B., Kubischik, M., Hoffmann, K., & Bremmer, F. (2003). *Neural correlates of visual localization and perisaccadic mislocalization*. *37*, 537–545.

Lewicki, M. S., Olshausen, B. A., Surlykke, A., & Moss, C. F. (2014). Scene analysis in the natural environment. *Frontiers in Psychology*, *5*, 199. https://doi.org/10.3389/fpsyg.2014.00199

Liberman, A. M., Harris, K. S., Hoffman, H. S., & Griffith, B. C. (1957). The Discrimination of Speech Sounds within and across Phoneme Boundaries. *Journal of Experimental Psychology*, *54*(5), 358–368. https://doi.org/Doi 10.1037/H0044417

Lissmann, H. W. (1958). on the Function and Evolution of Electric Organs in Fish. *Journal of Experimental Biology*, *35*(1), 156-. http://jeb.biologists.org/content/jexbio/35/1/156.full.pdf

Lissmann, H. W. (1963). Electric Location by Fishes. *Scientific American*, *208*(3), 50–59. https://doi.org/10.1038/scientificamerican0363-50

Lohr, B., Wright, T. F., & Dooling, R. J. (2003). Detection and discrimination of natural calls in masking noise by birds: Estimating the active space of a signal. *Animal Behaviour*, *65*(4), 763–777. https://doi.org/10.1006/anbe.2003.2093

Lohuis, T. D., & Fuzessery, Z. M. (2000). Neuronal sensitivity to interaural time differences in the sound envelope in the auditory cortex of the pallid bat. *Hearing Research*, *143*(1–2), 43–57. https://doi.org/10.1016/S0378-5955(00)00021-6

Maler, L. (2009). Receptive field organization across multiple electrosensory maps. I. Columnar organization and estimation of receptive field size. *Journal of Comparative Neurology*, *516*(5), 376–393. https://doi.org/10.1002/cne.22124

Maler, Leonard. (2007). Neural strategies for optimal processing of sensory signals. In *Progress in Brain Research* (2007/10/11, Vol. 165, pp. 135–154). https://doi.org/10.1016/S0079-6123(06)65009-7

Maler, Leonard. (2009a). Receptive field organization across multiple electrosensory maps. I. Columnar organization and estimation of receptive field size. *Journal of Comparative Neurology*, *516*(5), 376–393. https://doi.org/10.1002/cne.22124

Maler, Leonard. (2009b). Receptive field organization across multiple electrosensory maps. II. Computational analysis of the effects of receptive field size on prey localization. *Journal of Comparative Neurology*, *516*(5), 394–422. https://doi.org/10.1002/cne.22120

Maler, Leonard, Sas, E. K. B., & Rogers, J. (1981). The cytology of the posterior lateral line lobe of high-frequency weakly electric fish (gymnotidae): Dendritic differentiation and synaptic specificity in a simple cortex. *The Journal of Comparative Neurology*, *195*(1), 87–139. https://doi.org/10.1002/cne.901950107

Mathis, A. (1990). Territorial salamanders assess sexual and competitive information using chemical signals. *Animal Behaviour*, *40*(5), 953–962. https://doi.org/https://doi.org/10.1016/S0003-3472(05)80997-2

McDermott, J. H. (2009). The cocktail party problem. *Current Biology*, *19*(22), R1024–R1027.

https://doi.org/10.1016/j.cub.2009.09.005

McGregor, P. K. (1993). Signalling in territorial systems: a context for individual identification, ranging and eavesdropping. *Philosophical Transactions - Royal Society of London, B*, *340*(1292), 237–244. https://doi.org/10.1098/rstb.1993.0063

Metzen, M. G., Huang, C. G., & Chacron, M. J. (2018). Descending pathways generate perception of and neural responses to weak sensory input. *PLOS Biology*, *16*(6), e2005239.

Metzner, W. (1999). Neural circuitry for communication and jamming avoidance in gymnotiform electric fish. *The Journal of Experimental Biology*, *202*(Pt 10), 1365–1375.

Metzner, W., & Juranek, J. (1997). A sensory brain map for each behavior? *Proceedings of the National Academy of Sciences*, *94*(26).

Modrell, M. S., Bemis, W. E., Northcutt, R. G., Davis, M. C., & Baker, C. V. H. (2011). Electrosensory ampullary organs are derived from lateral line placodes in bony fishes. *Nature Communications*, *2*(1), 3142–3146. https://doi.org/10.1038/ncomms1502

Nelson, M. E., & MacIver, M. A. (1999). Prey capture in the weakly electric fish Apteronotus albifrons: Sensory acquisition strategies and electrosensory consequences. *The Journal of Experimental Biology*, *202*(10), 1195–1203. https://doi.org/PMID: 10210661

Nelson, M. E., MacIver, M. A., & Coombs, S. (2002). Modeling Electrosensory and Mechanosensory Images during the Predatory Behavior of Weakly Electric Fish. *Brain, Behavior and Evolution*, *59*(4), 199–210. https://doi.org/10.1159/000064907

Okada, J., & Toh, Y. (2006). Active tactile sensing for localization of objects by the cockroach

antenna. *Journal of Comparative Physiology A: Neuroethology, Sensory, Neural, and Behavioral Physiology*, *192*(7), 715–726. https://doi.org/10.1007/s00359-006-0106-9

Ölveczky, B. P., Baccus, S. A., & Meister, M. (2003). Segregation of object and background motion in the retina. *Nature*, *423*(6938), 401–408. https://doi.org/10.1038/nature01652

Pedraja, F., Perrone, R., Silva, A., & Budelli, R. (2016). Passive and active electroreception during agonistic encounters in the weakly electric fish Gymnotus omarorum. *Bioinspiration and Biomimetics*, *11*(6), 065002. https://doi.org/10.1088/1748-3190/11/6/065002

Petzold, J. M. J. M., Marsat, G., & Smith, G. T. T. (2016). *Co-adaptation of electric organ discharges and chirps in South American ghost knifefishes (Apteronotidae)*. *110*(3). https://doi.org/10.1016/j.jphysparis.2016.10.005

Postlethwaite, C. M., Psemeneki, T. M., Selimkhanov, J., Silber, M., & MacIver, M. A. (2009). Optimal movement in the prey strikes of weakly electric fish: A case study of the interplay of body plan and movement capability. *Journal of the Royal Society Interface*, *6*(34), 417–433. https://doi.org/10.1098/rsif.2008.0286

Rasnow, B. (1996). The effects of simple objects on the electric field of Apteronotus. *Journal of Comparative Physiology A*, *178*(3), 397–411. https://doi.org/10.1007/BF00193977

Rasnow, B., Assad, C., & Bower, J. M. (1993). Phase and amplitude maps of the electric organ discharge of the weakly electric fish, Apteronotus leptorhynchus. *Journal of Comparative Physiology A*, *172*(4), 481–491. https://doi.org/10.1007/BF00213530

Reid, J. M., Arcese, P., Cassidy, A. L. E. V., Hiebert, S. M., Smith, J. N. M., Stoddard, P. K., Marr,

A. B., & Keller, L. F. (2005). Fitness Correlates of Song Repertoire Size in Free-Living Song Sparrows (Melospiza melodia). *The American Naturalist*, *165*(3), 299–310. https://doi.org/10.1086/428299

Saunders, J., & Bastian, J. (1984). The physiology and morphology of 2 types of electrosensory neurons in the weakly electric fish Apteronotus leptorhynchus. *Journal of Comparative Physiology*, *154*(2), 199–209. https://doi.org/10.1007/BF00604985

Singh, N. C., & Theunissen, F. E. (2003). Modulation spectra of natural sounds and ethological theories of auditory processing. *The Journal of the Acoustical Society of America*, *114*(6 Pt 1), 3394–3411. https://doi.org/10.1121/1.1624067

Smith, C. U. M. (2008). Biology of sensory systems. In *TA - TT* - (2nd ed). John Wiley & Sons. https://doi.org/ LK - https://worldcat.org/title/228114883

Smith, Z. M., Delgutte, B., & Oxenham, A. J. (2002). Chimaeric sounds reveal dichotomies in auditory perception. *Nature*, *416*(6876), 87–90. https://doi.org/10.1038/416087a

Stamper, S. A., Madhav, M. S., Cowan, N. J., & Fortune, E. S. (2012). Beyond the Jamming Avoidance Response: weakly electric fish respond to the envelope of social electrosensory signals. *Journal of Experimental Biology*, *215*(23), 4196–4207. https://doi.org/10.1242/jeb.076513

Stamper, S. A., Roth, E., Cowan, N. J., & Fortune, E. S. (2012). Active sensing via movement shapes spatiotemporal patterns of sensory feedback. *Journal of Experimental Biology*, *215*(9), 1567–1574. https://doi.org/10.1242/jeb.068007

Szabo, T. (1974). *Anatomy of the Specialized Lateral Line Organs of Electroreception BT - Electroreceptors and Other Specialized Receptors in Lower Vertrebrates* (T H Bullock, A. Fessard, P. H. Hartline, A. J. Kalmijn, P. Laurent, R. W. Murray, H. Scheich, E. Schwartz, T. Szabo, & A. Fessard (eds.); pp. 13–58). Springer Berlin Heidelberg. https://doi.org/10.1007/978-3-642-65926-3_2

Theunissen, F. E., Sen, K., & Doupe, A. J. (2000). Spectral-temporal receptive fields of nonlinear auditory neurons obtained using natural sounds. *The Journal of Neuroscience : The Official Journal of the Society for Neuroscience*, *20*(6), 2315–2331. https://doi.org/10.1523/JNEUROSCI.20-06-02315.2000

Vinje, W. E., & Gallant, J. L. (2002). Natural stimulation of the nonclassical receptive field increases information transmission efficiency in V1. *The Journal of Neuroscience*, *22*(7), 2904–2915. https://doi.org/20026216

Von Der Emde, G., Schwarz, S., Gomez, L., Budelli, R., & Grant, K. (1998). Electric fish measure distance in the dark. *Nature*, *395*(6705), 890–894. https://doi.org/10.1038/27655

Vonderschen, K., & Chacron, M. J. (2011). Sparse and dense coding of natural stimuli by distinct midbrain neuron subpopulations in weakly electric fish. *Journal of Neurophysiology*, *106*(6), 3102–3118. https://doi.org/10.1152/jn.00588.2011

Xu, Z., Payne, J. R., & Nelson, M. E. (1996). Logarithmic time course of sensory adaptation in electrosensory afferent nerve fibers in a weakly electric fish. *Journal of Neurophysiology*, *76*(3), 2020–2032. https://doi.org/10.1152/jn.1996.76.3.2020

Yu, N., Hupé, G., Garfinkle, C., Lewis, J. E., Longtin, A., & Fortune, E. (2012). Coding Conspecific Identity and Motion in the Electric Sense. *PLoS Computational Biology*, *8*(7), e1002564. https://doi.org/10.1371/journal.pcbi.1002564

Zakon, H., Oestreich, J., Tallarovic, S., & Triefenbach, F. (2002). EOD modulations of brown ghost electric fish: JARs, chirps, rises, and dips. *Journal of Physiology, Paris*, *96*(5–6), 451–458. https://doi.org/10.1016/S0928-4257(03)00012-3

Zupanc, G. K. H., Sîrbulescu, R. F., Nichols, A., & Ilies, I. (2006). Electric interactions through chirping behavior in the weakly electric fish, Apteronotus leptorhynchus. *Journal of Comparative Physiology A: Neuroethology, Sensory, Neural, and Behavioral Physiology*, *192*(2), 159–173. https://doi.org/10.1007/s00359-005-0058-5

Chapter 2

Prologue

I have introduced the challenges of conspecific localization in our model system in the previous chapter. Specifically, I described how we still don't have a comprehensive description of the signals as it reaches the receptor array. As a consequence, we do not know the spatial structure of the input to the system. This information must then be encoded by the receptor and it is not clear how the structure of the population of receptors copes with noise to encode the signal accurately. To address these gaps in knowledge, in this chapter, I estimate the strength of the signal reaching the fish from a conspecific and then, model the responses of the heterogenous population of receptors to get a conservative estimate of the accuracy of detection and localization.

Note: This chapter is taken directly from a paper that was sent for publication:

"Ramachandra, K. L., Milam, O. E., Federico Pedraja, Jenna Cornett & Marsat, G. (2023).Detection and localization of conspecifics in ghost knifefish are influenced by the relationship between the spatial organization of receptors and signals."

My contribution to this paper represents 2/3 of the content: Ramachandra, Milam and Marsat designed the experiments, Ramachandra and Pedraja modelled the Electric Image and analyzed the data, Milam and Cornett stained and quantified the receptors, Ramachandra and Marsat modelled the receptors and analyzed the data. Ramachandra and Marsat wrote the paper with inputs form Milam.

Abstract

The detection and localization of signals relies on arrays of receptors and their spatial organization plays a key role in setting the accuracy of the system. Electrosensory signals in weakly electric ghost knifefish are captured by an array of receptors covering their body. While we know that spatial resolution for small objects, such as prey, is enhanced near the head due to a high receptor density, it is not clear how receptor organization influences the processing of global and diffuse signals from conspecifics. We investigated the detection and localization accuracy for conspecific signals and determined how they are influenced by the organization of receptors. To do so we modeled the signal, its spatial pattern as it reaches the sensory array, and the responses of the heterogeneous population of receptors. Our analysis provides a conservative estimate of the accuracy of detection and localization (specifically azimuth discrimination) of a conspecific signal. We show that beyond 20 cm the conspecific signal is less than a few percent the strength of the baseline self-generated signal. As a result, detection and localization accuracy decreases quickly for more distant sources. Detection accuracy at distances above 40 cm decreases rapidly and detection at the edge of behaviorally observed ranges might require attending to the signal for several seconds. Angular resolution starts to decrease at even shorter distances (30 cm) and distant signals might require behavioral or neural coding mechanisms that have not been considered here. Most importantly, we show that the higher density of receptors rostrally enhances detection accuracy for signal sources in front of the fish, but contributes little to the localization accuracy of these conspecific signals. We discuss parallels with other sensory systems and suggest that our results highlight a general principle. High receptor convergence in systems with spatially diffuse signals contributes to

detection capacities, whereas in systems with spatially delineated signals, receptor density is associated with better spatial resolution.

Introduction

Whether it is the early detection of a predator, the accurate localization of a mate, or finding food sources based on weak cues, the sensitive detection and localization of sensory signals can be an advantage. Signal detection and localization typically rely on an array of sensory receptors; their sensitivity, number, and spatial organization play a key role in setting the accuracy of the system. For example, visual resolution is enhanced by the high receptor density in the retina's fovea, sound localization is largely enabled by the binaural configuration of the auditory system, and moths can detect the presence of just a few pheromone molecules due to the number and convergence of olfactory receptors (Ashida and Carr, 2011; Provis et al., 2013; Rospars et al., 2014). While the spatial structure and size of the receptor array clearly shape the sensitivity of the system, it is not always clear how the configuration of the receptors is related to detection accuracy versus localization.

The electrosensory system in fish is an exquisite example of sensitivity. In ghost knifefish in particular, survival depends on navigating, detecting prey, and communicating through this active sense. They generate a constant weak electric field with their electric organ (EO) and any distortions of this field by preys or objects in their environment are picked up by an array of receptors covering the skin of the fish (Nelson et al., 1997; Pedraja et al., 2014). Distortions from an object or prey will impact only a spatially defined subset of receptors on the corresponding portion of skin onto which the electric image (EI) of the object is projected. By activating the corresponding portions of the topographic maps higher in the sensory system, spatial information is encoded in a sort of labeled-line code reminiscent of the way the visual or somatosensory system is organized. Furthermore, similar to these modalities (i.e., fovea of the

retina), regions of higher receptor density towards the head and snout of the fish provides a higher spatial resolution particularly useful in the last stage of prey capture as the target approaches the fish's mouth (MacIver et al., 2001; Nelson and Maciver, 1999). They also detect and communicate with one another through this electric sense (Allen & Marsat, 2018; Knudsen, 1975; Petzold et al., 2016). The ongoing electric organ discharge (EOD) is a spatially diffuse signal that can reach globally all the receptors of the other fish's body. Localization of such signals would thus have to rely on differences in the signal strength at different input locations, similar to the way the auditory system compares binaural inputs to localize sound sources (see Milam et al., 2019, for review). While it is clear that the high rostral density of receptors can enhance the spatial accuracy for objects, it is not clear how it influences the processing of diffuse and global signals from another fish's EOD. More specifically, we are interested in determining how the spatial organization and density of receptors interact with the spatial structure of EOD signals to influence the detection and localization of conspecific signals.

The EOD generated by the long EO located in the caudal 2/3 of the fish can be approximated as a dipole whose polarity switches during each EOD cycle (Rasnow et al., 1993). The resulting signal is a quasi-sinusoidal output with frequencies between 500 Hz and 1000 Hz (in *A. leptorhynchus*, the focal species in this paper; (Zupanc and Maler, 1993). Although weak, this signal will travel several tens of cm and will permit the long-range detection of the conspecific (Pedraja et al., 2016). Behavior studies demonstrated that frequent interactions occur at distances of 30 cm or less, but there is evidence from field studies that these fish might be able to detect and navigate toward one another at distances in the 1-meter range (this upper limit has not been quantified systematically; (Henninger et al., 2018; Stamper et al.,

2012; Stamper et al., 2013; Zupanc et al., 2006). These distant signals will reach the receptors with low intensity as the strength of electric signals decreases exponentially with distance. The signal from a distant fish will combine with the signal of the fish's own EOD resulting in a combined electric field with sinusoidal amplitude modulations designated as the beat. If the distant fish's signal reaches the focal fish with an amplitude $1/10^{th}$ the strength of the self-generated EOD, this beat modulation will have an amplitude of $1/10^{th}$ the undisturbed EOD. These weak beat contrasts are the signals that must be encoded to detect a conspecific and differences in contrast at receptors across the fish's body constitute the localization cues. The mathematical framework to estimate the strength and structure of the electric field during social interactions has been detailed in previous studies (Caputi and Budelli, 2006; Castello et al., 2000; Gómez-Sena et al., 2014; Kelly et al., 2008). It can be used to quantify the strength of the signal as it reaches each receptor to obtain a complete characterization of the sensory input structure due to an approaching conspecific.

Ghost knifefish possess several types of electroreceptors, we focus here on p-unit tuberous receptors that constitute the vast majority of electroreceptors, are tuned specifically to encode conspecific signals, and are responsible for encoding the amplitude of these beat contrasts (Bennett et al., 1989). Previous estimates of p-units receptor density range from 9-15 per mm^2 on the head region to 0.6-3.4 over the trunk area (Carr et al., 1982). A thorough quantification of receptor density as a function of dorso-ventral/rostro-caudal location in *A. leptorhynchus* is not yet available. Receptor sensitivity and response properties have been extensively studied and several neural models of p-units are available (Benda et al., 2005; Chacron et al., 2005; Goense and Ratnam, 2003; Gussin et al., 2007; Nelson et al., 1997; Ratnam

and Nelson, 2000). This large population of several thousand receptors will converge to the primary sensory area in the hindbrain, the electrosensory lateral line lobe, and the information is then transmitted down the sensory pathway (Lannoo et al., 1989; Maler et al., 1991). To estimate the information carried by the population of receptors about realistic signals, two key elements must be considered. First, we must take into account the response properties of the receptors, their sensitivity/noisiness, and their heterogeneity across the population. Second, we must consider the structure of the stimuli and how signals from different locations will cause input strengths that vary across the receptor positions.

In this paper, we aim to clarify how spatially realistic signals from conspecifics are encoded by the population of electroreceptors. Our approach includes using a model of the fish's electric field to quantify the EI strength at each receptor location. This input drives a model of the p-unit population consisting of heterogeneous leaky-integrate-and-fire units calibrated based on the extensively documented properties of this population. We then use a decoding analysis to estimate the information that can be extracted from the receptor population and provide a conservative estimate of the expected detection and localization accuracy. We specifically hypothesize that the high density of receptors rostrally will enhance detection and localization accuracy, particularly in the frontal quadrant. We tested this hypothesis by altering the structure and density of the receptor population and confirming that detection accuracy depends on receptor density. Surprisingly, we show that localization is relatively less influenced by receptor density and that the high rostral density does not enhance localization accuracy for frontal azimuth. Our results highlight the intricate relationship between the spatial structure of signals and the spatial organization of sensory receptors.

Methods

Quantification of electroreceptor distribution

Weakly electric brown ghost knifefish, *Apteronotus leptorhynchus*, were obtained from a tropical fish supplier (Segrest Farms, FL, USA). Fish care and use were approved by West Virginia University IACUC.

Fish were euthanized then fixed in a 50mL aliquot containing a 40mL solution of 4% paraformaldehyde, and preserved for up to 7 days. After tissues were completely fixed, 5mg of eosin Y was added to the aliquot containing the preserved fish. Stained fish were analyzed under a fluorescent microscope with a light wavelength of 530nm. A stereotaxic system was used to move the fish and place a $1mm^2$ sampling grid at different locations along the fish's body, tuberous receptors inside the grid were visually identified and counted. We collected 581 samples from 18 fish measuring on average 14 cm in length.

A coarse 3D mesh model of the fish was created using Maya 2019 (Autodesk, Inc) based on average measurements of our fish and images of the rostral, dorsal, and lateral profiles. The quadrangle mesh model has 218 planar faces. For each face, the corresponding measured receptor densities were averaged. Average receptor densities for each face were mapped along a rostro-caudal and dorsal-ventral plane. A 3-dimensional 5^{th}-degree polynomial was fitted to obtain a smooth, interpolated, estimate of receptor density as a function of body location. Using a more detailed mesh model (the same used for EI calculation; see below), we randomly generated receptor locations for each face according to our density function.

EI model

The electric image model used in this study was based on the established methods developed by Caputi and Budelli (Caputi and Budelli, 1995; Caputi and Budelli, 2006; Caputi et al., 1998), and implemented using software developed by Rother (Rother et al., 2003). More details on the model can be found in these publications and it is described here briefly. The EI model requires the creation of a reconstruction of the geometry and electrical properties of the fish bodies and their placement in the surrounding water. This information is used to calculate the transcutaneous voltage at specific nodes along the skin of the fish. The model makes the following assumptions:

1. All the media are ohmic Therefore, $J(x) = \sigma(x)E(x), \sigma(x) > 0$ (1)

   Where J(x) is the current density at point x and E(x) is the electric field at the same point.

2. There are no capacitive effects so at no point in space is there an accumulation of charge. $\frac{\delta p(x)}{\delta(t)} = 0$ (2)

3. The model is an electrostatic approximation (Bacher, 1983)

4. The fish and other objects that make up the environment are immersed in an infinite water medium. Each object in the environment is covered by a thin resistive layer (the skin in the case of the fish), which can be homogeneous or heterogeneous.

The model is based on the charge density equation which, under the above assumptions, implies that the charge generated by the sources f(x) is equal to the charge diffusion:

$$\frac{\delta p(x)}{\delta(t)} = f(x) - \nabla.J(x) \quad (3)$$

Combining equations 1 and 2 we get

$$\nabla . J(x) = f(x) \Rightarrow \sigma \nabla . E(x) = f(x) \quad (4)$$

The electric field E(x) can be expressed as $E(x) = -\nabla\varphi$ therefore:

$$\sigma \nabla^2 \varphi(x) = -f(x) \quad (5)$$

Equation (5) is a partial differential equation known as the Poisson equation and can be solved for every point in space, in our case the fish boundaries by using the boundary element method (BEM) as proposed by Assad (Assad and Bower, 1997). The method determines the boundary conditions by solving a linear system of M•N equations for M poles and N nodes, with the unknown variables being the transepithelial current density and voltage at each node (Pedraja et al., 2014). The shape of the 3D fish mesh model consists of 49 ellipses composed of 17 nodes each (i.e., 835 nodes) defining 1,666 triangular faces between the nodes (Rother et al., 2003). The size of the fish was kept constant at 14 cm in length in this paper and the water conductivity is 300 µS and the skin and internal conductivity of the fish were 100 and 10,000 µS respectively. The 2 poles for each fish were positioned 9.3 and 10.5 cm from the rostral tip of our 14 cm fish. We use the middle of this dipole (i.e., the center of our "electric organ") to define the position from which the signal originates.

Calculations of signal strength at receptor locations

We calculate the transdermal voltage when only the focal fish is present (*Vf*) or when both focal and sender fish are present (*Vfs*), in which case the peak voltage is determined at the top of the beat cycle (EODs in phase). The strength of the EI caused by the sender fish at each node *i* on the surface of the focal fish was defined as a contrast *c*:

$$c = \frac{Vfs_i - Vf_i}{Vf} \quad (6)$$

The contrast value for receptor location within each triangular face was interpolated from the values at the nodes that define the face using a barycentric coordinates system. Considering a triangle with values *N* at the nodes (vertices) and coordinates *X, Y, Z*. A receptor inside the triangle will have a contrast value *R* according to the weighted value of the nodes. The weights *W* can be found by solving:

$$X_R = W1 \cdot X_{N1} + W2 \cdot X_{N2} + W3 \cdot X_{N3} \quad (7)$$

$$Y_R = W1 \cdot Y_{N1} + W2 \cdot Y_{N2} + W3 \cdot Y_{N3} \quad (8)$$

$$Z_R = W1 \cdot Z_{N1} + W2 \cdot Z_{N2} + W3 \cdot Z_{N3} \quad (9)$$

And contrast at the receptor location is calculated as:

$$R = W1 \cdot N1 + W2 \cdot N2 + W3 \cdot N3 \quad (10)$$

Although the EI model was thoroughly calibrated based on experimental recording on actual fish (Pedraja et al., 2014; Pedraja et al., 2016), we performed transcutaneous recordings on 3 pairs of fish and verified that the transdermal voltage contrast values that we are calculating correspond to the range of values that can be measured experimentally.

Receptor Modelling

We used a leaky integrate and fire (LIF) framework to model the receptors. The model includes noise σ and adaptation current with conductance g_α and reversal potential E_α, and is driven by an input *I*. The membrane voltage is calculated as:

$$\tau_m \frac{dV}{dt} = E_m - V + R_m(I + \sigma - g_\alpha(V - E_\alpha)) \quad (11)$$

The initial parameters of the model were based on existing models (Benda et al., 2005; Carlson and Kawasaki, 2006; Chacron et al., 2001; Nelson et al., 1997). Particularly, the noise was the product of a strength variable A_σ and a random process (specifically, two Ornstein–Uhlenbeck processes (refer to Chacron et al., 2001, for details). Adaptation current α was adjusted to match the time course of adaptation described experimentally (Benda et al., 2005). Conductance g_α is augmented by Δ_α after each spike and decays with time constant τ_α. When the membrane voltage reaches the threshold V_T it is reset to V_R and kept constant during a refractory period t_R. The input I to these p-unit model neurons replicates the input they would receive from receptor cells during social interactions. A sinusoidal EOD carrier signal with amplitude A_{EOD} was created with a frequency of 1000 Hz (the upper range of the naturally occurring EOD frequencies in this species was used for convenience), and modulated with a sinusoidal amplitude modulation (the "beat") of 30 Hz (other AM envelopes are used to validate our model, see Supplementary Material). This AM envelope signal was adjusted to a specific contrast as specified in the Results. A contrast of 0% indicates that the baseline EOD is unmodulated. Whereas a beat contrast of 100% causes the EOD amplitude to be 0 during the trough and twice the baseline EOD amplitude at the peak of the beat. To emulate the current direction and sensitivity as the signal passes through the receptor cells before it reaches the p-unit neurons, the modulated EOD is halfwave rectified after a baseline bias β was subtracted.

Parameters were adjusted to create a prototypical neuron with response properties matched to published data (Bastian, 1981; Benda et al., 2005; Chacron et al., 2005; Grewe et al., 2017; Gussin et al., 2007b; Nelson et al., 1997; Ratnam & Nelson, 2000). We used a wide range of response parameters to validate our model: firing rate, coefficient of variation,

response sensitivity to random amplitude modulations, response sensitivity and time course to steps and responses to beat stimuli (see Supplementary Figure S1). This prototypical neuron with response properties matched to the average experimental values served as our original seed; this set of parameter values are given in Supplementary Information Table S1.

We then used this original seed to create a heterogeneous population that replicates the range of response properties observed experimentally through an iterative process of diversifying the population and constraining the response properties. A heterogeneous array of parameters sets was created (8,000 sets) from the original seed values by slightly varying randomly several parameters: t_R, R_m, τ_m, V_T, A_σ, τ_α, Δ_α, and β. From this array, 12 seeds were selected by choosing sets of parameters that, again, best replicate the average response properties. These sets were further diversified randomly, and from these new arrays, 26 seeds were chosen by selecting neurons that replicate the average coding properties, but that span the range of spontaneous firing rates measured experimentally (Chacron et al., 2001; Gussin et al., 2007; Ratnam and Nelson, 2000). From these 26 seeds, the parameter sets were further diversified and we retained 9,200 sets of parameters by rejecting sets for which the response properties do not fit in the range of response properties determined experimentally. Therefore, our pool of neurons replicates the average and range of response properties measured experimentally. From this pool, 5 equivalent but different populations of 8,195 receptors were created by randomly assigning one of the 9,200 neurons to each receptor location. All data shown in the results reflect averages across these 5 populations.

Decoding analysis

Population responses to different stimuli were compared with our decoding analysis to determine how accurately signals could be detected or discriminated considering the differences in response patterns for these stimuli. The framework used for our decoder has been described and validated thoroughly in previous publications (Marsat et al., 2023; Allen and Marsat, 2018; Allen and Marsat, 2019; Allen et al., 2021; Marsat and Maler, 2010). It was shown that this analysis measure is directly correlated with the information content of the responses about the stimuli. We describe the method briefly here. Importantly, the only difference with the established measure described in Marsat et al. (2023) is that we do not use the detailed time-course of each neural response (i.e., the full spike trains) but use the peak-to-though firing rate to quantify the response of the neuron. To calculate the peak-to-trough firing rate, the binarized spike trains are smooth with a sliding square window of 16.67 ms (half a beat cycle) to obtain an instantaneous firing rate. For each beat cycle, the difference between the maximum of the instantaneous firing rate and the minimum gives us our measure of peak-to-through firing rate. These peak-to-trough measures can be averaged over several cycles of the beat, or we can use the values for single beat cycles as specified in the different Results section. When no beat stimulus is provided, the analysis is unchanged and the peak-to-trough is calculated over each consecutive 33.34 ms segments of response (i.e., a 30 Hz period).

Pairs of responses are compared by the analysis: responses to stimuli from two different azimuths are compared in the angular resolution analysis while in the detection analysis the response to the sender fish's signal is compared to the response when no second fish is present (i.e., baseline firing due to the focal fish's own signal). For each individual neuron *i* (out of *n*

total neurons*)*, the similarity between the probability distributions *P(x)* of responses (the peak-to-trough firing rate *x*) to the two stimuli (*R* and *B*) is calculated based on the area difference $\Omega_{(P_R,P_B)}$ between the two distributions:

$$\Omega_{(P_{Ri},P_{Bi})} = \sum_x |P_{Ri}(x) - P_{Bi}(x)| \quad (12)$$

AD values are normalized to 1 across the *n* neurons to obtain a weight W:

$$W_i = H_0(\Omega_{(P_{Ri},P_{Bi})} - \frac{1}{n}\sum_n \Omega_{(P_{Rn},P_{Bn})} + 1) \quad (13)$$

where H_0 is the Heaviside step function. The peak-to-trough firing rates for each neuron are multiplied with these weights before being used in our Euclidean distance calculations (see below). As a consequence of this weighting, the neurons that respond very differently to the two stimuli will contribute more to Euclidean distance between the population responses and the neurons that respond similarly to the two stimuli will contribute little to the Euclidean distance. Since the sum of the weight for a population is 1, the overall firing rate of the population is unchanged by the weighting procedure.

The Euclidean distance *D* between pairs of weighted responses (R_a and R_b) is calculated between responses to the same stimulus or between responses to the two different stimuli being compared:

$$D = \sqrt{\sum_{nt}(R_a - R_b)^2} \quad (14)$$

These Euclidean distances are used to determine how well an ideal observer could discriminate between responses to the two stimuli. The distribution of distances between responses to the same stimulus D_{xx} and the distribution of distances between responses to the two different stimuli, D_{xy}, are used for an ROC analysis. In this analysis, a threshold distance *T* is

varied. For each threshold, the probability of non-discrimination (P_D) is calculated as the sum of $P(D_{xy}>T)$ and the probability of false discrimination (P_F) is calculated as the sum $P(D_{xx}>T)$. The error rate E is taken as the minimum error across threshold given:

$$E = \frac{1}{2}P_F + \frac{1}{2}(1 - P_D) \tag{15}$$

This error rate is used in the various parts of the result as specified therein, and we consider that reliable detection or discrimination happens when the error rate is below 0.05.

Results

Since ghost knifefish can detect and localize each other based on the electric signals they continuously emit; both fish are thus senders and receivers at the same time. To simplify the description of our results we describe the fish for which we describe the electric image (EI) and sensory responses as the focal fish. The "other" fish that needs to be detected and localized by the focal fish is designated as the sender fish. A number of studies have characterized the EI that one fish cause on another fish's body (Kelly et al., 2008; Pedraja et al., 2016). The results presented in these papers are not always easily related to electrophysiological studies because many experiments on the responses of sensory neurons in this system calibrate the signals as a relative contrast in the measured voltage. For example, many studies present the response properties to conspecific signal of 5-10% contrast (Fotowat et al., 2013; Metzen et al., 2018). Since our goal is to use the estimate of signal strength as an input to neuron models that match their known response properties, we quantify the EI strength as a relative contrast in the transdermal potential difference. If the signal from the sender is as strong as the focal fish's own baseline signal at a given point on their body, the signal strength will be 100% and the EOD will vary from close to 0 mV (at the trough of the beat) to twice the baseline EOD strength (at the peak of the beat cycle).

Expressing the signal as a contrast highlights the challenges that the fish encounters when interacting with a conspecific due to the rapid decay of signal strength with distance. Figure 1 displays the signal strength during a common scenario a sender fish approaching and then moving away from the focal fish. When the fish are separated by only a few centimeters (position 2), the EI has a strong gradient that goes from a strong signal (25% contrast) on

portions of the body closest to the sender to a very weak signal close to 0% contrast. For convenience, we will refer to the region of the electric image with the strongest signal as the hot spot. While this hotspot is well defined when the sender is close-by, the EI is much more diffuse when the sender is further away and there is a weaker gradient between the hotspot and the areas with a weaker signal. For example, in Fig 1B, the difference between the hot spot near the head (position 1) or tail (position 3) is less than 1% stronger than the portions with the weakest signal. The positions 1 and 3 depicted here correspond to a distance (30 cm) at we know fish can detect each other and display active interactions (Henninger et al., 2018; Zupanc and Maler, 1993; Zupanc et al., 2006). The known extreme sensitivity of this system is thus highlighted here since detecting the sender 30 cm away involves detection of a 1% modulation, and localizing this signal requires deciphering a gradient in this signal of less than 1% across the body surface.

The EI stimulates an array of receptors covering the fish's skin and the spatial structure of this sensory array will dictate how the spatial structure of the signal is captured. Receptor density for different portions of the fish's body has been characterized in a closely related species (Carr et al., 1982), but we needed a more detailed quantification of variations in receptor density across the fish's body (Fig 2A). Our data confirm the general organization of receptor density: a region of high density on the snout and head, of medium density on the dorso-rostral portion of the trunk that decreases both ventrally and caudally (Fig 2B). Based on this spatially precise empirical data, we incorporated a population of p-unit receptor locations on the 3D mesh model used for EI calculations that varies smoothly in density as a function of

rostro-caudal and dorso-ventral position (Fig 2C). In the rest of this study, we will use an "average" fish that measures 14 cm long and includes ~8,195 receptor locations.

We calculated the stimulus intensity for each receptor location for the various iterations of the EI calculation; the result for the 3 positions illustrated in Fig 1 is shown in Fig 3A (note that for this figure, the blue-red color scale covers the contrast range for each position). We wanted to quantify how the strength of the EI changes with the position of the sender relative to the focal fish. To do so, we ran the model for 864 relative positions where the two fish are at 12 distances that vary from nearly touching to 75 cm apart and for 72 different azimuths around the focal fish while always having the sender fish's heading towards the focal fish. To estimate the maximal strength of the signal for each location, we used the strength of the signal at the center of the hot spot on the focal fish. We plot this value as a color scale at the position of the middle of the electric organ of the sender fish (Fig 3B). We can see that the strength of the signal decreases sharply with distance as expected. The portions of the figure with contrast above 20% (yellow-white shades) represent positions where the fish are nearly touching (with the sender fish head-on). The decrease in signal strength with distance follows the expected power law such that contrast drops to 10% by 10-15 cm and is only a few percent when the sender is 20-30 cm away (Fig 3C).

The EI model helps us quantify the cues that the sensory system can use to detect and localize the source of these signals. To better understand the accuracy with which detection and localization could occur, the strength of these signal must be compared with the noise that the sensory system experiences. We therefore use the deterministic model of EI signal strength described above as an input to a population of model neurons that includes realistic noise. We

based our receptor model on established parameters of leaky-integrate-and-fire that includes adaptation, noise, and a refractory period, to replicate the response properties of p-units (Benda et al., 2005; Chacron et al., 2005; Grewe et al., 2017; Gussin et al., 2007; Nelson et al., 1997). Based on this prototype p-unit model, with properties matched to the average characteristics of p-units, we diversified the model parameters to create a heterogeneous population matching the range of properties observed experimentally (see Methods for details). For the model to provide a biologically reasonable estimate of how accurately this population encodes spatial cues, it is vital to calibrate the sensitivity, heterogeneity and noisiness of the responses to reflect the measured properties of the neurons. Our calibration involved matching the model responses to published values for a range of stimulus types and analysis methods (see Methods and Supplementary Figure S1). The population is then stimulated with conspecific signals (beat stimuli) at intensity levels that is dictated by the EI image for various relative fish positions. Figure 4 shows the response pattern of the population for two of the positions used in Figure 1 and 3. Response strength is quantified as the difference between the peak and though of the instantaneous firing rate during each stimulus cycle (here normalized relative to spontaneous activity). We can see differences in response strength due to the spatial contrast in the EI but also differences across receptors due to heterogeneity that makes some neurons more sensitive.

Firing rate modulation across one stimulus cycle replicates the experimentally measured sensitivity (Fotowat et al., 2013; Henninger et al., 2018; Pedraja et al., 2014; Pedraja et al., 2016; Zupanc et al., 2006) The strength of the electric image quickly decreases with distances and reaches levels below 1% contrast at ranges where the fish still detect and interact with

each other (e.g., 30 cm). Our model replicates the fact that for these weak signals, the response modulation is barely above variations in firing rate that naturally occur in the absence of a second fish (Fig 5). Figure 5C shows that, although the responses for nearby fish (14 cm and 22.5 cm in this figure) are visibly different from spontaneous response, signals from more distant fish (40 cm, 75 cm in this figure) cause much more subtle differences in response strength. This is true when looking at the distribution of responses for cycles of the beat, for responses averaged across time (grey or color portion of the distribution plots), or overall responses averaged across time and neurons (white lines).

The sensitivity with which a conspecific signal would be detected will depend on the coding and decoding mechanisms implemented by the nervous system. It is beyond the scope of this article to explore all possible coding and decoding algorithms that could contribute to the sensitivity of the system, but as a first step towards understanding the sensitivity of this system, we aim to provide a lower-bound on accuracy. To do so, we only consider peak-to-trough firing rate to quantify response strength as it is the most salient aspect of the response that varies with stimulus strength. The responses of individual receptors will be combined at higher levels of the nervous system and this can help average out noise in the responses. However, the way these responses are combined would require various assumptions, matched to the architecture of high brain areas, that would lead to a complex modelling effort and speculations on decoding procedure. For this reason, and to remain within a “lower-bound” perspective, we map each population response in Euclidean space where each dimension represents the response strength of a neuron (i.e., response strength is not averaged across neurons). Reliable detection would occur if the strength of the population response is markedly

different from the response when no signal is present; in other words, when the stimulus response is far from baseline responses in this Euclidean space representation. Our analysis therefore uses a weighted Euclidean distance followed by an ROC analysis to quantify the reliability with which stimulus responses can be differentiated from baseline. This analysis could be done on “instantaneous responses”, considering the response of the population (peak-to-trough for each receptor) for a single cycle of the stimulus which would give us a response accuracy (i.e., probability of error) for each fish positions. Behavioral responses typically occur after attending the signal for a certain period of time, and more accurate detection occurs after several seconds of the stimulus than after the first cycle. We therefore integrate the response of each neuron across time (average the peak-to-trough across several beat cycles) to estimate how detection accuracy would change as information is accumulated with time. We consider that accurate detection occurs when less than 5% detection error would occur and plot in Figure 6 the amount of time that accurate detection would require. Our analysis shows that accurate detection could occur within a single cycle of the stimulus for fish that are within 20 cm of the focal fish (Fig 6A, 6C). Detection accuracy decreases with distance and thus it takes more time to reliably detect the stimulus. As a result, a fish 60-70 cm away would require integrating the signal for several seconds to be able to reliably tell that another fish is present.

Detection accuracy is undoubtedly influenced by the fact that thousands of receptors contribute to transmitting this information. The distribution of these receptors is not uniform across the fish’s body. In particular, the rostral end of the fish (head region) has a density of receptors 5-10 times higher than the caudal end (tail region). We hypothesize that this foveal organization supports an enhanced sensitivity in the frontal quadrant relative to the fish.

Alternatively, the increased density in receptors plays an important role in localizing small objects like prey with higher resolution, but does not enhance perception of conspecific in specific regions of space. This is a plausible alternative because conspecific signals cause a more diffuse EI that stimulate a majority of the receptors over the receiver's body. To test our hypothesis, we reduced the density of receptors to make it uniform over the entire body and equal to the low density found at the caudal end of the fish (Supplementary Figure S2). Our resulting population has 2,770 receptors compared to 8,195 for the full population. The difference in detection sensitivity is displayed in Figure 6B and reveals the enhancement in sensitivity afforded by the increased density in the rostral portion of the body. The difference is negligeable when the sender is very close because accuracy is high and a decrease in the number of receptors encoding the stimulus is not sufficient to affect performance. For very distant signals (e.g., 75 cm), the lower rostral density causes a decrease in sensitivity that is fairly uniform across azimuth (see also Supplementary Figure S3). This can be explained by the fact that distant signals cause diffuse EI patterns that vary by less than 1% across the body (e.g., see Figure 1). As a result, the head region is stimulated at a level nearly identical to the tail region even if the sender fish is located behind the focal fish. There is, however, a clear difference as a function of azimuth for medium distances (35-50 cm; Figure 6B and Supplementary Figure S3). The higher density of receptors on the head provides a clear advantage in detection accuracy in the frontal quadrants (i.e., requires less time until accurate detection occurs). We further verified the idea that having a larger population of receptors allows the population to encode the presence of the stimulus more reliably by decreasing further the density of our uniform population of receptors by 2-, 4- and 8-fold (resulting in

population sizes of 1,385, 693 and 347 receptors respectively). Our analysis confirms that a higher density of receptors allows more accurate detection for distances where the signal is faint (Figure 6C).

We next inquire about the spatial information about the angular position of the sender fish relative to the focal fish: its azimuth (in front=0°; behind= 180°). To do so, we compare the responses to stimuli at various positions and quantify how reliably these responses could be discriminated based on the same weighted Euclidean distance analysis used above. Error probability will thus depend on two factors, angular separation between the two stimuli and duration of stimulus evaluated whereas in our previous detection analysis the latter was the only factor considered. To be able to display our results conveniently, we chose to keep the duration of the stimulus integration to 1s. This value is a compromise between expecting accurate angular discrimination instantaneously (~1 cycle) and expecting the sender fish to remain in a relatively fixed position for seconds in order for angular position to be accurately estimated. Using this 1s integration time, we determined the angle that needed to separate two stimuli to lead to reliable discrimination (<5% error) and call this value angular resolution (Figure 7). Our results show that angular resolution is accurate to a few degrees (<5°) when the sender is within 10-20 cm and decreases sharply between 20 and 40 cm such that beyond 40 cm, azimuth could not be reliably determined (angular resolution>180°). If we repeat the analysis using different integration times (Fig 7B); as expected, the sharp decrease in angular resolutions moves from being for positions 20 cm away when a single cycle of the beat is considered to being 40-50 cm away when 3.3s of the stimulus is being averaged. Our analysis suggests that for the most distant positions tested (75 cm) angular position could not be

resolved even when the stimulus is being integrated for several seconds. Together with the results of Figure 6, these finding thus suggest that for the more distant signals only detection would occur, and the position of the sender would not be accurately determined without relying on additional behavioral or neural mechanisms (see Discussion).

Angular resolution does not appear to be equally good for a given distance as a function of the azimuth of the sender (e.g., front vs. side vs. back). This can be seen in Figure 7A where the color patterns around the focal fish are not perfectly circular. In particular, worse angular resolution occurs at a shorter distance in the back quadrant compared to the front. We suspected that the way we equalized distance across angle could cause a bias. The center of the focal fish is taken as the average receptor position and the center of the sender as the middle between the two emitting poles that constitute the EOD source. Center-to-center distance and azimuth were used to set our relative positions. In this arrangement, a fish at 130° (in the back quadrant, see fish illustrated in Fig 7A) rotating 5° would not only change azimuth but also come closer to the focal fish if we consider the two closest points on each fish's bodies. Note that this is not an issue in our detection analysis since our accuracy measure does not depend on the comparisons between two stimuli locations but only on the absolute location of a single stimulus. We therefore repeated our angular resolution analysis by comparing angular resolutions where the distance between the rostral tip of the sender and the closest point on the body of the receiver is kept constant (the dots in Fig 8A show the positions of the rostral tip of the sender used in our analysis). We found that angular resolution is better in the frontal quadrants than at the back (Fig 8A, 8C). Surprisingly, it is not best directly in front of the focal fish (0°) but rather on the side (90°). Since we expected the high density of receptors on the

head of the fish to help enhance localization accuracy, we hypothesize that angular resolution is particularly good as the edge of the hotspot caused by the sender sweeps across the region of high receptor density (which could correspond to sender positions around ~90°). To test the contribution of higher receptor density towards the heads, we repeated the analysis with the "uniform" receptor population used in the previous section that has an equally low receptor density across the whole body. This uniform population of receptors did not perform much worse than our full population, and in particular there is no striking difference directly in front (0°) or the side (90°) of the fish where resolution is best. Azimuth determination was not possible (angular resolution>180°) when the fish were two body lengths apart (28 cm) but at one body length, the higher density of receptors provided a small advantage. Specifically, there are only a few spots at ~45° and ~125° where the higher receptor density on the rostral portion of the body helps to enhance angular resolution (Fig 8B, 8C). We confirm that decreasing the population density further decreases angular resolution and this is particularly obvious for more distant stimuli (one body length), where localization is still possible but angular resolution is not great (Fig 8D).

Our results demonstrate that the angular resolution is relatively poor at the back and is slightly better on the side than the front. This effect cannot be attributed to the higher density of receptor towards the head. Therefore, we questioned whether this effect could be due to the geometry of the fish's body and how it interacts with the geometry of the electric field. We hypothesize that a small change in angle on the side will cause a relatively bigger change in the electric image than a similar angle difference at the back. A sender fish at 90° azimuth would have its EI hotspot centered on the flat surface of the side of the focal fish whereas for frontal

(0°) or caudal (180°) azimuth, the EI hotspots are centered on the pointy rostral and caudal ends of the fish. We quantified how much difference in EI a sender at various azimuth would cause on the focal fish and integrated this difference across the body surface. We found that it correlates strongly with the differences in angular resolution that we have estimated for various azimuth and distances (Figure 8E). Our analysis supports the conclusion that differences in angular resolution as a function of azimuth is in part due to the geometry of the fish and their electric fields.

Discussion

By using a model of weakly electric fish EI and carefully normalizing how we calculate the distance between the relevant points on the two fish, we presented a clear quantification of the strength of the EI as a function of distance. Our results suggest that strong signals of more than a few percent beat contrast, only occur at distances below 15-20 cm. This finding is in agreement with empirical data and consistent with the fact that when two fish actively interact (e.g., chasing each other and courtship), they are typically in close proximity (Fotowat et al., 2013; Zupanc and Maler, 1993).The relationship we show is quantitatively informative only in a simplified case: a given fish size (and EOD strength) with a fixed heading angle (sender head-on towards focal fish). The strength of the electric image as a function of distance will depend on environmental factors (water conductivity), the individuals interacting (their size and EOD strength), and on moment-by-moment changes in the relative heading angle of each fish. All these factors could be taken into account in a more extensive analysis of EI during social interactions, but it is beyond the scope of our paper. It is also important to point out that additional improvements on the model could provide additional details on the structure and dynamics of the EI such as replicating the bending of the fish's body or having the EO modeled with more spatio-temporal details rather than being a simple fixed dipole. We note that since the strength of the EI at a given receptor location depends on distance and relative heading angles, the strength of the beat AM (its envelope) cannot serve as a reliable indicator of distance or movement towards/away. Rather, reliable spatial information must take into account the differences in EI strength over the body of the receiver. This is obvious for localizing

the azimuth of the target but can also help resolve the distance since a fish close-by will cause EIs with sharper contrasts across the body while distant fish will elicit more uniform EIs.

We used, for the first time in this system, a model of the full population of receptors, replicating their heterogeneous response properties and their spatially realistic input patterns. This allowed us to provide a conservative estimate of the detection range that this sensory input could support. We found that, depending on how the information is extracted, detection would still be possible at 75 cm. This range is comparable to behavioral interactions that report instances where a fish detected and moved towards another or simply interacted electrically with one another at ranges above 60 cm (Henninger et al., 2018; Stamper et al., 2012; Yu et al., 2012). Our sensitivity estimates might, in fact, come short of the sensitivity observed behaviorally, but this might be because we intentionally provide a conservative estimate. Our estimate relies on a decoding analysis that does not try to replicate sophisticated decoding procedures that could be implemented by the nervous system. Our analysis uses a “Euclidean distance” perspective to quantify similarity in responses where the response of each neuron is kept as separate dimensions. The nervous system will, in various steps of its pathway, combine neural responses and thereby average out noise. An optimized procedure (e.g., using a principal component approach) could be implemented but it would need to be tailored to each stimulus/task being considered. Any realistic attempt to leverage the convergence of receptor input that is performed by higher sensory area would be a major undertaking that could not be simply added to this study. We also use a simple measure of response strength (peak-to-trough firing rate) and although it is likely one of the key elements of the response, other aspects could be considered. Particularly, synchrony among receptors has been shown to encode frequency

modulations that occur during communication (Benda et al., 2006; Metzen et al., 2020). It is possible that changes in synchrony occur as the stimulus strength changes and encode information that could enhance the detection and localization accuracy. Further experiments are required to better understand the importance of population synchrony in this context. Other neural mechanisms could be present and enhance the sensitivity of the system. We know for example that the presence of negative correlations in inter-spike intervals suppresses noise at low frequencies and could enhance the coding of low-frequency stimuli (lower than the frequency we use in this paper; (Chacron et al., 2001). For this reason, we propose that our sensitivity estimates are conservative estimates that can serve as a starting point in estimating the limits in detection and localization abilities.

Our analysis indicates that reliable detection or localization would require integration of the signals over a certain period of time by higher brain areas. This is a realistic perspective as behavioral performance in various systems will be more accurate for ongoing than for brief stimuli (Dizon and Litovsky, 2004; Gai et al., 2013). For example, estimates of the direction of motion in a “random dot display” integrates over time in the visual system of primates to reach a reliable decision after seconds of attending the stimulus (Ditterich et al., 2003; Kim and Shadlen, 1999). For weakly electric fish, it is not unrealistic to assume that the stimulus can be integrated over several hundred ms to support accurate detection and localization, but it is not clear that this integration could occur over tens of seconds particularly when relative movement could require location estimate to be updated frequently. As a first step, our analysis considered spatially fixed signals, but it will thus be imperative in future studies, to take into account both the spatial and temporal dynamic of the conspecific signals. According to this

perspective, localization accuracy, and thus behavioral decisions, depends on the spatial dynamic during the interaction. Moreover, this spatial dynamic can be leveraged as a means to collect spatial information. Various behavioral strategies can contribute to localizing a stimulus. For example, when localization is difficult, movements towards the target that result in the signal strength increasing can help confirm the position of the second fish (Fagan et al., 2013; Kaushik et al., 2020). Lateralization, rather that precise azimuth localization, can be used while a fish moves towards a target: if a stimulus is perceived as coming from the left or right, corrective turns realign the target. The individual would therefore move towards the target in a zig-zag pattern; this mechanism has been proposed to contribute to behavior in various systems (Beetz and el Jundi, 2023; Gerhardt et al., 2023; Pollack et al., 1984).

Detection could rely on the convergence of the whole population of receptors thereby efficiently averaging out noise. Furthermore, the high receptor density rostrally improves detection for frontal azimuth because the EI hotspot will be centered on this high receptor density area and thus lead to a high convergence of strong responses. Localization, however, must rely on comparison of the EI strength across the body. When comparing the responses to stimuli from different azimuths, our analysis focusses on the neural responses that differ between the stimuli by weighing heavily the contribution of these neurons. This procedure to optimize the extraction of spatial information is essential because the EI might differ only slightly between two stimuli and thus the responses of most neurons will be identical across the stimuli locations. For localization, it is thus the convergence of the responses of a subset of neurons, that differ in activation between the locations being compared, that can support the accurate discrimination of azimuth. Surprisingly, we found that the high density of receptors on

the rostral portion of the fish, does not lead to a better discrimination of the frontal azimuth. This result could reflect the fact that the receptors on the head will have a stronger difference in response at the edge of the hot spot elicited by the sender moving across these receptor locations. We suggest that this would occur as the leading, or trailing, edge of the hotspot sweeping across the high-density areas. This could explain the modest increases in spatial resolution due to the increased rostral receptors density that we observed around 60° and 120°. This is in contrast with the contribution of the high density of receptors during prey capture (i.e., small objects) where localization accuracy is enhanced for the head and snout regions. The structure and convergence of receptors thus play different roles in the detection and localization of objects and conspecifics: while high density and convergence contribute markedly to spatial coding of objects, it mostly contributes to detection accuracy for conspecific signals.

In other systems, regions of high receptor density are typically associated with high spatial resolution. It is the case of the foveal region of the retina and of high receptor density regions of the somatosensory system like the fingers or lips in humans (Catania and Catania, 2015; Dacey, 1994; Nakamura et al., 1998). In other systems faced with spatially diffuse signals, like the auditory or olfactory systems, the extraction of spatial information typically relies on the comparisons between a limited number of input (e.g., 2 ears) and high convergence of receptors is more tightly involved with the accurate detection, rather that localization, of the signals (Carr and MacLeod, 2010; Chapman, 1982; Okada and Toh, 2006; Schnupp and Carr, 2009). Our result on the electrosensory system suggests that this is a general principle guiding the relationship between signal structure and the organization of the sensory arrays. We argue

that for signals that are spatially diffuse, receptor density and convergence will benefit detection abilities and spatial information is extracted by comparing inputs at different locations without relying on a higher number of inputs to enhance localization. For signals that are spatially localized, a topographic mapping system is advantageous and localization accuracy directly depends on the spatial resolution of the input array. The electrosensory system provides a powerful way to compare these systems and reveal organizing principles because it processes both localized and diffuse signals for which receptor organization and convergence play different roles.

References

Allen, K. M. and Marsat, G. (2018). Task-specific sensory coding strategies are matched to detection and discrimination performance. *J Exp Biol* **221**, jeb170563.

Allen, K. M. and Marsat, G. (2019). Neural Processing of Communication Signals: The Extent of Sender–Receiver Matching Varies across Species of Apteronotus. *eNeuro* **6**,.

Allen, K. M., Salles, A., Park, S., Elhilali, M. and Moss, C. F. (2021). Effect of background clutter on neural discrimination in the bat auditory midbrain. *J Neurophysiol* **126**, 1772–1782.

Ashida, G. and Carr, C. E. (2011). Sound localization: Jeffress and beyond. *Curr Opin Neurobiol* **21**, 745–751.

Assad, C. and Bower, J. M. (1997). Electric field maps and boundary element simulations of electrolocation in weakly electric fish. *Engineering and Applied Science* **PhD**,.

Bacher, M. (1983). A new method for the simulation of electric fields, generated by electric fish, and their distorsions by objects. *Biol Cybern* **47**, 51–58.

Beetz, M. J. and el Jundi, B. (2023). The influence of stimulus history on directional coding in the monarch butterfly brain. *J Comp Physiol A Neuroethol Sens Neural Behav Physiol*.

Benda, J., Longtin, A. and Maler, L. (2005). Spike-Frequency Adaptation Separates Transient Communication Signals from Background Oscillations. *Journal of Neuroscience* **25**, 2312–2321.

Benda, J., Longtin, A. and Maler, L. (2006). A synchronization-desynchronization code for natural communication signals. *Neuron* **52**, 347–358.

Bennett, M. V. L., Sandri, C. and Akert, K. (1989). Fine structure of the tuberous electroreceptor of the high-frequency electric fish,Sternarchus albifrons (gymnotiformes). *J Neurocytol* **18**, 265–283.

Caputi, A. and Budelli, R. (1995). The electric image in weakly electric fish: I. A data-based model of waveform generation in Gymnotus carapo. *J Comput Neurosci* **2**, 131–147.

Caputi, A. A. and Budelli, R. (2006). Peripheral electrosensory imaging by weakly electric fish. *Journal of Comparative Physiology A* **192**, 587–600.

Caputi, A. A., Budelli, R., Grant, K. and Bell, C. C. (1998). The electric image in weakly electric fish: physical images of resistive objects in Gnathonemus petersii. *J Exp Biol* **201**, 2115–28.

Carlson, B. A. and Kawasaki, M. (2006). Ambiguous Encoding of Stimuli by Primary Sensory Afferents Causes a Lack of Independence in the Perception of Multiple Stimulus Attributes. *Journal of Neuroscience* **26**, 9173–9183.

Carr, C. E. and MacLeod, K. M. (2010). Microseconds Matter. *PLoS Biol* **8**, e1000405.

Carr, C. E., Maler, L. and Sas, E. (1982). Peripheral organization and central projections of the electrosensory nerves in gymnotiform fish. *J Comp Neurol* **211**, 139–153.

Castello, M. E., Aguilera, P. A., Trujillo-Cenoz, O. and Caputi, A. A. (2000). Electroreception in Gymnotus carapo: pre-receptor processing and the distribution of electroreceptor types. *Journal of Experimental Biology* **203**,.

Catania, K. C. and Catania, E. H. (2015). Comparative studies of somatosensory systems and active sensing. *Sensorimotor Integration in the Whisker System* 7–28.

Chacron, M. J., Longtin, A. and Maler, L. (2001). Negative interspike interval correlations increase the neuronal capacity for encoding time-dependent stimuli. *J Neurosci* **21**, 5328–43.

Chacron, M. J., Maler, L. and Bastian, J. (2005). Electroreceptor neuron dynamics shape information transmission. *Nat Neurosci* **8**, 673–678.

Chapman, R. F. (1982). Chemoreception: the significance of receptor numbers. *Adv Insect Physiol* **16**, 247–356.

Dacey, D. M. (1994). Physiology, Morphology and Spatial Densities of Identified Ganglion Cell Types in Primate Retina. *Ciba Found Symp* **184**, 12–34.

Ditterich, J., Mazurek, M. E. and Shadlen, M. N. (2003). Microstimulation of visual cortex affects the speed of perceptual decisions. *Nature Neuroscience 2003 6:8* **6**, 891–898.

Dizon, R. M. and Litovsky, R. Y. (2004). Localization dominance in the median-sagittal plane: Effect of stimulus duration. *J Acoust Soc Am* **115**, 3142–3155.

Fagan, W. F., Lewis, M. A., Auger-Méthé, M., Avgar, T., Benhamou, S., Breed, G., Ladage, L., Schlägel, U. E., Tang, W. W., Papastamatiou, Y. P., et al. (2013). Spatial memory and animal movement. *Ecol Lett* **16**, 1316–1329.

Fotowat, H., Harrison, R. R. and Krahe, R. (2013). Statistics of the Electrosensory Input in the Freely Swimming Weakly Electric Fish Apteronotus leptorhynchus. *Journal of Neuroscience* **33**, 13758–13772.

Gai, Y., Ruhland, J. L., Yin, T. C. T. and Tollin, D. J. (2013). Behavioral and modeling studies of sound localization in cats: Effects of stimulus level and duration. *J Neurophysiol* **110**, 607–620.

Gerhardt, H. C., Bee, M. A. and Christensen-Dalsgaard, J. (2023). Neuroethology of sound localization in anurans. *J Comp Physiol A Neuroethol Sens Neural Behav Physiol* **209**, 115–129.

Goense, J. B. M. and Ratnam, R. (2003). Continuous detection of weak sensory signals in afferent spike trains: The role of anti-correlated interspike intervals in detection performance. *J Comp Physiol A Neuroethol Sens Neural Behav Physiol* **189**, 741–759.

Gómez-Sena, L., Pedraja, F., Sanguinetti-Scheck, J. I. and Budelli, R. (2014). Computational modeling of electric imaging in weakly electric fish: Insights for physiology, behavior and evolution. *Journal of Physiology-Paris* **108**, 112–128.

Grewe, J., Kruscha, A., Lindner, B. and Benda, J. (2017). Synchronous spikes are necessary but not sufficient for a synchrony code in populations of spiking neurons. *Proc Natl Acad Sci U S A* **114**, E1977–E1985.

Gussin, D., Benda, J. and Maler, L. (2007). Limits of Linear Rate Coding of Dynamic Stimuli by Electroreceptor Afferents. *J Neurophysiol* **97**, 2917–2929.

Henninger, J., Krahe, R., Kirschbaum, F., Grewe, J. and Benda, J. (2018). Statistics of natural communication signals observed in the wild identify important yet neglected stimulus regimes in weakly electric fish. *J Neurosci* 0350–18.

Kaushik, P. K., Renz, M. and Olsson, S. B. (2020). Characterizing long-range search behavior in Diptera using complex 3D virtual environments. *Proc Natl Acad Sci U S A* **117**, 12201–12207.

Kelly, M., Babineau, D., Longtin, A. and Lewis, J. E. (2008). Electric field interactions in pairs of electric fish: Modeling and mimicking naturalistic inputs. *Biol Cybern* **98**, 479–490.

Kim, J. N. and Shadlen, M. N. (1999). Neural correlates of a decision in the dorsolateral prefrontal cortex of the macaque. *Nature Neuroscience 1999 2:2* **2**, 176–185.

Knudsen, E. I. (1975). Spatial aspects of the electric fields generated by weakly electric fish. *Journal of Comparative Physiology ? A* **99**, 103–118.

Lannoo, M. J., Maler, L. and Tinner, B. (1989). Ganglion cell arrangement and axonal trajectories in the anterior lateral line nerve of the weakly electric fish Apteronotus leptorhynchus (Gymnotiformes). *Journal of Comparative Neurology* **280**, 331–342.

MacIver, M. A., Sharabash, N. M. and Nelson, M. E. (2001). Prey-capture behavior in gymnotid electric fish: motion analysis and effects of water conductivity. *Journal of Experimental Biology* **204**,.

Maler, L., Sas, E., Johnston, S. and Ellis, W. (1991). An atlas of the brain of the electric fish Apteronotus leptorhynchus. *J Chem Neuroanat* **4**, 1–38.

Marsat, G. and Maler, L. (2010). Neural Heterogeneity and Efficient Population Codes for Communication Signals Marsat G, Maler L. Neural heterogeneity and efficient population codes for communication signals. *J Neurophysiol* **104**, 2543–2555.

Marsat, G., Daly, K. C. and Drew, J. A. (2023). Characterizing neural coding performance for populations of sensory neurons: comparing a weighted spike distance metrics to other analytical methods. *bioRxiv* 778514.

Metzen, M. G., Huang, C. G. and Chacron, M. J. (2018). Descending pathways generate perception of and neural responses to weak sensory input. *PLoS Biol* **16**, e2005239.

Metzen, M. G., Hofmann, V. and Chacron, M. J. (2020). Neural Synchrony Gives Rise to Amplitude- and Duration-Invariant Encoding Consistent With Perception of Natural Communication Stimuli. *Front Neurosci* **14**, 79.

Milam, O. E., Ramachandra, K. L. and Marsat, G. (2019). Behavioral and Neural Aspects of the Spatial Processing of Conspecifics Signals in the Electrosensory System. *Behavioral Neuroscience* **133**, 282–296.

Nakamura, A., Yamada, T., Goto, A., Kato, T., Ito, K., Abe, Y., Kachi, T. and Kakigi, R. (1998). Somatosensory Homunculus as Drawn by MEG. *Neuroimage* **7**, 377–386.

Nelson, M. E. and Maciver, M. A. (1999). Prey capture in the weakly electric fish Apteronotus albifrons: sensory acquisition strategies and electrosensory consequences. *J Exp Biol* **202**, 1195–203.

Nelson, M. E., Xu, Z. and Payne, J. R. (1997). Characterization and modeling of P-type electrosensory afferent responses to amplitude modulations in a wave-type electric fish. *Journal of Comparative Physiology A* **181**, 532–544.

Okada, J. and Toh, Y. (2006). Active tactile sensing for localization of objects by the cockroach antenna. *J Comp Physiol A Neuroethol Sens Neural Behav Physiol* **192**, 715–726.

Pedraja, F., Aguilera, P., Caputi, A. A., Budelli, R. and Nobel, S. (2014). Electric Imaging through Evolution, a Modeling Study of Commonalities and Differences. *PLoS Comput Biol* **10**, e1003722.

Pedraja, F., Perrone, R., Silva, A. and Budelli, R. (2016). Passive and active electroreception during agonistic encounters in the weakly electric fish Gymnotus omarorum. *Bioinspir Biomim* **11**, 065002.

Petzold, J. M., Marsat, G. and Smith, G. T. (2016). Co-adaptation of electric organ discharges and chirps in South American ghost knifefishes (Apteronotidae). *J Physiol Paris* **110**, 200–215.

Pollack, G. S., Huber, F. and Weber, T. (1984). Frequency and temporal pattern-dependent phonotaxis of crickets (Teleogryllus oceanicus) during tethered flight and compensated walking. *Journal of Comparative Physiology A* **154**, 13–26.

Provis, J. M., Dubis, A. M., Maddess, T. and Carroll, J. (2013). Adaptation of the central retina for high acuity vision: Cones, the fovea and the avascular zone. *Prog Retin Eye Res* **35**, 63–81.

Rasnow, B., Assad, C. and Bower, J. M. (1993). Phase and amplitude maps of the electric organ discharge of the weakly electric fish, Apteronotus leptorhynchus. *Journal of Comparative Physiology A* **172**, 481–491.

Ratnam, R. and Nelson, M. E. (2000). Nonrenewal statistics of electrosensory afferent spike trains: implications for the detection of weak sensory signals. *J Neurosci* **20**, 6672–83.

Rospars, J. P., Grémiaux, A., Jarriault, D., Chaffiol, A., Monsempes, C., Deisig, N., Anton, S., Lucas, P. and Martinez, D. (2014). Heterogeneity and Convergence of Olfactory First-Order Neurons Account for the High Speed and Sensitivity of Second-Order Neurons. *PLoS Comput Biol* **10**, e1003975.

Rother, D., Migliaro, A., Canetti, R., Gómez, L., Caputi, A. and Budelli, R. (2003). Electric images of two low resistance objects in weakly electric fish. *Biosystems* **71**, 169–177.

Schnupp, J. W. H. and Carr, C. E. (2009). On hearing with more than one ear: lessons from evolution. *Nat Neurosci* **12**, 692–697.

Stamper, S. A., Madhav, M. S., Cowan, N. J. and Fortune, E. S. (2012). Beyond the Jamming Avoidance Response: weakly electric fish respond to the envelope of social electrosensory signals. *Journal of Experimental Biology* **215**, 4196–4207.

Stamper, S. A., Fortune, E. S. and Chacron, M. J. (2013). Perception and coding of envelopes in weakly electric fishes. *Journal of Experimental Biology* **216**,.

Yu, N., Hupé, G., Garfinkle, C., Lewis, J. E., Longtin, A. and Fortune, E. (2012). Coding Conspecific Identity and Motion in the Electric Sense. *PLoS Comput Biol* **8**, e1002564.

Zupanc, G. K. H. and Maler, L. (1993). Evoked chirping in the weakly electric fish Apteronotus leptorhynchus : a quantitative biophysical analysis. *Can J Zool* **71**, 2301–2310.

Zupanc, G. K. H., Sîrbulescu, R. F., Nichols, A., Ilies, I., Sirbulescu, R. F., Nichols, A., Ilies, I., Sîrbulescu, R. F., Nichols, A., Ilies, I., et al. (2006). Electric interactions through chirping behavior in the weakly electric fish, Apteronotus leptorhynchus. *J Comp Physiol A Neuroethol Sens Neural Behav Physiol* **192**, 159–173.

Figures

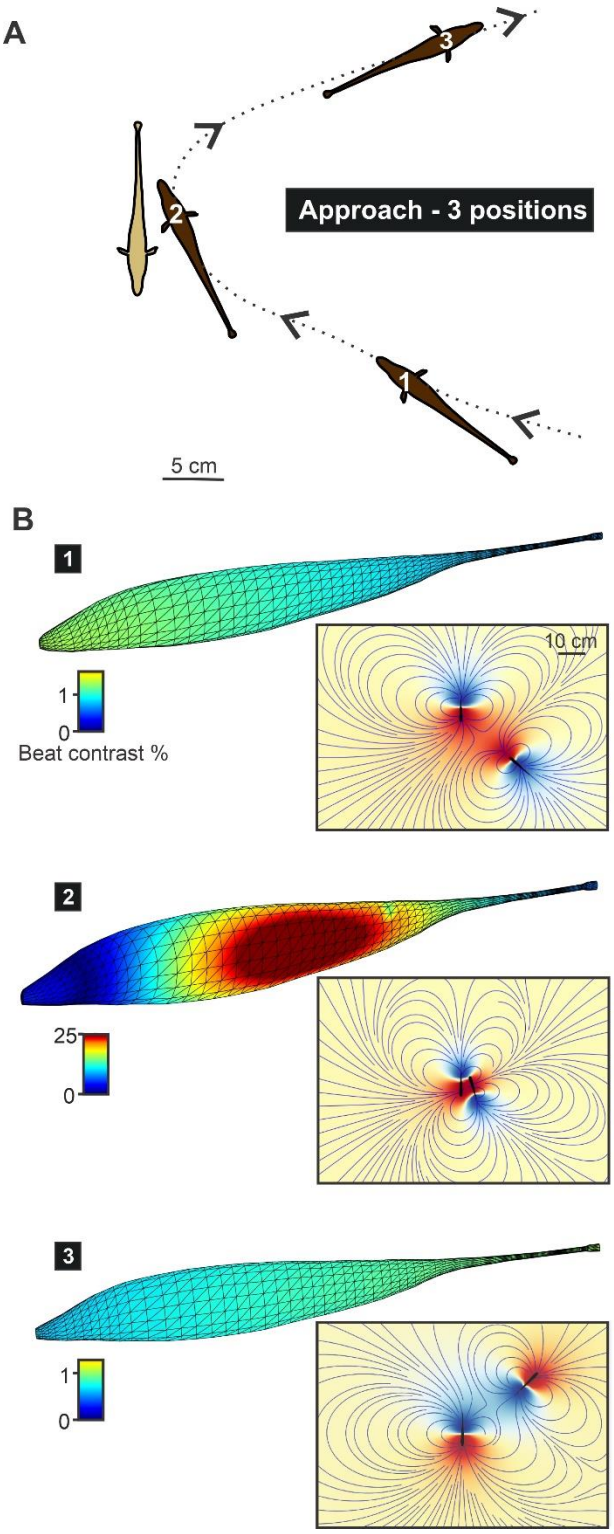

Figure 1: Model of the electric image during social interactions. The model takes into account the relative position of the two fish to estimate the strength of the EI caused by one fish (designated as "sender") onto the body of the other ("focal" fish). **A.** Three relative positions are illustrated here representing different phases of a fish approaching the focal fish. **B.** The EI is quantified based on the strength of the transdermal voltage at the peak of the beat AM caused by the interaction of the fish's EODs. The strength of this AM is then normalized to the baseline EOD strength (i.e., EOD amplitude when only the focal fish is present) to obtain an EI strength expressed as percent contrast. 0% contrast indicates that the signal from the sender fish has no impact on the receiver and 100% contrast indicates that the sender's signal is as strong as the focal fish's own EOD. We can see that for the 2

more distant positions, the signal strength is weak (<1%) and there are only minute differences in signal strength across the receiver's body. When the sender is very close, however, a salient "hot spot" has a much stronger EI strength than other portions of the body (note the different color scales for each image). We show as an inset on the right, the electric field with current lines (grey lines), and the iso-potential lines are depicted for the near-field range as a color gradient (red or blue depending on polarity). The perspective in this inset is from the top as in A) while the EI illustrations in B) present a perspective of the side of the focal fish being approached by the sender.

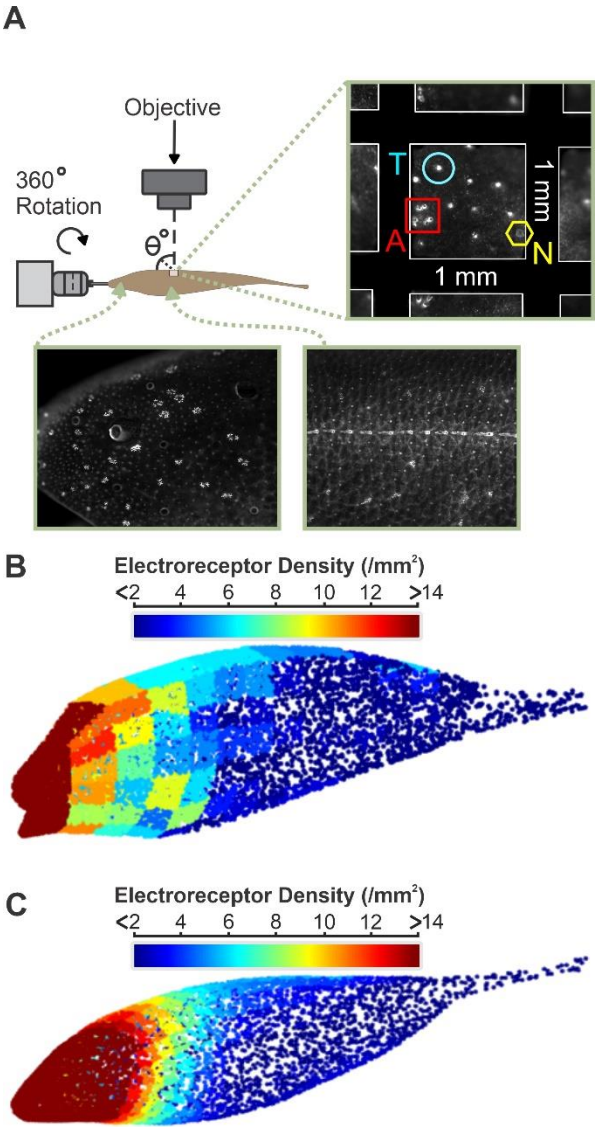

Figure 2: Spatial structure of the receptor array. **A.** Receptor density across the body of the fish was determined experimentally. Eosin Y-stained specimen were examined and cutaneous receptors of different types were identified (e.g., Neuromast labelled N, ampullary labelled A, or tuberous receptors, labelled T in the inset on the top right). The number of tuberous receptors in 1mm^2 areas was averaged across samples for each face of a coarse 3D mesh model of the fish (**B**). Receptor density as a function of body position was then smoothed by fitting a 5th degree polynomial and mapped onto the fine mesh model used in the EI model (**C**). For each face of this 3D mesh, random receptor positions were selected according to the receptor density attributed to each face. The receptor positions that we generated are marked by the dots in B) and C) and their color reflect the density of receptors for the corresponding position.

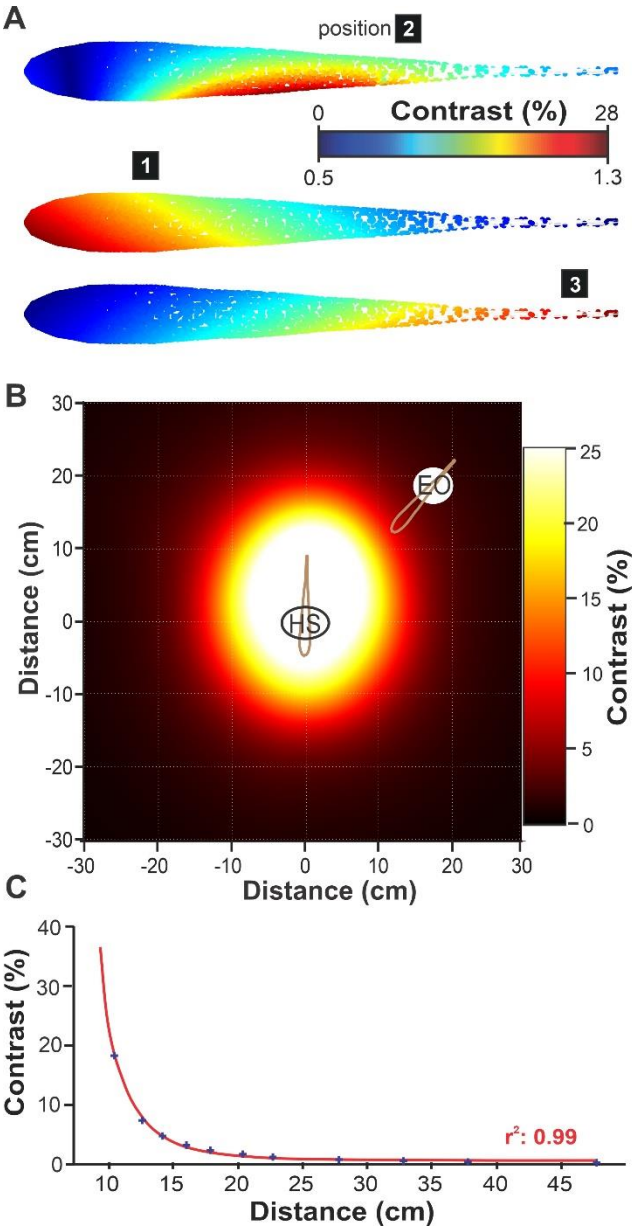

Figure 3: EI strength as a function of relative position of the two fish. A. The strength of the EI from the sender was calculated for each receptor position. It is displayed here for the 3 relative fish positions illustrated in Figure 1 (note the difference in color scale for position 2 vs 1 and 3). The focal fish are presented here from a top perspective. **B.** The strength of the electric image is characterized as a function of distance and azimuth. The EI for 864 relative positions (12 distances x 72 azimuths) was calculated and the strength of the signal in the "hot spot" (HS; taken as the average of the 5% most strongly activated receptors) is depicted by the color scale. The position of the sender fish for position is based on the center of the EO and the data points have been repositioned to reflect the distance between the center of the HS on the focal fish and the EO of the sender rather than the center of the focal fish. The EI strength values (contrast %) have been interpolated between data points. **C.** Average contrast values in the HS across azimuth and for fish displayed as a function of the distance between the

hot spot and EO centers. The relationship follows a cubic power law (red best fit curve: $c=1.6\cdot10^{4}\cdot x^{-3}$).

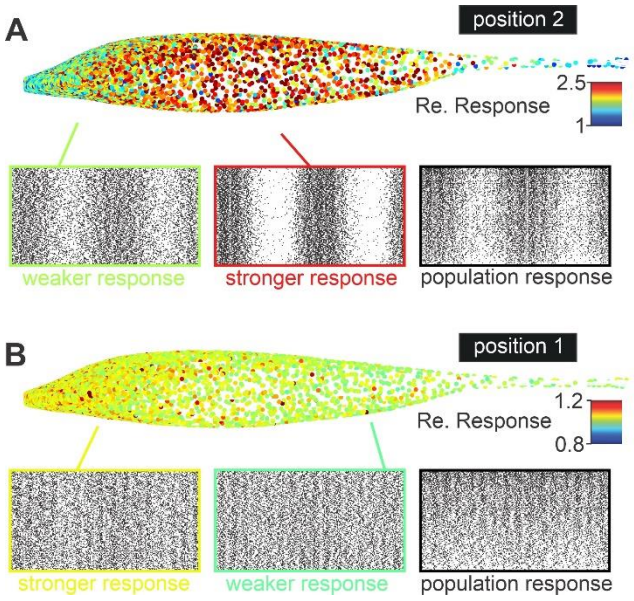

Figure 4: Heterogeneous population response in modelled receptors. A. LIF models with heterogeneous response properties were stimulated with realistic inputs that match the spatio-temporal structure of conspecific signals. In the color map (top), each receptor's response is quantified as the peak-to-trough firing rate modulation and normalized relative to spontaneous modulations in firing rate occurring when no second fish is present (i.e., a relative response of 1 reflects modulations in firing rate similar to spontaneous activity). The two raster plot insets on the left show the response patterns of two individual neurons from portions of the fish's body that are more or less strongly stimulated. The raster plot on the right shows the population response: we show a stack of 800 randomly selected receptor responses ordered from weakest peak-to-trough responses (bottom) to strongest responses (top). **B.** We display the same elements as in panel A. but the position of the sender fish is more distant (position 1 of Figure 1) compared to nearby relative position used in A. (position 2 from Figure 1).

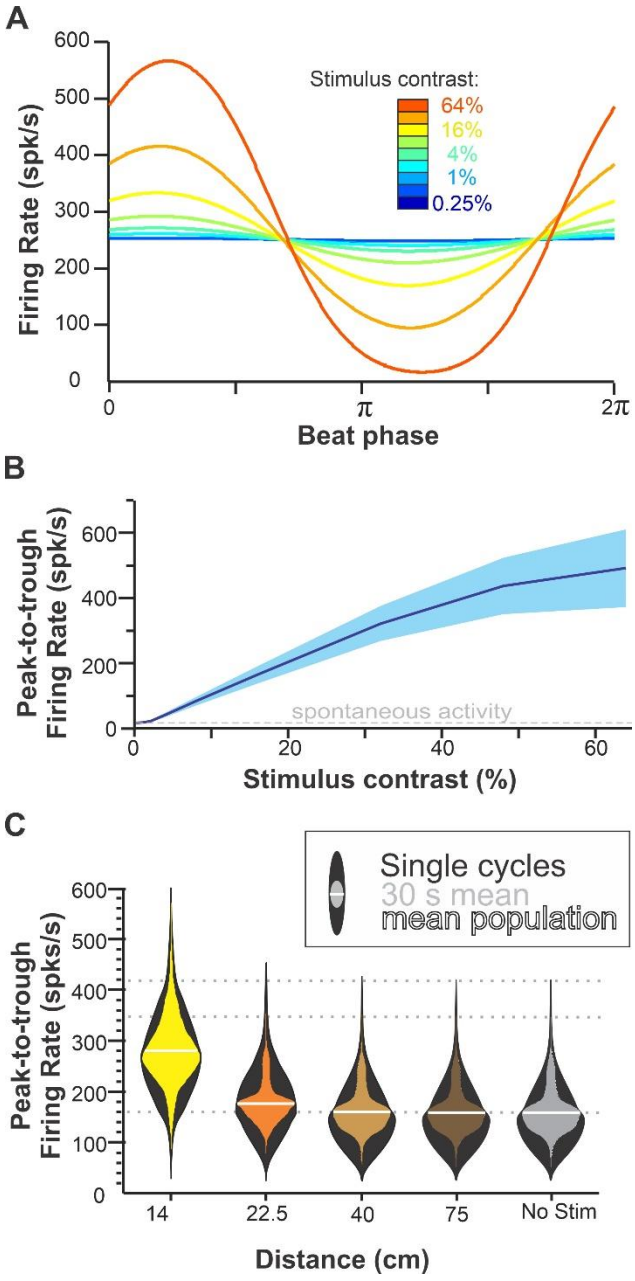

Figure 5: Sensitivity of the receptor model replicates responses to beat stimuli. A. Mean firing rate (averaged across all receptors) during a single cycle of a 30 Hz AM beat stimulus for different contrast intensity. The model produced modulations in firing of just a few spikes/s peak-to-through for the weakest intensities and of a few hundred spikes/s for the stronger intensities. **B.** F-I curves display the strength of the response as a function of the stimulus intensity (mean across the population ± s.d.). Average peak-to-through firing rate quantified in a similar way but during spontaneous activity (no sender fish) is display (grey dashed line) and we can see that for the weakest stimuli the average response is similar to spontaneous activity. Response sensitivity has been calibrated to match published data (Bastian, 1981; Nelson et al., 1997; see also Methods and Supplementary Figure S1). **C.** The distribution of responses strength across the population of receptors is displayed for sender fish positioned at different distances (azimuth 90º). The outer distributions (black violin plots) show the variability of peak-to-through firing rate on single cycles of the beat for single neurons. The inner

distributions (colored violin plots) show the variability across neurons but for each neuron peak-to-trough firing rate is averaged across the whole stimulus (900 cycles, 30 s). The mean of this distribution (i.e., also averaged across neurons) is displayed as a white line. Dotted grid lines (in grey) are provided in the background to help notice minute differences in the distributions. The fact that only subtle differences between the distributions for stimuli at distances of 40 cm or more compared to responses in the absence of second fish highlights the difficulty in detecting these distant signals.

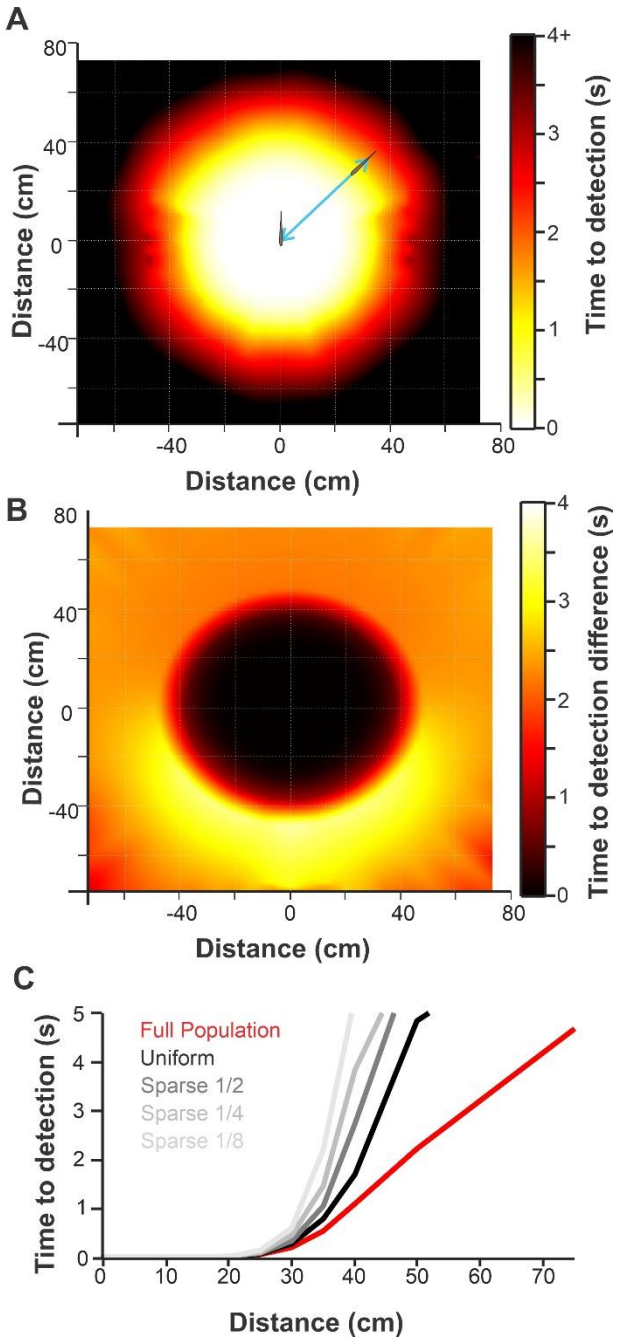

Figure 6: Estimates of detection sensitivity as a function of relative fish position and the influence of receptor density distribution. A. Detection sensitivity is quantified as the time it would take to reliably detect the presence of the sender's signal and is displayed as a function of the relative position of the sender. For each position (12 distances x 72 azimuth) the peak-to-trough responses of the population are compared to spontaneous responses. As peak-to-trough is averaged across cycles of the beat (increased time to detection), detection becomes more reliable because noise is averaged out. We display the stimulation time required for our decoder to reach reliable detection (<5% error; see Methods for more details). Each position is defined by the distance and azimuth between the center of the receptor positions in the focal fish and the center of the EO in the sender fish. Values for each data point are then interpolated across space to obtain the smoothly varying color plots. **B.** Decrease in detection sensitivity (increased time to detection) caused by reducing the density of receptors in dense areas (i.e., making it uniformly low like the

density in the caudal portion of the body). The decrease in density makes uniformly no difference nearby (black region). It uniformly increases time to detection when the sender is very distant (distant black area in panel A). It has a most pronounced effect at mid distance (40-50 cm) in the frontal azimuth (yellow area) where time to detection increases from 1-2 s to 2-6 s (see also Supplementary Figure S3) showing that the rostral high density of receptors can increase detection sensitivity in the frontal quadrant. C. The overall detection sensitivity (time to detection averaged across azimuth) decreased markedly at distances above 30 cm when receptor density is made uniformly low (black line compared to red line) and decreases further when receptor density is made even sparser (1/2, 1/4 or 1/8 the size of the uniform population; grey curves).

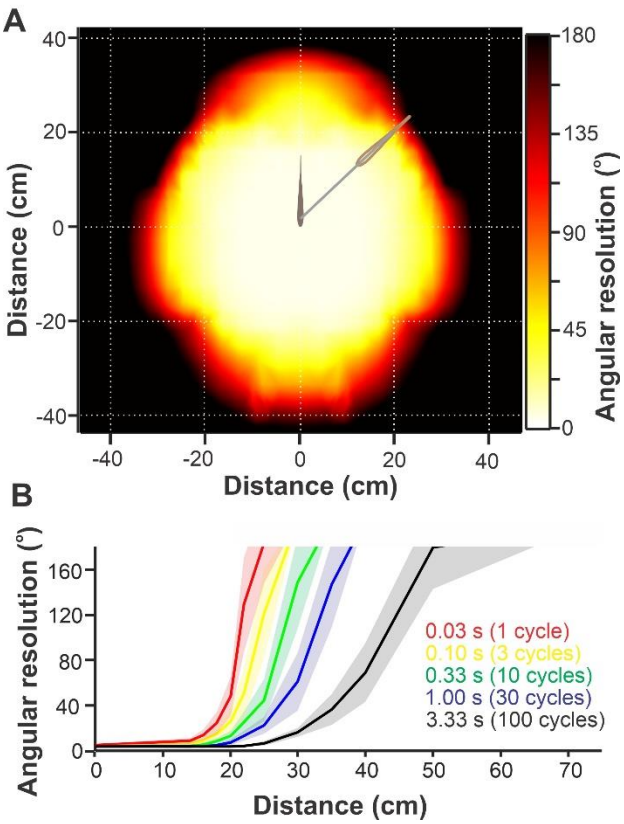

Figure 7: Estimates of angular resolution supported by the receptors' response accuracy. A. Angular resolution estimated as a function of distance and azimuth of the sender. The analysis is based on the average peak-to-trough firing rate (30 cycles average, i.e., 1 s) of each receptor for a given stimulus location. Population responses for a sender at a given test azimuth was compared, by our decoder, to responses for a sender at various angular displacement (clock-wise or counter-clock-wise; distance kept fixed). The smallest angle that allows 95% accurate discrimination between the responses was taken as the angular resolution. Failure to discriminate responses for stimuli locations 180º apart (black regions on the graph) indicates an inability to localize reliably the azimuth of the sender's location. Data points for 72 test azimuths and 12 distances (i.e., 864 positions) were generated, taking the center of receptors location for the focal fish and the center of the EO for the sender fish as position values. Data values are then interpolated to obtain the smoothly varying color plot. **B.** The angular resolution (mean ± s.d. across azimuth) can be calculated based on peak-to-trough responses of the receptors to a single cycle of the stimulus or on the peak-to-trough averaged across several cycles. Averaging the response across cycles corresponds to a decoder that integrates the response across time to get a more accurate estimate of response strength. Consequently, angular resolution

improves as the decoder integrates across more time, but in all cases we still see a sharp change in resolution from very accurate (e.g., at distances below 20 cm) to very poor (e.g., above 50 cm).

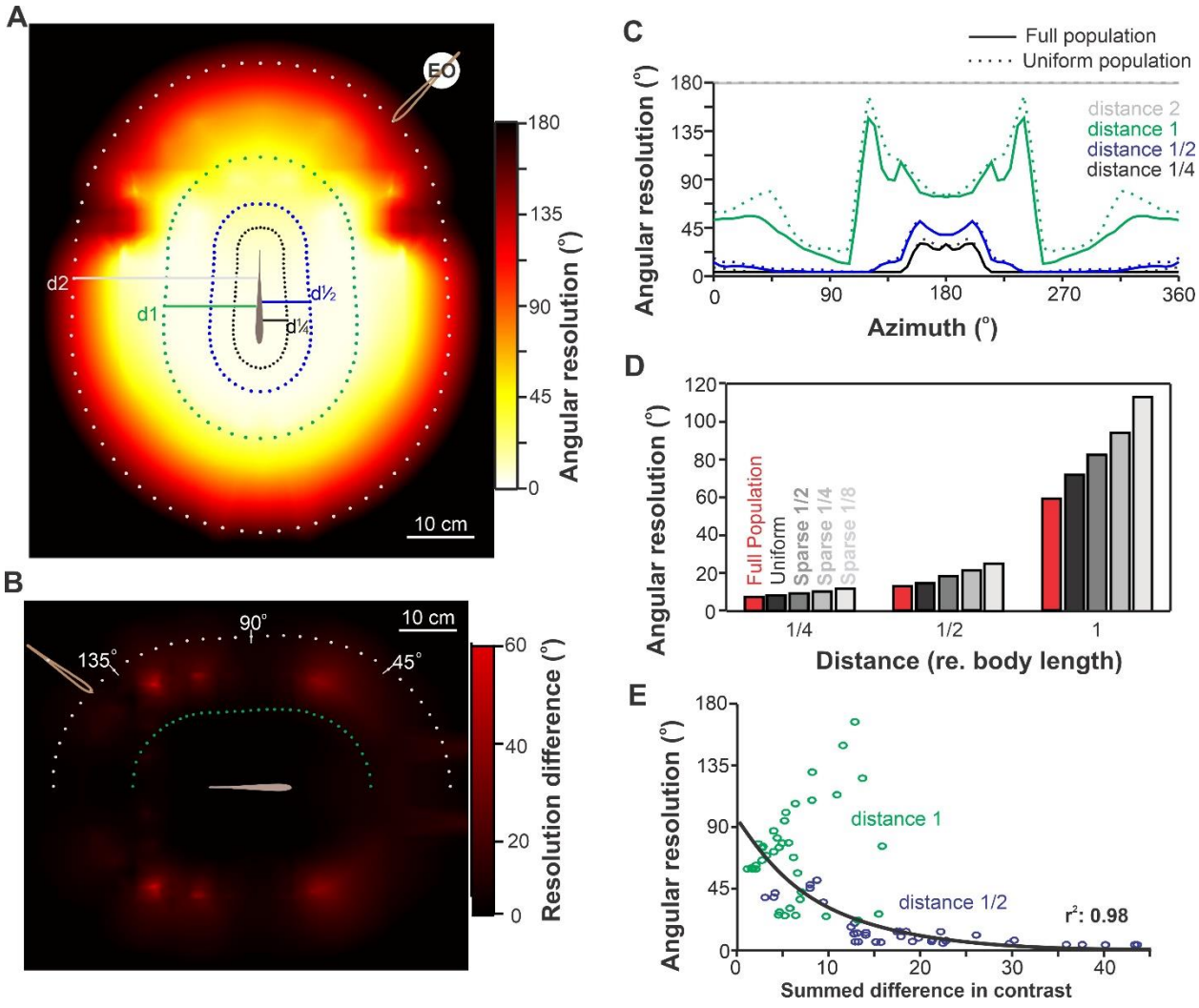

Figure 8: Receptor density and angular resolution as a function of azimuth. A. Angular resolution for a sender fish at various positions around the focal fish was calculated as in Figure 7, but the way distance is normalized across angles is different. We still compare, with our decoder, positions at different angles while keeping the distance equal. Here distance is set by the distance between the rostral tip of the sender and the closest point on the surface of the focal fish. The fish are thus separated by a fixed gap set to 1/4, 1/2, 1 or 2 body lengths (i.e., 3.5, 7, 14 and 28 cm respectively). In Figure 7, the gap between the fish was not consistent across azimuth since the distance was set between the center of receptor locations in the focal

fish and the center of the EO in the sender. For example, the rostral tip of the sender was closer to the skin of the receiver when it was at 180º than when it was at 0º. The positions of the rostral tip of the sender, for the 72 angles and 4 distances, are marked with dots on this figure. Datapoints for various positions are still mapped on the color graph at the position of the middle of the EOD of the sender and the color gradient interpolated between datapoints. **B.** Decreasing the density of receptors in dense areas (i.e., making receptor density uniformly as low as density in the caudal portion of the body) causes decreases in angular resolution. This resolution decrease is strongest in the red area of the graph. We note that this decrease is relatively limited and not concentrated in the frontal quadrant. **C.** Angular resolution as a function of azimuth, distance and receptor density. This is the same data used to generate panels A and B but shown here in 2D. The change in resolution as a function of azimuth is clearly visible even when receptor density is uniform across the body **D.** Angular resolution averaged across azimuths for different receptor density patterns. The full population is compared to a uniform lower density population or to populations made even sparser (1/2, 1/4 or 1/8 the uniform population). Decreasing the receptor density decreases angular resolution. **E.** Changes in EI for small angular displacements (averaged across 5°, 10° and 15° displacements) are compared across azimuth and related to the angular resolution of the system. For a given displacement, the difference in EI was characterized by integrating the difference in EI strength across the body surface. This EI difference was calculated for various azimuth and at the 2 distances (1 or 1/2 body length apart) that give medium angular resolutions. We show that the EI difference correlates with angular resolution with an exponential relationship (black best-fit curve, r^2=0.98).

Supplementary Information

Table S1: Model parameters used for the prototypic seed neuron (see Methods for details).

Description	Name	Value	Description	Name	Value
Membrane time constant (s)	τ_m	$15 \cdot 10^{-4}$	Noise strength (A)	A_σ	$15 \cdot 10^{-9}$
Lean reversal potential (V)	E_m	$-70 \cdot 10^{-3}$	Adaptation reversal potential (V)	E_α	$-80 \cdot 10^{-3}$
Membrane resistance (Ω)	R_m	$15 \cdot 10^{5}$	Adaptation increment (V)	Δ_α	$14.5 \cdot 10^{-8}$
Spiking threshold (V)	V_T	$-49 \cdot 10^{-3}$	Adaptation time constant (s)	τ_α	$50 \cdot 10^{-3}$
Reset potential (V)	V_R	$-70 \cdot 10^{-3}$	EOD amplitude (A)	A_{EOD}	$1.7 \cdot 10^{-7}$
Refractory period (s)	t_R	$9 \cdot 10^{-4}$	EOD baseline bias (A)	β	$3 \cdot 10^{-8}$

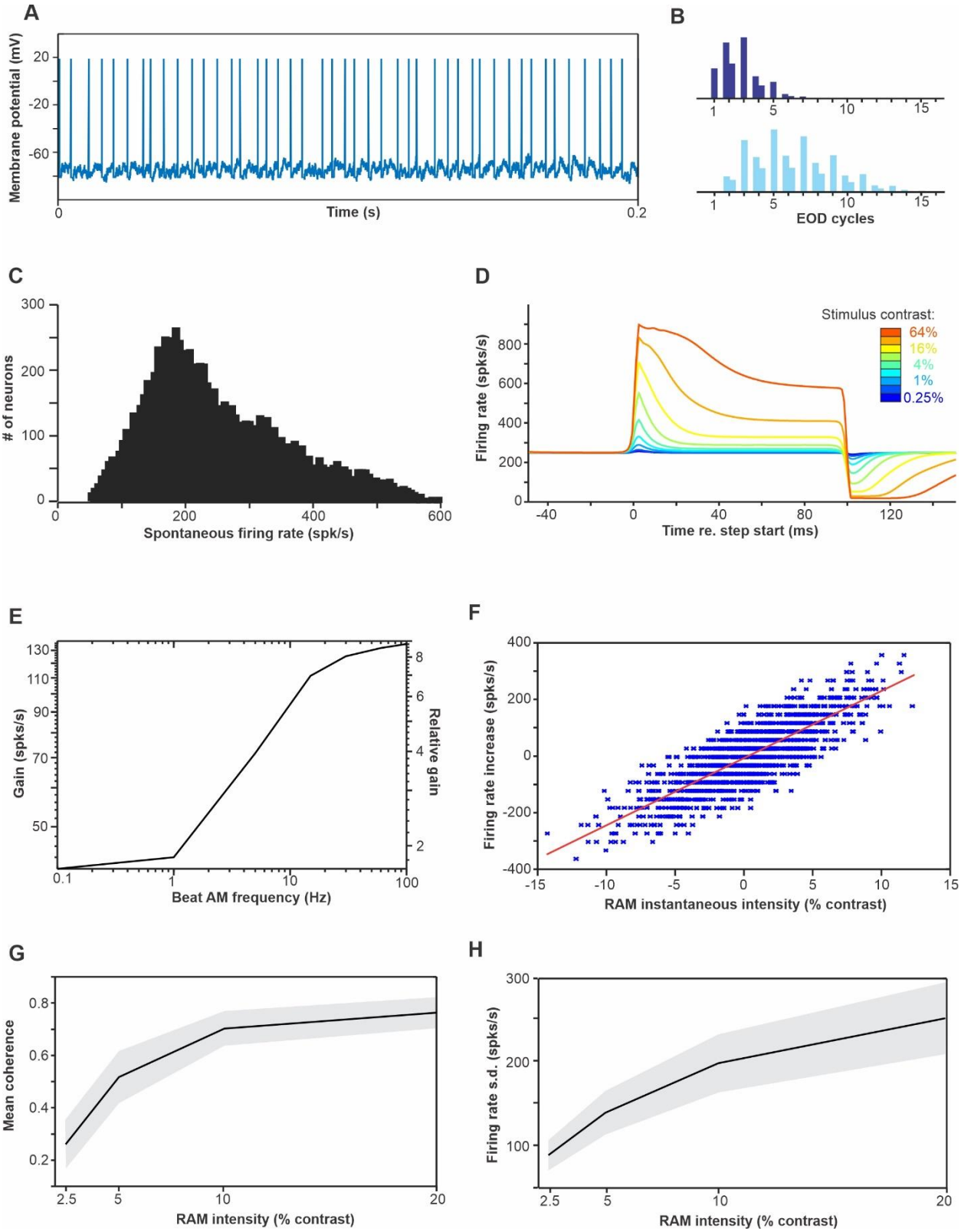
A
Membrane potential (mV)
20
-20
-60
0
Time (s)
0.2
B
1
5
10
15
1
5
10
15
EOD cycles
C
# of neurons
300
200
100
0
0
200
400
600
Spontaneous firing rate (spk/s)
D
Firing rate (spks/s)
800
600
400
200
0
Stimulus contrast:
64%
16%
4%
1%
0.25%
-40
0
40
80
120
Time re. step start (ms)
E
Gain (spks/s)
130
110
90
70
50
Relative gain
8
6
4
2
0.1
1
10
100
Beat AM frequency (Hz)
F
Firing rate increase (spks/s)
400
200
0
-200
-400
-15
-10
-5
0
5
10
15
RAM instantaneous intensity (% contrast)
G
Mean coherence
0.8
0.6
0.4
0.2
2.5
5
10
20
RAM intensity (% contrast)
H
Firing rate s.d. (spks/s)
300
200
100
2.5
5
10
20
RAM intensity (% contrast)

Figure S1: Average response properties of the heterogeneous population of modeled receptors.

A. Example of the membrane potential and spiking pattern of a model response (spontaneous activity). **B.** Inter-spike interval histogram of 2 different model neurons (spontaneous activity) showing phase locking to the EOD period and different firing tendencies. Note that the x-axis is expressed in multiples of the EOD period but since we used an EOD frequency of 1,000 Hz for simplicity, this also corresponds to ms. **C.** Distribution of spontaneous firing rate across our entire population. This distribution was achieved by selecting 26 seed neurons with firing rates unevenly distributed along this range and diversifying model parameters based on these seeds (see Methods). This range and distribution replicates published data (Bastian, 1981; Grewe et al., 2017; Ratnam & Nelson, 2000). In particular, the mean spontaneous firing rate was 251 spk/s with a CV of 0.45. **D.** Responses to step increases in EOD intensity. The strength of the peak response, the steady-state response, and the adaptation time course was matched to published data (Benda et al., 2005). **E.** Response gain to beat stimuli of different AM frequencies. Although we did not explore systematically the response of our model at different beat frequencies in the results section, we calculated the gain for a range of AM frequencies. This analysis helps us to evaluate the sensitivity of the neurons (see the absolute scale on the left) and it also helps to assert that the adaptation dynamic replicates some of the tuning properties of the neurons (see the relative scale on the right; gain for an AM of 1 Hz is normalized to 1). This average gain curve is comparable to experimental data (Chacron et al., 2005; M. E. Nelson et al., 1997). **F.** Relative firing rate during random amplitude modulations. We replicated a published analysis of receptors sensitivity

(Gussin et al., 2007a) that measure the relative firing rate (relative to average) in successive 32 ms windows during the response to a low frequency (0 to 4 Hz) random amplitude modulation. We note that our scale is different than theirs: our ± 5% values correspond to the absolute contrast of the stimulus (i.e., s.d. of 10% contrast) whereas the scale in their Fig 3 has ± 50% being the min-to-max of their 10% contrast stimulus. When converted to the same scale, we find a gain slope of 23.7 spk/s/% (± 5.8 s.d.) comparable to the 17.7 spk/s/% (range 3.2 to 40.2) they found. **G.** Mean coherence at 10-30 Hz for random amplitude modulations (0-100 Hz) of different overall intensities (contrast). We qualitatively matched the coherence to values found in previous publications (Chacron et al., 2005; Grewe et al., 2017). **H.** Firing rate modulation in response to random amplitude modulations (0-300 Hz). We replicated the analysis in Grewe et al. (2017; see their figure S1A) that plots the standard deviation of the response (averaged over trials) as a function of stimulus contrast. Their population averages go from approximately 100 spk/s for 2.5% contrast to 200 spk/s at 20% contrast with a large variability among the population; we have a population average between 90 spk/s and 250 spk/s respectively.

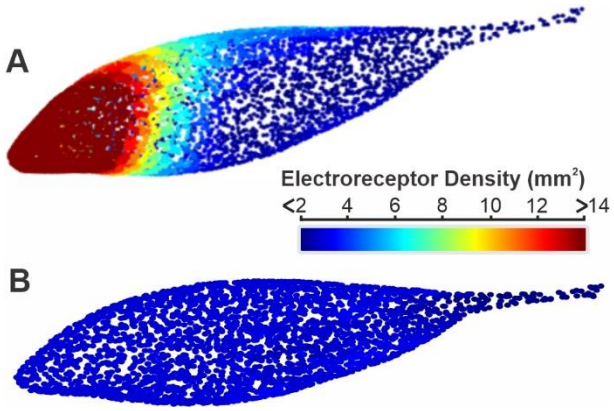

Figure S2: Receptor density compared between our full population (A) and our uniformly low-density population (B). Each dot shows the position of a receptor and the color reflects the density of the receptor at this location. The uniform population was created by selecting, for each face of the mesh model, a subset of receptors from the full population to match the density of 2 receptors per mm^2.

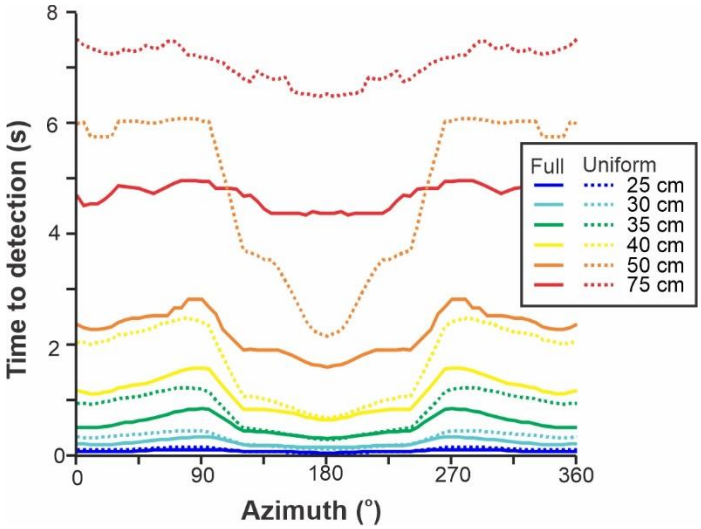

Figure S3: Detection performance as a function of source location and receptor structure. We compare a full population of receptors that includes a high density in rostral regions with a population that has a uniform density across the body matching the low density of the caudal region of the body (see Figure S2B). We present here the results for distances above 25 cm where we can see differences across azimuth and population structures. Our decoder considers that the response strength of receptors can be integrated across time and thus more noisy, weak responses require integration across longer periods to reach a reliable detection performance. We plot here the integration time required for our decoder to reach 95% detection accuracy and plot this here as a function of stimulus location.

Chapter 3

Prologue

In the previous chapter, I characterized the structure of the signal reaching the fish and the response of the receptors. I also calculated the detection and localization accuracy. In the above case, the stimuli were from a stationary fish i.e., no movement involved. However, in the natural environment, free movement contributes to creating a more dynamic sensory problem for the fish. Therefore, to further understand how the sensory signal can guide behavior we first need to characterize the movement patterns characteristic of social interactions. Here I characterize the movement pattern during agnostic encounters and delineate the movement sequences these fish display.

This chapter will be included in a publication that will be submitted as *"Ramachandra, K. L., Sophia Keith & Marsat, G. (2023). Movement patterns during social interactions in Ghost Knifefish."*

My contribution to this paper represents the majority of the content: Ramachandra and Marsat designed the experiments, Ramachandra performed the experiments with help from Keith, Ramachandra analyzed the data, and Ramachandra wrote the paper with help from Marsat.

Abstract

Despite behavior being very variable, we can typically decompose it in sequences of stereotyped movements and we can identify distinct categories of motor patterns. Interaction occurring during conflict is one of the most common types of social interaction that ethologists have focused on. For a given species, conflict resolution typically follows a specific progression allowing each individual to assess their relative capacity. Weakly electric fish is an important model system used to better understand sensory processing and the evolution of signaling. Although we have numerous reports on the communication underlying agonistic encounters in these fish, no systematic description of the physical interactions taking place are available. Here we aimed to provide a thorough characterization of the distinct movement patterns observed during agonistic encounters. To do so we performed behavioral recording of pairs of fish placed in a variety of situations. We identified nine categories of movements and show that specific sequences of these behavior are displayed by the fish. Our results indicate that conflict resolution in these fish follows a cumulative assessment strategy where distinct aggressive moves are produced in a variable sequence. This study provides a strong framework to delineate how agonistic interactions unfold in these fish and can serve as the foundation to provide a quantitative understanding of the signals experienced during these behavior and how sensory processing can support targeted actions.

Introduction

Behavior is the result of complex motor and decision-making process that make it inherently very variable. Nevertheless, we can often categorize behavior in distinct sequences or identify stereotyped movement patterns that occur in succession to constitute behavioral responses. This is true of a simpler invertebrate system, a fly for example that produces stereotyped grooming movement, alternating the grooming of different body parts (Mueller et al., 2021). It is also true of vertebrates, for example, courtship in bowerbirds consists of a repertoire of moves and signals that are produced in a variable order (Mitoyen et al., 2019; Patricelli et al., 2002). Another illustration of this fact comes from agonistic interactions in red deer that follow a strict sequence of stereotyped displays (Clutton-Brock et al., 1979). An important step in understanding animal behavior is to identify these distinct behavioral patterns and reveal how these patterns are stringed into specific predictable sequences. The classical ethogram approach has been instrumental in clarifying how sequences of motor patterns are assembled into complex behaviors. In this paper, we aim to better understand the sequences of movements occurring during agonistic encounters in gymnotiform weakly electric fish.

Weakly electric fish are nocturnal and live in muddy, turbid water which makes vision rather ineffective to guide navigation. To overcome this issue these fish evolved an electric organ that runs along the caudal portion of the fish (Baker et al., 2013). In *Apteronotus*, the species studied in this study, the electric organ produces a constant semi-sinusoidal wave of electricity for the entirety of the fish life called the electric organ discharge or EOD(Bullock et al., 1986; Maler, 2007). The distortions in the fish EOD caused by objects and animals allow the

fish to map its environment. Weakly electric fish thereby possess an active electrosense where the EOD (Lissmann, 1951), and its environment-imposed distortions, is perceived by electroreceptors on the skin. Anything in their environment that is more or less resistive than water will cause a distortion of this electric field and cast an “electric shadow” (Rasnow, 1996) on the sensory surface. The ability of the fish to navigate and locate prey based on the electrosense is well characterized (Nelson et al., 1999; Postlethwaite et al., 2009; Stamper et al., 2012; Von Der Emde et al., 1998). They also rely heavily on this electrosense when interacting with conspecifics to identify, communicate and locate each other (Kolodziejski et al., 2007; Zakon et al., 2002; Zupanc et al., 2006). During social interaction, the spatially diffuse electric fields of each weakly electric fish combine in the water. Due to the changing phase relationship of the two EOD, the combined signal contains amplitude modulations known as the "beat” (Heiligenberg, 1975). Because the beat signal results from the presence of a conspecific, it carries information about a conspecific’s location, for example, the signal will be strong on the side where the other individual is located. Lab and field studies show that weakly electric fish can leverage the spatial cues in the signal to localize a conspecific. A field study by Henninger and colleagues used grids of electrodes placed in river streams and creeks to triangulate and track individuals in their natural environment over long periods of time (Henninger et al., 2018). This study details the range of detection of conspecifics via this electrosense and their data suggests that weakly electric fish routinely communicate with each other over distances of up to 30 cm, while also revealing that two fish can detect and localize a conspecific at distances of 1 meter or more. For example, they documented a resident fish-initiated attack towards an intruder located 1.7 meter away.

In this paper, we focus on agonistic social interactions. During such interactions, they perform precisely coordinated maneuvers relative to one another. For example, the fish chase each other at high speed in the dark. The task appears simple however requires precise and rapid localization of the other individual based on the electrosensory signal. Casual observations of fish interacting allow us to appreciate how navigation guided by this electrosense permits rapid and accurate movements but we do not have a systematic characterization of the kinematic of interacting fish. Understanding the kinematic of interacting fish is important to understand the spatiotemporal structure of the signal and the cues used to localize conspecifics. Understanding the structure of stereotyped and behaviorally relevant behavior can help understand how signals are processed. For example, a study on stereotyped movement in hoverflies shows how spatial information from the retinal flow reflected an active sensing strategy to enhance spatial processing (Geurten et al., 2010). We have only casual observations of such stereotyped behavior in interacting fish (e.g., chases, lunges…) but we lack a systematic understanding of the kinematic occurring during social behaviors.

In this paper, we recorded the interaction of pairs of fish and categorized movement patterns and their sequence. We identified nine distinct patterns of movement and our results show that they are sequenced in specific order during agonistic interactions. We conclude that agonistic interactions in knifefish is consistent with the cumulative assessment model of conflict resolution. This data allows us to better understand the dynamic of conflict in these fish. Also, the detailed characterization of relative movement patterns will allow a quantitative description of the sensory signals that underlie the perception of conspecifics and thus directed movements. This study is thus fundamental, not only because it characterizes a key behavior in

this important model system but because it serves as an essential prerequisite to clarifying how sensory processing supports behavior.

.

Methods

Animals and Housing

Wild-caught fish *Apteronotus leptorhynchus* were obtained from commercial fish suppliers. The water was maintained at 27^{o}C and a conductivity of 200-300 µS and the room was subject to a reverse light cycle. The sex and age of the fish cannot be determined from visual inspection. A given fish was never tested more often than once a day. Animal care and experimental protocols were approved by West Virginia University IACUC.

Behavioral Paradigm

In order to get data on social interactions, fish were placed in a range of situations (experiment 1a-c, see figure 1) where they interact with each other. We note that due to the limits of the laboratory setting, we cannot consider all possible stereotyped movements that these fish might exhibit in the wild, for example during courtship. Our analysis will focus on agonistic and inquisitive behaviors routinely displayed in the lab. The fish were placed in the experimental tanks 100 x 100 cm with an open octagonal area. The water was kept at the similar conditions to the housing tanks. The chasing behavior was filmed using a video camera (Allied Vision, MantaG-4719B NIR) in IR light and recording occurred at their peak active period shortly after lights are turned off for the day. Videos were captured at 30 frames per second with a spatial resolution of 2033 x 2022 pixels. A single camera was sufficient to capture the relevant movement patterns (i.e., 2D motion) because these fish are typically bottom dwellers and thus the vast majority of their movement can accurately be described in 2D. We intervened if the interaction became aggressive to the point where they could be harmed if they continued.

Experiment 1a: Resident-intruder scenario. These fish will compete over the best shelters (Fugère et al., 2011). A fish was introduced into the experimental tank a day (~24 hrs.) before the start of the experiment to fully explore the experimental arena. A single shelter is placed in the center of the tank: a clear plastic tube where the fish are used to hiding Once the resident fish was habituated, an intruder fish was introduced. The recordings captured the first 20 minutes of interactions where the probability of interactions was highest.

Experiment 1b: Competition over food. Social interactions can also occur when foraging for food. Two fish were housed in separate enclosed areas in opposite corners of the experimental tank. For the training, each fish was let out of their area individually, and food - just enough to feed one fish- was placed at the center of the tank. The fish were free to swim and explore until they found the food. The training phase continued until the fish were able to go towards the feeder as soon as the shelter door was open (up to 10 days for some experiments). Once both the fish had successfully learned the task they were allowed to come out of the feeder at the same time and this forced the fish to interact. Each trial lasted only 5 minutes as after 5 minutes the fish for the majority of the time were uninterested in each other and were seen exploring corners of the tank.

Experiment 1c: Targeted investigation. The presence of an unknown neighboring fish can elicit investigative social interactions. Both fish were placed at the same time in a mesh enclosing so that they can sense and locate each other. The fish were placed at various positions relative to one another. Once they are habituated for 15 min, the focal fish was allowed out of the enclosure to go investigate its neighbor. The focal fish was allowed to

explore for 2 minutes before the other fish was let out of the arena and their interactions were recorded for an additional 5 minutes.

Analysis

Video Tracking

From the behavioral recordings, we tracked the animal's position (center of the body, head, and tail) based on the contrast between the light background and dark fish body using a custom-written semi-automatic tracking program in MATLAB (2019a, MathWorks). We tested several automatic tracking software available for tracking multiple animals (Mathis et al., 2018; Nath et al., 2019; Pereira et al., 2019; Walter & Couzin, 2021) however due to the unique swimming patterns and tail flicks which caused higher motion blur the available software were unable to reliably track the fish. Hence, we developed our own tracking system. The tracking algorithm first creates a mean image from the majority of the frames to establish a background that we subtracted from each frame to get only the fish in the frame and remove the rest of the tank and accessories. To determine the position of the fish the centroid was calculated from the extracted shape of the fish. Given that the head of the fish has a larger area compared to the tail, by comparing the areas, the bulkier area was assigned as a head and the other as a tail. If for some reason the fish was obstructed from view for a few frames, the position in the surrounding frames was used to interpolate the position. There were also instances where the fish get very close which could lead to the swapping of identities between the fish. Such instances were flagged automatically and an experimenter visually confirmed tracking and manually corrected any discrepancies.

Once the coordinates of the fish were calculated, we determined the absolute and relative kinematics of interest (relative azimuth, heading, speed, and distance between fish). The distance between the fish was calculated as a simple Euclidian distance between the two centroids of the fish. To calculate the speed, we calculated the distance the fish traveled between successive frames. The heading angle was calculated as the angle between the centroid of the fish and the head of the fish. While the relative azimuth is calculated as the difference between the heading of the second fish and the angle between the centers of the two fish.

Identification of Behaviors

We tested several quantitative ways to delineate and identify different movement patterns (see Results) but we also performed visual inspection to establish the different behavior categories and mark each video with a moment-by-moment description of the movement pattern the fish are performing. Pattern identification by humans is still a very powerful way to qualitatively describe behavior and this traditional method has been used successfully in numerous studies (MacNulty et al., 2007; Mas-Muñoz et al., 2011; Xu et al., 2012). Four experimenters were involved in visual inspection of the recordings and the videos were marked by at least two experimenters to confirm that marking was consistent across experimenters. Since we found very little discrepancy, we are confident that the results are accurate.

We identified nine unique behavioral movement patterns. For each behavior, the start and stop time and the movement pattern label were noted in order to create a continuous frame-by-frame commentary of the video. The distance between the fish and the position of

one fish with respect to the other played an important role in labeling some of the behavior. If the fish were far away from each other or the fish were swimming without interacting we categorize them as *"passive avoidance"*: the fish avoided each other by being stationary or swimming slowly in separate portions of the tank. *"Active avoidance"* occurs when both fish are swimming close to each other but avoiding directly coming into the path of the other fish or one fish is stationary and the other fish is swimming close to the stationary fish but actively making sure not to get to close to the fish. *"Approach"*, in which one fish actively swims towards the other fish and usually results in one of the aggressive behaviors. *"Recede"* is when one or both fish move away from each other. These four are referred to as general movement patterns and we also identified several patterns more specifically associated with agonistic interactions. A few chasing behaviors were identified. *"Linear chase"* is very common and consists of one fish chasing another fish from behind in a linear trajectory over a certain distance and at high speed. A *"Circular chase"* occurred when both the fish were involved in a circular trajectory. The trajectory could be turns always in the same sense or sequences of mixed left and right turns. *"Failed chases"* occur when one fish starts to pursue another fish, but it ends before there is a sequence where it follows the fish over a distance. *"Mouth wrestling"*, in which the fish fought face to face pushing and biting each other keeping their mouth open a significant portion of the time. Contrary to mouth wrestling patterns in other fish, there rarely were sequences with the fish grabbing each-other by the mouth and wrestling that way. Nevertheless, the behavior has enough similarities with mouth wrestling in these other species that we felt it was appropriate to label it that way. Finally, *"Bite/lunge"* is defined as when the aggressive fish lunges to bite usually the tail or midbody of the other fish.

Transition matrix

We calculated the probability of transition from one behavior to another as a conditional probability problem that was normalized relative to the probability that happened in no preferred sequence. The probability was calculated as *Relative Probability* = $P_{(2nd|1st)}$ / P_{2nd*} were $P_{(2nd|1st)}$ is the conditional probability that behavior *2* follows behavior *1* and P_{2nd*} is the probability of behavior *2* among all behaviors except behavior *1*. We calculated a confidence interval by shuffling the sequence of behaviors in each video and calculated again the relative probability for each sequence. We took a 95% upper and lower threshold given this distribution of randomly sequenced relative probabilities. Relative probabilities above or below these thresholds are marked as significantly different from chance.

EI model

The electric image used in this study was based on the established methods developed by Caputi and Budelli (Caputi et al., 1998; Caputi & Budelli, 1995) and implemented using software developed by Rother (Rother et al., 2003). More information can be found in these publications and in a previous paper where we adapted and used this electric image model (Ramachandra et al, 2023).

Results

Behavioral scenarios and movement tracking

We aimed to capture a diversity of interaction patterns by setting up pairs of fish in different scenarios. We have not explored the wide range of behaviors that could be observed in natural conditions, for example, courtship, and focused on a category easy to replicate in the laboratory. Specifically, we placed fish that are in non-breeding conditions, in a large arena in situations where they encountered an unfamiliar conspecific of either sex. Three scenarios were established to stimulate the fish to interact (Figure 1; see methods): 1-resident-intruder, 2- competition of a resource (food), and 3- targeted investigation. While we were able to capture 40 hrs. of interactions, 15 hrs. of recording during these experiments (n=25 fish pairs) consisted of the fish being passively in their own space and were not analyzed. These fish are typically bottom dwellers and the vast majority of their movements can be captured through a 2D characterization. Even if the behavioral recording where limited to 2D video (1 camera from the top) automatic tracking with available software did not provide reliable results due to the movement patterns unique to these fish (e.g., swimming backwards and laterally) and to the fact that two fish coming together were often mislabeled as one-another. We devised our own automatic tracking software (Figure 2) that included a manual validation step: bouts of movement where tracking accuracy was expected to be prone to errors (e.g., fish come together and there is uncertainty about which fish continues to which trajectory) was flagged. Visual confirmation and manual adjustments could then be implemented where needed. As a result, tracking is rapid, accurate, and requires minimal human intervention. The algorithm determines the “center of mass” of each fish, their rostral and caudal extremity (curvature can

be calculated), and their heading angle for each frame. This software is now publicly available (Supplementary Information) and might particularly benefit research on these fish with unique movement patterns. From these position data, we calculated a wide range of parameters that could have been useful to characterize the movement patterns of one focal fish relative to the other: distance, azimuth, relative heading angle, speed (relative or absolute), and the relative direction of movement. The time-course of these values, or their variability in small time windows, was used as input to our movement patterns analyses.

Movement patterns

One of our main goals was to identify recurring movement patterns that these fish employ when interacting with one another. Indeed, casual observations of fish interacting suggest that stereotyped movement patterns can occur. Chases for example are striking example of common behavior that seem to consist of specific relative movement (one fish behind the other chasing it at high speed and close distance). We thus hypothesized that relative movement data would form clusters reflecting a set of stereotyped movement patterns such as chasing. We used different approaches to categorize movement patterns. A classical qualitative approach (see methods) involved the experimenters visually classifying movement patterns and marking moment-by-moment interactions. We also implemented quantitative approaches to clustering movements to automatically identify stereotyped patterns and score the behavioral recordings.

We identified 9 types of movement during our qualitative analysis (Figure 3). Some of these movement patterns can be further divided based on the role of each fish in the behavior when the behavior is asymmetrical. For example, chases could be subdivided and chasing or

being chased. We will consider these subdivisions below and first focus on the 9 broad categories of movement behaviors (see supplemental video). Three of the kinetic measurement were most useful to characterize the relative movements: absolute speed, relative distance, and relative azimuth. These measures consider a focal fish which, in this analysis, was taken as the fish initiating the behavior (e.g., chaser rather than chasee).

Several of the identified behaviors consist of simple movements of the fish relative to one another. The most common behavior was passive avoidance where the fish avoided each other by either being stationary or swimming slowly in the opposite ends of the tank. We observe this behavior over 65% of the time in the recordings. We defined it as an active avoidance situation where the fish are closer to each other and actively swimming but avoiding coming directly next to each other. We also observe a bout where one fish came directly towards the other (approach) or away (recede). When the fish are interacting more dynamically, we identified 4 main behaviors. Linear chases are common types of interactions in which one fish is located behind another and is chasing the other along a linear path. Sometimes behaviors that looked like chases failed to proceed to a full-fledged chase. Chases could also include numerous twists and turns and are designated as circular chases. Brown ghost often open their mouth and/or perform biting motion, presumably as threat displays. It appears that many of these actions do not result in physical harm (we would have stopped interactions that could have escalated to that point) but they are the most serious displays of aggression. We differentiated a behavior we describe as mouth wrestling from biting movement initiated by one fish towards the other. Some species of fish perform behaviors more rightfully described as mouth wrestling (e.g., in cichlids, Brick, 1998) where the fish lock

mouths together and exert force on one another. We see here a mouth-to-mouth fighting behavior that shares some similarities even though their mouths are not locked together. They are face-to-face in close proximity with their mouth open and produce biting and grabbing movements with forceful movements towards each other. Other biting behaviors are more unidirectional. One fish lunge at the other from various relative angles (e.g., from the side) often accompanied by biting motion. It is often directed at the mid-body or tail of the other fish and may not end with actual physical contact even when the fish on the receiving end did not move away to avoid it. It is possible that actual bites and lunges/pretend bites are two levels of this threat behavior.

We characterized the kinetic patterns of these behavior (see methods) and display 3 important aspects of the relative movement properties: speed, distance, and relative azimuth. A few general observations about these characteristics are worth noting. For the more general swimming behaviors (Fig 4) we note that swimming speeds are typically in the lower range and we see few bouts of fast swimming at speeds above 5cm/s, contrary to agonistic behaviors (Fig 5) that can involve faster swimming (e.g., linear chases). Some of these movement behaviors involve the fish being far away from each other, partly due to the definition of the behavior. For example, passive avoidance requires the fish to be distant so they don't need to actively avoid each other while moving. Other movement behavior seems to occur at closer ranges. In particular, it is interesting that targeted approaches occur only when the fish are withing 30-40 cm of each other. Agonistic behaviors (Fig 5) also happen in a fairly close range of less than 30 cm, the distance center-to-center being most often in the 0-20 cm range. We also note that some behavior involves specific relative azimuthal positions: fish receding has the other fish

behind them, chases have the chasers in behind them, and mouth wrestling happens face-to-face. Other behavior does not involve specific relative angles, for example, biting or even approaches involve a variety of relative angles. We note that this diversity or relative azimuth is made more diverse by the fact that these fish can swim side-ways or backward so the direction of their movement doesn't automatically align with their heading angle.

Although only a few kinematic and relative positions properties are detailed here we used various other aspects in our attempts at quantitative analysis. We used several approaches to try to identify stereotyped patterns of movement. We tried clustering analysis using various techniques (e.g., K-means), dimensionality reduction methods (e.g., PCA, tSNE), and unsupervised neural networks (SOM maps, UMAP and HDBSCAN). While we had limited success with subsets of behaviors, these methods failed to identify clear clusters when our whole dataset is used. Dissection of the behaviors identified visually -and their properties' distributions- indicated that although we can categorize behaviors using specific criteria as boundaries, the behaviors are very variables and fall along a continuum with indistinct boundaries between the categories. This is illustrated by mapping the behaviors we identified using 6 kinetic parameters (plotting them using PCA to reduce it to 3 dimensions; Figure 6). The visually identified behavior mostly falls along distinct regions of space but high-density clusters separated by boundaries with fewer data points are not visible. We have not explored all possible ways to analyze the data, and the fact that we can visually identify distinct behaviors suggests that categorization is possible, but the complexity of the problem makes it an endeavor that will have to be tackled in future efforts.

Ethograms

Next, we question whether specific sequences of behavior can be observed. Alternatively, the probability of a given behavior being followed by a specific second one is random and simply reflects the different propensity of the different behaviors. For example, a bite could be systematically followed by a chase but never by active avoidance. We calculated the conditional probabilities of transitions from one behavior to another and normalized it considering the random probability of each sequence (Figure 7). As a result, a value of 1 indicates a random chance for the specific sequence. A value of 2 for example indicates a probability twice larger than chance to have the specific sequence. We calculated a 95% confidence interval based on random shuffling of behavior sequences and mark with an asterisk probability significantly more or less likely than chance. We see that most sequences are significantly different than chance indicating that specific sequences of behavior occur. We note a few general patterns. First, fish cycle in and out of passive avoidance with approaches recedes. Approaches are followed by one of the agonistic behaviors: chases, biting, or mouth-wrestling. The agonistic behaviors are interspersed with active avoidance and are rarely followed immediately by another type of agonistic behavior. The bout of agonistic interactions ends with one of the aggressive moves (chase, mouth wrestling) leading to one of the fish moving away and entering a passive avoidance state.

Discussion

The goal of this study was to characterize movement patterns and delineate behaviors during agonistic interactions. In order to do so, we developed a semi-automatic rapid tracking system that can track the position of the fish. Using azimuth, speed, and distance as factors we characterized 9 unique stereotyped behavior in interacting fish. For each of the behavior, we were able to create a quantitative description of the behaviors. An important result of our study is to have identified the distance ranges at which active interactions occur. We found that clear interaction starts occurring at 40 cm but the bulk of interactions occur at short ranges below 20 cm. in a recent modeling study that includes the estimate of sensory signals and receptor responses during social interactions we found that accuracy decreases sharply at comparable ranges of 30-40 cm. We suggest that our behavioral data support the idea that more distant fish might be detected, and with searching strategies, they can be localized, but the fast and accurate localization necessary for high-speed interactions like chases are restricted to shorter ranges below 40 cm.

We showed that certain behaviors involve specific spatial relationship; a linear chase for example involve on fish behind the other. For other behaviors, the distribution of angle is wide and involves a variety of angles. This is partly due to the unique nature of the knifefish swimming capacity: unlike other fish, they can swim sideways and backward with ease and this makes the angle distribution more variable. Nevertheless, our findings emphasize the need to have a precise estimate of target azimuth. It is interesting to consider chases and in particular circular chases that involve frequent turns as the fish will need precise and rapid localization abilities. It would be intriguing to investigate this motor behavior through analytical approaches

resembling engineering system control. This would allow us to discern the respective influences of motor performance factors (such as lag) and sensory accuracy (the precision of locating the target) on the observed azimuth variability.

Due to the high variability in the behavior, automatic clustering and identification of stereotyped behaviors were not readily achieved. Given that visual categorization was possible, we believe that sophisticated analytical procedures should be able to automatically cluster and identify stereotyped behavior. Human visual pattern recognition is a highly performant system and replicating its performance is not trivial. We believe that several factors make this task particularly hard. The behaviors can vary greatly in duration. In behavioral analysis, extracting features from fixed-length time bins can limit the representation of natural timing variations in behaviors (Klaus et al., 2017; Marshall et al., 2021). To address this, alternative approaches such as change-point detection or the use of features robust to temporal variation can be advantageous (Costa et al., 2019; Mearns et al., 2020; Szigeti et al., 2015). Also, we are considering multi-animal interactions which increases exponentially the number of parameters that can be relevant. When dimensionality reduction is necessary, it's important to test different hyperparameters, as they can significantly affect the results. Additionally, algorithms like t-SNE and UMAP, commonly used for dimensionality reduction, are sensitive to initialization and can generate different embeddings each time they are run (Karpenko et al., 2020; McInnes et al., 2018). The primary challenges in clustering data include selecting an appropriate algorithm, specifying a suitable distance metric, and determining the number of clusters. To evaluate the quality of obtained clusters, it is recommended to apply clustering validation metrics such as the silhouette score, the Calinski-Harabasz criterion, or the gap

statistic (Caliński & Harabasz, 1974; Rousseeuw, 1987; Tibshirani et al., 2001). Ensemble clustering, which involves clustering the data multiple times with perturbations, can be more effective in identifying stable and consistent solutions. Dimensionality reduction can also be incorporated within an ensemble clustering framework to ensure stability when dealing with stochastic algorithms and embedding hyperparameters (Ronan et al., 2016). We argue that our visual identification of behavior was sufficient to characterize major categories of movement patterns and their sequence. Given the complexity of the issue, it became obvious that a quantitative automated clustering effort was beyond the scope of this article but it would constitute and interesting follow-up study.

The next step to developing a reliable model that can be used to help further understand the neural basis of sensory processing should be to look deeper into the differences in another prototypical behavior of weakly electric fish, and chirping patterns. It was beyond the scope of this study to examine the changes in the chirp frequencies during the chasing bouts. Studies have shown that during agonistic and exploratory behavior the fish chirp frequency and patterns change (Hofmann et al., 2014; Pedraja et al., 2016) A similar analysis can be done for interacting fish. We know, from existing studies, that the dominant fish or the more aggressive fish increases its chirp rate and the submissive fish decreases its chirp rate and frequency (Henninger et al., 2018; Hupe & Lewis, 2008; Pedraja et al., 2016; Triefenbach & Zakon, 2008) or chirp in an echo pattern (Zupanc et al., 2006; Zupanc & Maler, 1993). Pairing this communication element with the kinematics of agnostic behavior would help provide a more complete understanding of these social interactions.

An important motivation for our study was to quantify the relative position of fish during behaviorally relevant interaction in order to estimate the spatiotemporal structure of the signals that underlie behavior. Much of the interactions we described here require precise sensory estimates of the other fish's position to produce directed behaviors. Our behavioral analysis can be paired with models of electric field propagation to obtain a thorough quantification of the spatiotemporal dynamic of signals that must be processed. To illustrate this process, we show in Figure 8, the strength of the signal that would be experienced when one fish approaches the other (see Ramachandra et al.,2023 for more information). Our behavioral data complement recent studies (Ramachandra et al 2023, Pedraja et al., 2016) to argue that much of the sensory processing occurring during the realistic behavior occurs in the range of "weak signals". Electrophysiological studies of sensory responses often focused on responses in the upper range of these relevant intensities (Benda et al, 2006, Metzen et al, 2018). Furthermore, most studies on this system used stimuli with unrealistic spatial structures (Milam et al., 2018). Our current study can serve as the foundation to replicate more behaviorally relevant signal structures and target response properties that are particularly important in encoding the stimuli pattern identified here.

Our study also includes an ethogram study to better understand the sequences of behaviors occurring during agonistic interactions. A general pattern of how these interactions unfold emerged. Fish can be in a passive mode and are typically far away but move closer for more active interactions (i.e., "passive avoidance was paired with corresponding "approach" or "recede" movements). While actively engaged, the fish alternate periods of "active avoidance", where they remain separate but nearby, with one of the moves from a repertoire of aggressive

behaviors: various chasing patterns, biting, lunging or “mouth wrestling”. Theories of animal behavior typically classify conflict resolution strategies in one of three categories: energetic war of attrition, sequential assessment, or cumulative assessment (Bradbury & Vehrencamp, 2011). The behavior we describe here corresponds well with the latter. In this type of conflictual interaction, the opponent assesses each other by exchanging escalating or de-escalating moves from a repertoire. Crickets are a well-documented example of this strategy, they produce behaviors such as “antenna lash” or “rear kick” in variable sequences to provide accumulating evidence that they are the dominant individual (Hofmann & Schildberger, 2001; Lobregat et al., 2019). Here, we argue that the fact that aggressive behaviors are separated by short “active avoidance” periods makes it clear that each of these moves (i.e., a chase, a lunge…) are separate behavior from their repertoire. Future research could further investigate this perspective and systematically analyze how each individual provides accumulating evidence of their dominance through these distinct behaviors and how it relates to the establishment of dominance.

In conclusion, our study delineated a number of distinct movement patterns associated with agonistic encounters. By describing the spatiotemporal dynamic of the individuals during these interactions we lay the foundations for designing more realistic investigations of sensory processing to understand how it guides complex behaviors. Our study also anchored this agonistic interaction in established theories of conflict resolution thereby providing a rigorous framework to understand social dynamics in these fish.

References

Baker, C. V. H., Modrell, M. S., & Gillis, J. A. (2013). The evolution and development of vertebrate lateral line electroreceptors. *Journal of Experimental Biology*, *216*(13), 2515–2522. https://doi.org/10.1242/jeb.082362

Bradbury, J. W., & Vehrencamp, S. L. (2011). *Principles of animal communication* (2nd ed.). Sinauer Associates.

BRICK, O. (1998). Fighting behaviour, vigilance and predation risk in the cichlid fishNannacara anomala. *Animal Behaviour*, *56*(2), 309–317. https://doi.org/https://doi.org/10.1006/anbe.1998.0782

Bullock, T. H., Hopkins, C. D., Popper, A. N., & Fay, R. R. (1986). Electroreception. In *Eletroreception*. https://doi.org/10.1007/0-387-28275-0

Caliński, T., & Harabasz, J. (1974). A dendrite method for cluster analysis. *Communications in Statistics*, *3*(1), 1–27. https://doi.org/10.1080/03610927408827101

Caputi, A. A., Budelli, R., Grant, K., & Bell, C. C. (1998). The electric image in weakly electric fish: Physical images of resistive objects in Gnathonemus petersii. *Journal of Experimental Biology*, *201*(14), 2115–2128. https://doi.org/10.1242/jeb.201.14.2115

Caputi, A., & Budelli, R. (1995). The electric image in weakly electric fish: I. A data-based model of waveform generation in Gymnotus carapo. *Journal of Computational Neuroscience*, *2*(2), 131–147. https://doi.org/10.1007/BF00961884

Clutton-Brock, T. H., Albon, S. D., Gibson, R. M., & Guinness, F. E. (1979). The logical stag: Adaptive aspects of fighting in red deer (Cervus elaphus L.). *Animal Behaviour*, *27*, 211–225.

Costa, A. C., Ahamed, T., & Stephens, G. J. (2019). Adaptive, locally linear models of complex dynamics. *Proceedings of the National Academy of Sciences*, *116*(5), 1501–1510. https://doi.org/10.1073/pnas.1813476116

Fugère, V., Ortega, H., & Krahe, R. (2011). Electrical signalling of dominance in a wild population of electric fish. *Biology Letters*, *7*(2), 197–200. https://doi.org/10.1098/rsbl.2010.0804

Geurten, B. R. H., Kern, R., Braun, E., & Egelhaaf, M. (2010). A syntax of hoverfly flight prototypes. *Journal of Experimental Biology*, *213*(14), 2461–2475. https://doi.org/10.1242/jeb.036079

Heiligenberg, W. (1975). Theoretical and experimental approaches to spatial aspects of electrolocation. *Journal of Comparative Physiology A*, *103*(3), 247–272. https://doi.org/10.1007/BF00612021

Henninger, J., Krahe, R., Kirschbaum, F., Grewe, J., & Benda, J. (2018). Statistics of natural communication signals observed in the wild identify important yet neglected stimulus regimes in weakly electric fish. *The Journal of Neuroscience*. https://doi.org/10.1523/JNEUROSCI.0350-18.2018

Hofmann, H. A., & Schildberger, K. (2001). Assessment of strength and willingness to fight

during aggressive encounters in crickets. *Animal Behaviour*, *62*(2), 337–348. https://doi.org/10.1006/anbe.2001.1746

Hofmann, V., Geurten, B. R. H., Sanguinetti-Scheck, J. I., GÃ³mez-Sena, L., & Engelmann, J. (2014). Motor patterns during active electrosensory acquisition. *Frontiers in Behavioral Neuroscience*, *8*, 186. https://doi.org/10.3389/fnbeh.2014.00186

Hupe, G. J., & Lewis, J. E. (2008). Electrocommunication signals in free swimming brown ghost knifefish, Apteronotus leptorhynchus. *Journal of Experimental Biology*. https://doi.org/10.1242/jeb.013516

Karpenko, S., Wolf, S., Lafaye, J., Le Goc, G., Panier, T., Bormuth, V., Candelier, R., & Debrégeas, G. (2020). From behavior to circuit modeling of light-seeking navigation in zebrafish larvae. *ELife*, *9*, e52882. https://doi.org/10.7554/eLife.52882

Klaus, A., Martins, G. J., Paixao, V. B., Zhou, P., Paninski, L., & Costa, R. M. (2017). The Spatiotemporal Organization of the Striatum Encodes Action Space. *Neuron*, *95*(5), 1171-1180.e7. https://doi.org/https://doi.org/10.1016/j.neuron.2017.08.015

Kolodziejski, J. a, Sanford, S. E., & Smith, G. T. (2007). Stimulus frequency differentially affects chirping in two species of weakly electric fish: implications for the evolution of signal structure and function. *The Journal of Experimental Biology*, *210*(Pt 14), 2501–2509. https://doi.org/10.1242/jeb.005272

Lissmann, H. W. (1951). Continuous Electrical Signals from the Tail of a Fish, Gymnarchus niloticus Cuv. *Nature*, *167*(4240), 201–202. http://dx.doi.org/10.1038/167201a0

Lobregat, G., Gechel Kloss, T., Peixoto, P. E. C., & Sperber, C. F. (2019). Fighting in rounds: males of a neotropical cricket switch assessment strategies during contests. *Behavioral Ecology*, *30*(3), 688–696. https://doi.org/10.1093/beheco/arz005

MacNulty, D. R., Mech, L. D., & Smith, D. W. (2007). A Proposed Ethogram of Large-Carnivore Predatory Behavior, Exemplified by the Wolf. *Journal of Mammalogy*, *88*(3), 595–605. https://doi.org/10.1644/06-MAMM-A-119R1.1

Maler, L. (2007). Neural strategies for optimal processing of sensory signals. In *Progress in Brain Research* (2007/10/11, Vol. 165, pp. 135–154). https://doi.org/10.1016/S0079-6123(06)65009-7

Marshall, J. D., Aldarondo, D. E., Dunn, T. W., Wang, W. L., Berman, G. J., & Ölveczky, B. P. (2021). Continuous Whole-Body 3D Kinematic Recordings across the Rodent Behavioral Repertoire. *Neuron*, *109*(3), 420-437.e8. https://doi.org/https://doi.org/10.1016/j.neuron.2020.11.016

Mas-Muñoz, J., Komen, H., Schneider, O., Visch, S. W., & Schrama, J. W. (2011). Feeding behaviour, swimming activity and boldness explain variation in feed intake and growth of sole (Solea solea) reared in captivity. *PloS One*, *6*(6), e21393. https://doi.org/10.1371/journal.pone.0021393

Mathis, A., Mamidanna, P., Cury, K. M., Abe, T., Murthy, V. N., Mathis, M. W., & Bethge, M. (2018). DeepLabCut: markerless pose estimation of user-defined body parts with deep learning. *Nature Neuroscience*, *21*(9), 1281–1289. https://doi.org/10.1038/s41593-018-0209-y

McInnes, L., Healy, J., & Melville, J. (2018). *UMAP: Uniform Manifold Approximation and Projection for Dimension Reduction*. http://arxiv.org/abs/1802.03426

Mearns, D. S., Donovan, J. C., Fernandes, A. M., Semmelhack, J. L., & Baier, H. (2020). Deconstructing Hunting Behavior Reveals a Tightly Coupled Stimulus-Response Loop. *Current Biology*, *30*(1), 54-69.e9. https://doi.org/https://doi.org/10.1016/j.cub.2019.11.022

Milam, O. E., Ramachandra, K. L., & Marsat, G. (2018). *Behavioral and neural aspects of the spatial processing of conspecifics in the electrosensory system*. *November*, 1–39. https://doi.org/10.20944/preprints201811.0132.v1

Mitoyen, C., Quigley, C., & Fusani, L. (2019). Evolution and function of multimodal courtship displays. *Ethology*, *125*(8), 503–515. https://doi.org/10.1111/eth.12882

Mueller, J. M., Zhang, N., Carlson, J. M., & Simpson, J. H. (2021). Variation and Variability in Drosophila Grooming Behavior. *Frontiers in Behavioral Neuroscience*, *15*, 769372. https://doi.org/10.3389/fnbeh.2021.769372

Nath, T., Mathis, A., Chen, A. C., Patel, A., Bethge, M., & Mathis, M. W. (2019). Using DeepLabCut for 3D markerless pose estimation across species and behaviors. *Nature Protocols*, *14*(7), 2152–2176. https://doi.org/10.1038/s41596-019-0176-0

Nelson, M. E., Maciver, M. A., Nelson M Maciver M, Nelson, M. E., & Maciver, M. A. (1999). Prey capture in the weakly electric fish Apteronotus albifrons: sensory acquisition strategies and electrosensory consequences. *Journal of Experimental Biology*, *202*(10).

http://www.ncbi.nlm.nih.gov/pubmed/9487102

Patricelli, G. L., Uy, J. A. C., Walsh, G., & Borgia, G. (2002). Male displays adjusted to female's response. *Nature*, *415*(6869), 279–280. https://doi.org/10.1038/415279a

Pedraja, F., Perrone, R., Silva, A., & Budelli, R. (2016). Passive and active electroreception during agonistic encounters in the weakly electric fish Gymnotus omarorum. *Bioinspiration & Biomimetics*, *11*(6), 065002. https://doi.org/10.1088/1748-3190/11/6/065002

Pereira, T. D., Aldarondo, D. E., Willmore, L., Kislin, M., Wang, S. S.-H., Murthy, M., & Shaevitz, J. W. (2019). Fast animal pose estimation using deep neural networks. *Nature Methods*, *16*(1), 117–125. https://doi.org/10.1038/s41592-018-0234-5

Perrone, R., Pedraja, F., Valiño, G., Tassino, B., & Silva, A. (2019). Non-breeding territoriality and the effect of territory size on aggression in the weakly electric fish, Gymnotus omarorum. *Acta Ethologica*, *22*(2), 79–89. https://doi.org/10.1007/s10211-019-00309-7

Postlethwaite, C. M., Psemeneki, T. M., Selimkhanov, J., Silber, M., & MacIver, M. A. (2009). Optimal movement in the prey strikes of weakly electric fish: A case study of the interplay of body plan and movement capability. *Journal of the Royal Society Interface*, *6*(34), 417–433. https://doi.org/10.1098/rsif.2008.0286

Rasnow, B. (1996). The effects of simple objects on the electric field of Apteronotus. *Journal of Comparative Physiology A*, *178*(3), 397–411. https://doi.org/10.1007/BF00193977

Ronan, T., Qi, Z., & Naegle, K. M. (2016). Avoiding common pitfalls when clustering biological data. *Science Signaling*, *9*(432), re6–re6. https://doi.org/10.1126/scisignal.aad1932

Rother, D., Migliaro, A., Canetti, R., Gómez, L., Caputi, A., & Budelli, R. (2003). Electric images of two low resistance objects in weakly electric fish. *BioSystems*, *71*(1–2), 169–177. https://doi.org/10.1016/S0303-2647(03)00124-2

Rousseeuw, P. J. (1987). Silhouettes: A graphical aid to the interpretation and validation of cluster analysis. *Journal of Computational and Applied Mathematics*, *20*, 53–65. https://doi.org/https://doi.org/10.1016/0377-0427(87)90125-7

Stamper, S. A., Roth, E., Cowan, N. J., & Fortune, E. S. (2012). Active sensing via movement shapes spatiotemporal patterns of sensory feedback. *Journal of Experimental Biology*, *215*(9), 1567–1574. https://doi.org/10.1242/jeb.068007

Szigeti, B., Deogade, A., & Webb, B. (2015). Searching for motifs in the behaviour of larval Drosophila melanogaster and Caenorhabditis elegans reveals continuity between behavioural states. *Journal of The Royal Society Interface*, *12*(113), 20150899. https://doi.org/10.1098/rsif.2015.0899

Tibshirani, R., Walther, G., & Hastie, T. (2001). Estimating the Number of Clusters in a Data Set Via the Gap Statistic. *Journal of the Royal Statistical Society Series B: Statistical Methodology*, *63*(2), 411–423. https://doi.org/10.1111/1467-9868.00293

Triefenbach, F. A., & Zakon, H. H. (2008). Changes in signalling during agonistic interactions between male weakly electric knifefish, Apteronotus leptorhynchus. *Animal Behaviour*, *75*(4), 1263–1272. https://doi.org/10.1016/j.anbehav.2007.09.027

Von Der Emde, G., Schwarz, S., Gomez, L., Budelli, R., & Grant, K. (1998). Electric fish measure

distance in the dark. *Nature*, *395*(6705), 890–894. https://doi.org/10.1038/27655

Walter, T., & Couzin, I. D. (2021). TRex, a fast multi-animal tracking system with markerless identification, and 2D estimation of posture and visual fields. *ELife*, *10*, e64000. https://doi.org/10.7554/eLife.64000

Xu, F., Xie, L., Li, X., Li, Q., Wang, T., Ji, Y., Kong, F., Zhan, Q., Cheng, K., Fang, L., & Xie, P. (2012). Construction and validation of a systematic ethogram of Macaca fascicularis in a free enclosure. *PLoS ONE*, *7*(5), 1–12. https://doi.org/10.1371/journal.pone.0037486

Zakon, H., Oestreich, J., Tallarovic, S., & Triefenbach, F. (2002). EOD modulations of brown ghost electric fish: JARs, chirps, rises, and dips. *Journal of Physiology, Paris*, *96*(5–6), 451–458. https://doi.org/10.1016/S0928-4257(03)00012-3

Zupanc, G. K. H., & Maler, L. (1993). Evoked chirping in the weakly electric fish Apteronotus leptorhynchus – a quantitative biophysical analysis. *Canadian Journal of Zoology*, *71*(11), 2301–2310. https://doi.org/10.1139/z93-323

Zupanc, G. K. H., Sîrbulescu, R. F., Nichols, A., & Ilies, I. (2006). Electric interactions through chirping behavior in the weakly electric fish, Apteronotus leptorhynchus. *Journal of Comparative Physiology A: Neuroethology, Sensory, Neural, and Behavioral Physiology*, *192*(2), 159–173. https://doi.org/10.1007/s00359-005-0058-5

Figures

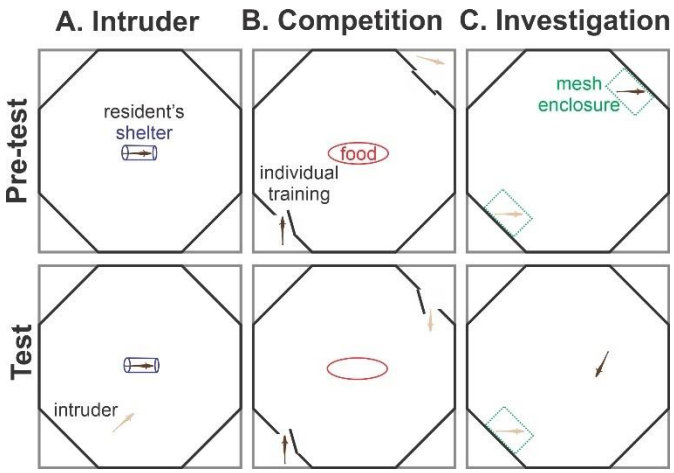

Figure 1: Behavioral paradigms. A. Resident-intruder scenario. A first fish is introduced in the tank 24hr before the test (pre-test; top panel) and a single shelter is provided (a clear plastic tube). As the recording starts (camera from the top, in IR light, at the beginning of their active nocturnal phase), a second fish -the intruder- in introduced in the tank (bottom panel). Recording continued for the 30 min after intruder introduction. **B.** Competition of food. Fish are trained for 10-12 days in the pre-test (top) by being introduced in the experimental tank at the beginning of their active phase; after 15 min of acclimatation, food is introduced in the center of the tank and the fish is allow to swim outside its shelter to go capture the food (live black worms). Two fish are trained over the same period but are by themselves in the tank during the pre-test. At the end of the training session, the fish know to go directly to the center to capture the food. During the test session, two fish are introduced at the same time in opposite portions of the tank with no food provided however, they experience competition as they encounter each other when going to food location . . **C.** Targeted investigation. Two fish are introduced on opposite sides of the tank in small mesh enclosure that allows the electric signals to propagate. In the pre-test period, the fish are simply allowed to sense each other from the distance for 30 min while remaining in their enclosure. We note that although the signals at that distance are weak, field data suggest this is still within the range they can perceive (REF Henninger, Fortune).

During the test recording period, one fish is let out of its enclosure and allowed to explore, possibly moving towards and around the other fish that is still in its enclosure. The arena is a square 1x1m which corners have been closed off with a divider to avoid providing a corner in which fish will tend to shelter. The arena is thus an octagon. Water level is low (20 cm) further constraining movement to 2D. IR lighting is provided from the bottom and the IR camera is recording from the top.

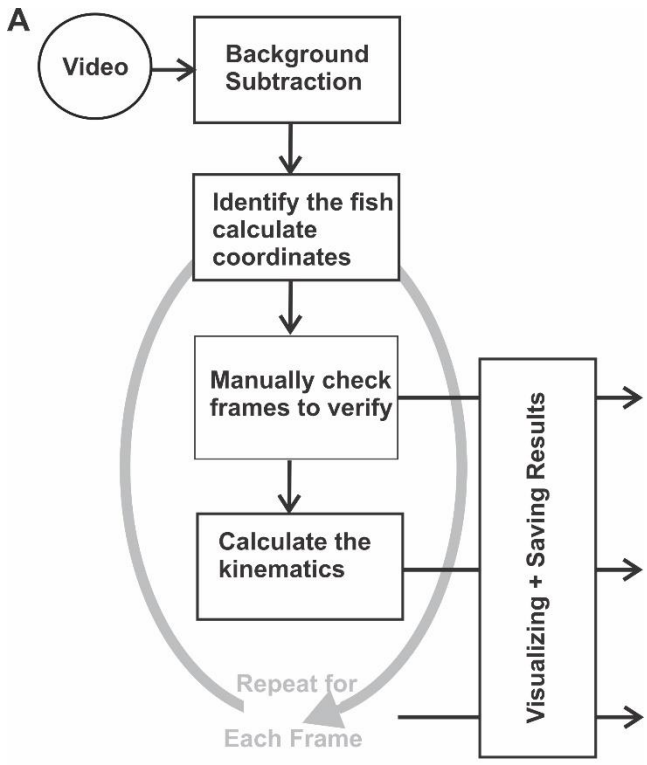

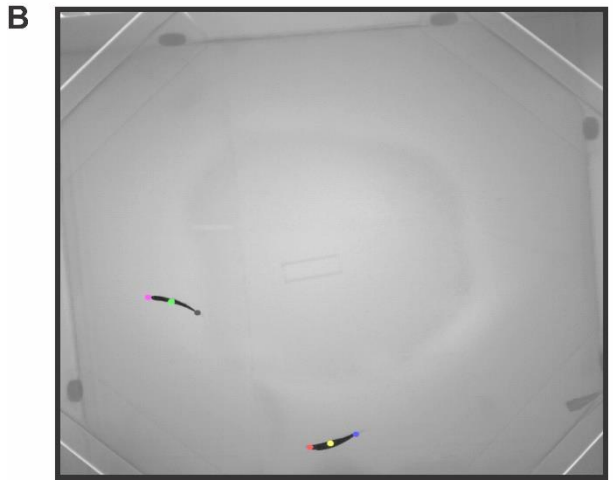

Figure 2 Tracking software package. A. The algorithm involves creating a mean background image and performing background subtraction to eliminate elements of the environment. Dark masses are then identified as the two fish and their position is determined. There can be instances where the fish get close in a way that leads to the swapping of identities between the fish. These frames are flagged and verified visually and corrected manually. Using the coordinates value different kinematic parameters were calculated. The software package also provides convenient ways to visualize the tracking results and save the data. **B.** Example of a frame of the video recording with the coordinates of the two fish marked. Note that the center of the centroids and the two extremities are identified (and rostral distinguished from caudal).

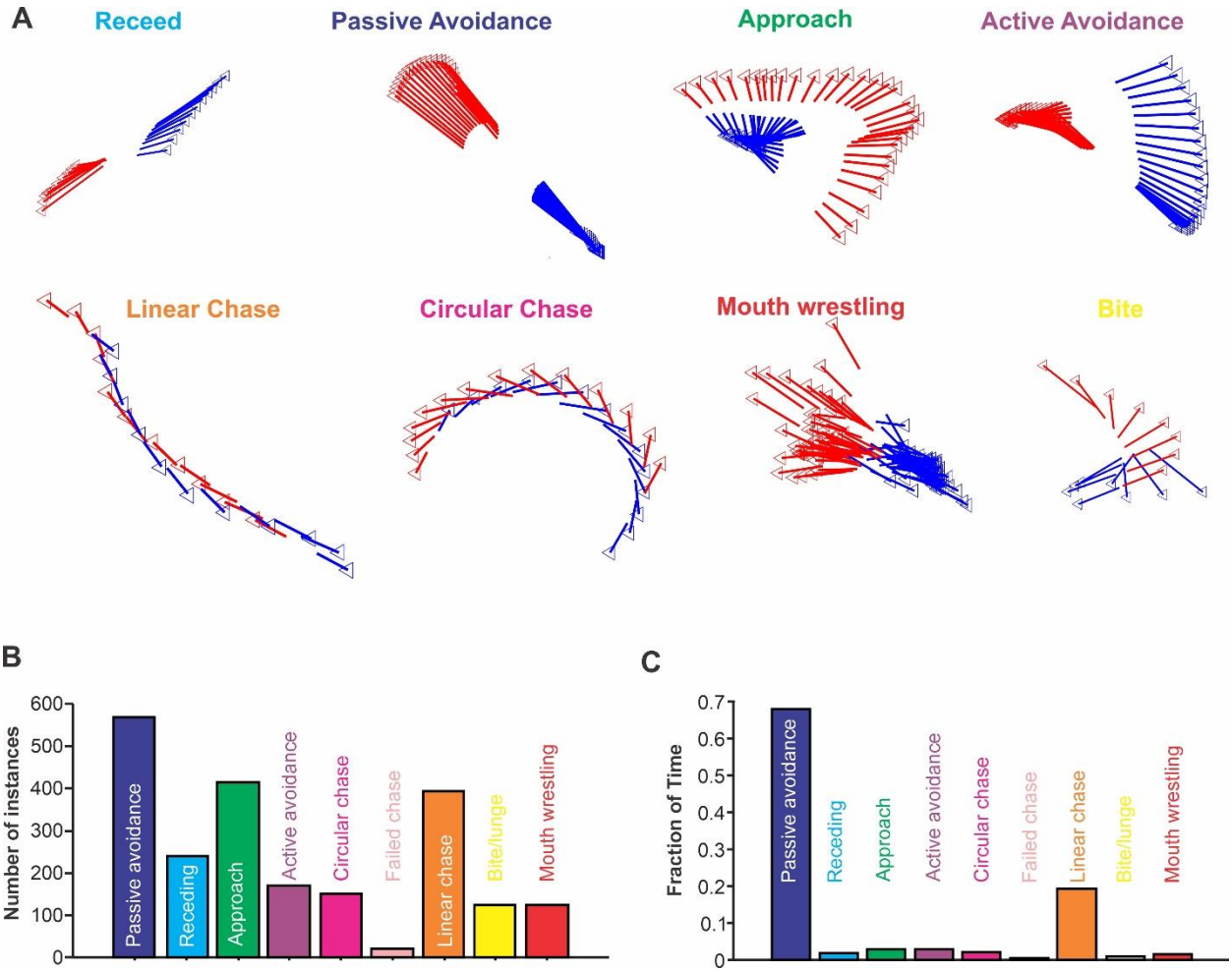

Figure 3: Relative movements categorized in 9 behaviors. A. Examples of sequences of relative positions during 8 behaviors. We do not show an example for failed chase but it will be similar in pattern to the beginning of a linear or circular chase. For the 8 examples shown, the center of each fish is marked by a triangle, and a line stem from the triangle in the direction of the center of the other fish thereby highlighting their relative positions. The color code used for the names of the behavior will be used throughout the paper with cool colors denoting the 4 general movement patterns (top row) and warm colors used for the 4 agonistic behaviors (bottom row). **B.** Number of bouts of each behavior present in our recordings. **C.** Fraction of the time spend doing each of the 9 behaviors.

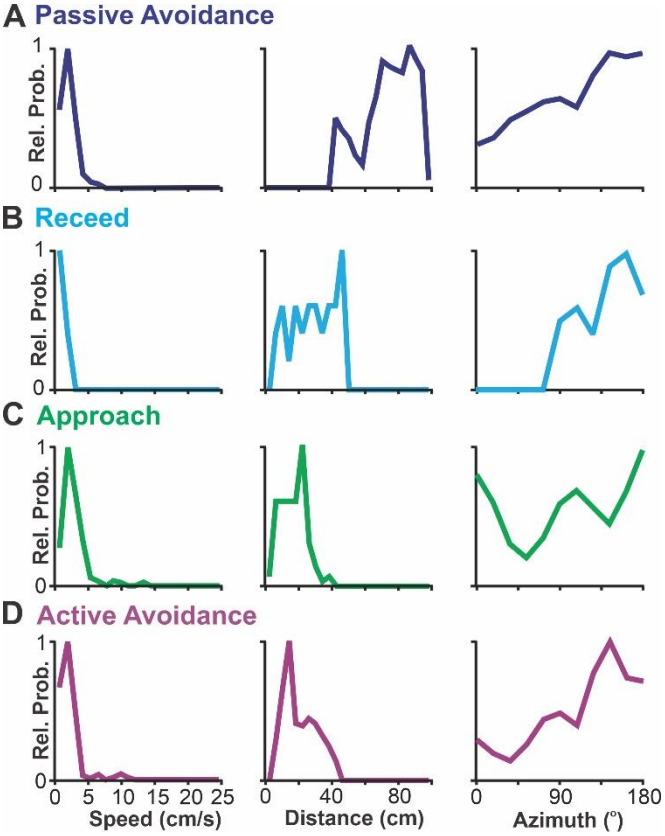

Figure 4. Distributions of the kinematics for the general movement behaviors. Based on the frame-by-frame positions of the fish during each behavior, we calculated a variety of relative position and kinematic measures; we show here the absolute speed of the focal fish (plots on the left), the distance between the two fish (plots in the middle), and the relative azimuth (plots on the right) of the second fish relative to the focal fish (i.e., 180° indicate a fish positioned behind the focal fish). The focal fish for approach/recede is the one performing the action. Probabilities were normalized to a peak of 1. Each behavior is described in a different row **A-D**.

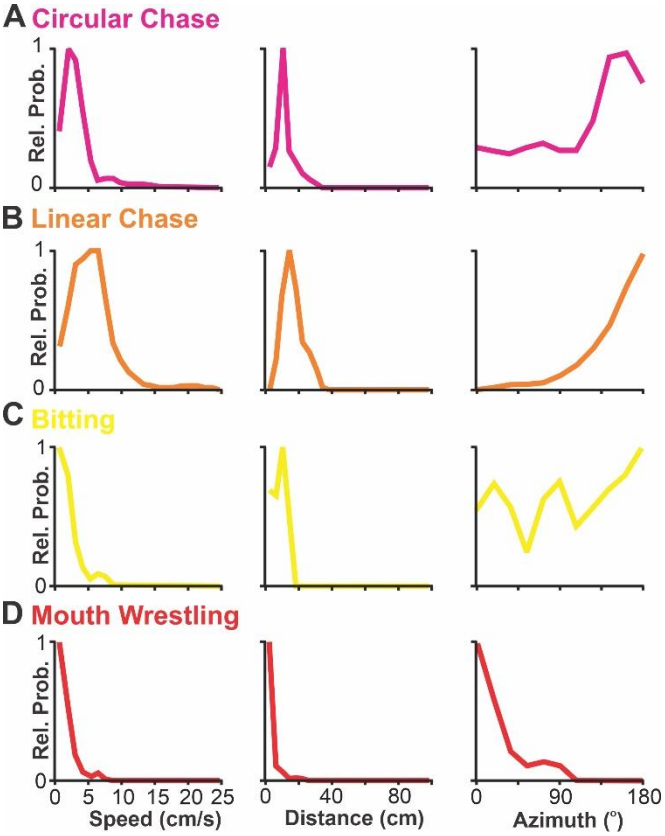

Figure 5: Distributions of the kinematics for the agonistic behaviors. Based on the frame-by-frame positions of the fish during each behavior, we calculated a variety of relative position and kinematic measures; we show here the absolute speed of the focal fish (plots on the left), the distance between the two fish (plots in the middle), and the relative azimuth (plots on the right) of the second fish relative to the focal fish (i.e., 180° indicate a fish positioned behind the focal fish). The focal fish is the one being chased or the one initiating the biting/wrestling. Probabilities were normalized to a peak of 1. Each behavior is described in a different row **A-D**.

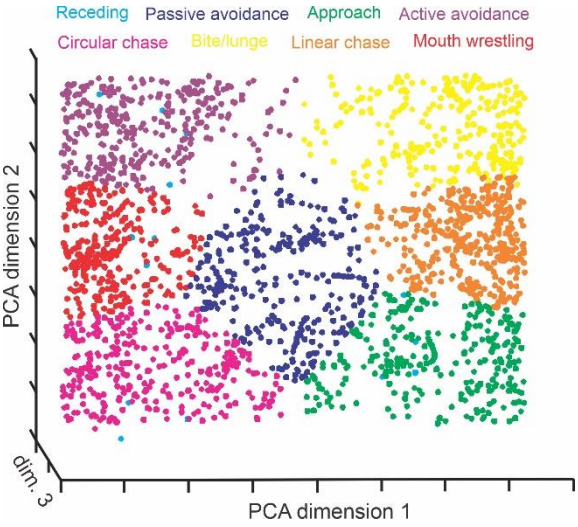

Figure 6: Clustering attempt for the bouts of movements that were also categorized manually. Various aspects or measures derived from the kinematic and relative positions of the fish were used to try to identify clusters of behaviors with stereotyped patterns of movements that could be delineated categorically through a clustering algorithm. We show here one such attempt were 6 measures are used and the dimensionality is reduced via PCA. Each data point was colored according to the behavior label assigned by experimenters through qualitative identification. Receding bouts do not fall in a single portion of this space but the other behaviors fall in specific portions of space in this specific analysis. However, clusters are not apparent and the boundaries between visually identified behaviors do not correspond to natural separations in the distribution of the data.

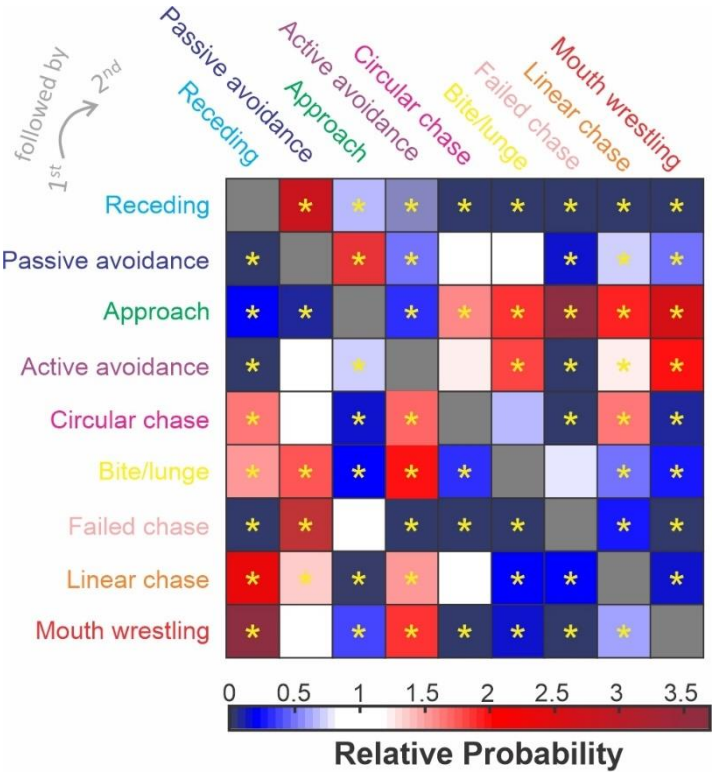

Figure 7. Relative probability of transition from one behavior to the next. We calculated the probability that one behavior (left labels, different rows) is followed by each of the other 8 behaviors (top labels, different columns). Therefore, before normalization, the sum of the probability for each row would be one since each behavior must be followed by one of the other 8 (never itself -cells in grey). Probability is then normalized relative to the probability of each behavior happening. As a result, a relative probability of 1 indicates a sequence that is as probable as chance whereas values much below/above 1 indicate sequences that are particularly common/rare. We calculated the range of values we could expect from random sequences by shuffling the order of behaviors (10000 iterations) to calculate a confidence interval and denote a star value above/below this interval.

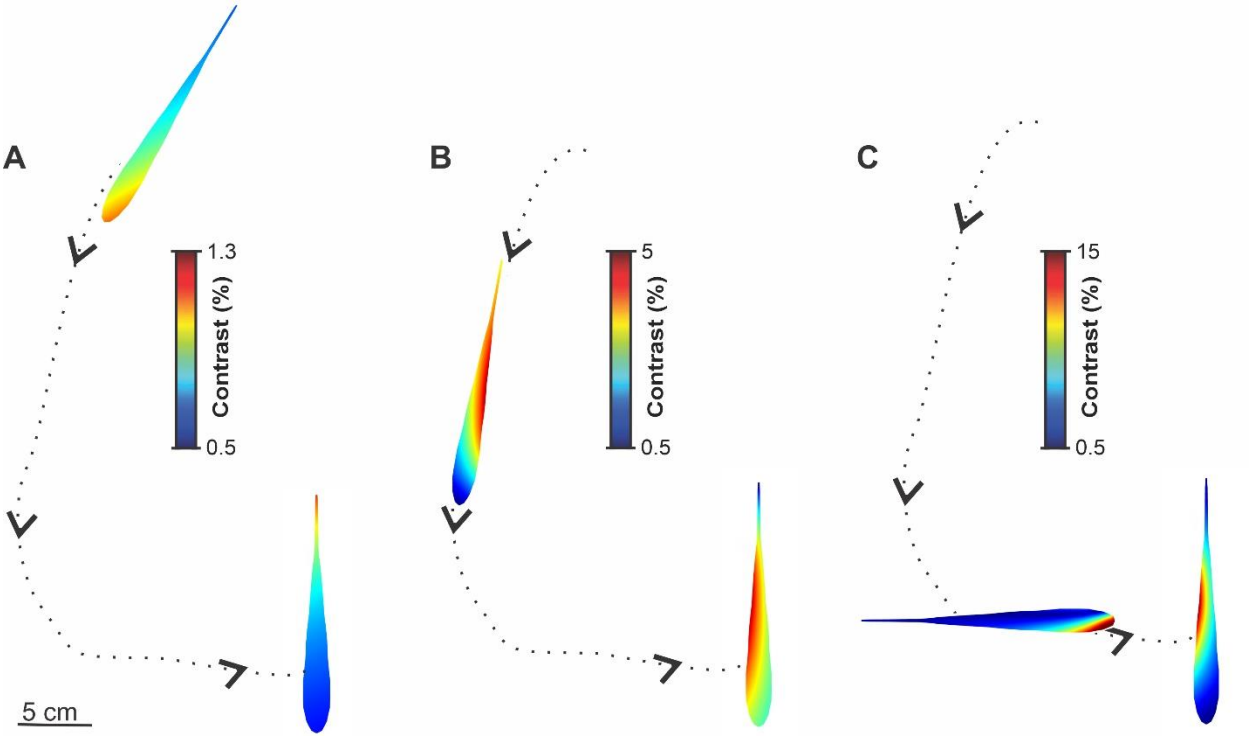

Figure 8: Illustration of the electric image experienced during an example behavior. The algorithm we used (see Ramachandra et al 2023 for details) Calculates the strength of the electric field present during the fish interactions. The signals that result from the addition of the second fish is designated as the electric image it casts on the receiver and it is shown here as a relative transdermal voltage. A contrast of 0 indicates that the electric field strength at that point is the same as if no second fish was present. A contrast of 100% indicates that the effect of second fish's signal at that point on the receiver's body is as strong as the receiver's own signal when no second fish is present. We show the electric images for three positions (**A-C**) along the trajectory of a fish approaching another.

Supplementary information

Supplementary method: Tracking Software package

All the tracking code and the example videos and images are available at (https://www.marsat.org/publications/code)

Instructions for running the tracker

1. Before even running the tracker, run the file preprocess.m. The preprocess function needs the filenames of the videos and the start and end times of the videos. This will create the background image needed for calculations.

2. Once preprocessing of the file is over, call the tracker by typing MultiTrack(it is case sensitive so pay attention to the caps) in the command window. Here all the user has to do is click on load meanimage which has been calculated from the preprocess script.

3. Then select in the drop menu the tracking which best suits your purpose. Irrespective of what is selected the script will ask for selecting the corners of the video to strip the video. The cutting of videos is different depending upon the need and experiment.

4. That should run the whole tracking which will then show an output with the original video and the tracked video playing side by side. The tracked image will the fish and will show the CM, head and tail positions Keep an eye on it to check for abnormalities. If the fish is not seen in the frame an additional script will predict the positions . However, do remember to check and see if the flip has been corrected. The easiest way is to plot the trajectory of the fish with the head if it is flipped you should be able to see the flipping. More about it in step 6.

5. In case the object is not recognizable by the program, the script will save those positions and then after the completion of the tracking, the script will automatically run a prediction script and then the user will be asked if the predicted positions are correct if not it will ask the user to select the head and tail. Please do it in this order only as the head and the tail positions for each fish as they are used for performing other calculations by the tracker.

6. Once the tracking is complete as a quick glance to see if the flips are all accounted for. In the GUI go to plotting and run the plotting for the experiment. It should plot the trajectory of the fish as a stick figure using the head positions. This can tell the user if there is any error in the head and the tail positions as in if the flips are not accounted for or there seems to be jumps in data.

Chapter 4: Discussion

Summary of the Data

In this dissertation, I evaluate the sensory input the fish receive during conspecific interactions. Specifically, I show how the location and orientation of the signal modulate the activation pattern of the electroreceptor array **(Chapter 2)**, and how the detection accuracy and the angular resolution depend on the distance and time scale of signals by modeling a heterogenous population of receptors **(Chapter 2).** I characterize the spatiotemporal dynamic of interacting fish to better understand the signals that guide social behaviors. **(Chapter 3)**.

The spatial Strength of a Conspecific signal varies as a function of distance and Angle

In Chapter 2, I present a model where I project the electric image of one fish onto another fish (referred to as the focal fish) to demonstrate how information about the conspecific's location and orientation is conveyed through the electric field and accurately captured by the electrosensory array. Experimental data published by Fotowat et al. (Fotowat et al., 2013) and Zupanc and Maler (Zupanc & Maler, 1993) support the finding that strong activation of the receptors occurs at distances less than 20 cm, which aligns with our own observations of behavior where fish typically interact at ranges below 30 cm (Chapter 3).

The activation pattern observed in the model exhibits a clear spatial structure, consistent with the distribution of electroreceptors across the skin of the focal fish. These receptors respond differently based on their location and orientation relative to the sender fish,

indicating that the differential response of the receptors provides the fish with information about the spatial location of the conspecific.

While gathering spatial information has been extensively studied in the auditory system, such as the research conducted by Konishi (Knudsen & Konishi, 1979), electrolocation of conspecific fish cannot rely on timing differences since the speed of light does not produce significant timing disparities. However, the electrosensory signal can result in amplitude differences, similar to the interaural level difference (ILD) utilized by the owl auditory system. In the auditory system, ILD sensitivity contributes to sound localization on the horizontal plane in mammals, and a binaural comparison occurs in the lateral superior olive. Sensitivity to these cues first emerges in the posterior nucleus of the ventral lateral lemniscus, where neurons receive excitation from one side and inhibition from the other (Takahashi & Keller, 1992).

The beat that occurs when the electric signals of two fish interact is influenced by the distance between them. As the fish moves closer, the beat becomes stronger, while it weakens as the distance increases. This phenomenon has been characterized through electrophysiological experiments in the laboratory, where the signals received by a fish exposed to one or several moving conspecifics were recorded (Fotowat et al., 2013; Yu et al., 2012)

Our model replicates this basic property: the contrast between the signals becomes stronger when the sender fish is closer to the receiver fish (>25% for distances <10 cm), but this contrast decreases rapidly as the distance increases (<5% for distances >30 cm). This decrease in contrast is due to the electric field decreasing in strength according to a power law, which

aligns with experimental findings reported by Caputi and Fotowat (Caputi et al., 2013; Fotowat et al., 2013).

Moreover, studies have shown that the strength of the signal reaching the receiver fish is not solely determined by the distance between the sender and receiver, but also by the orientation of the pair. Similar effects have been observed when stimulating the fish from different distances and angles (Rasnow et al., 1993)

Detection and localization of conspecific depends on the spatial structure of the fish

In Chapter 2 of this dissertation, a conservative estimate for the accuracy of localization and detection is given. The model was developed using a heterogeneous population of receptors that replicate responses to spatially realistic stimuli. This approach provides a conservative estimate of the detection range and localizing accuracy because we consider it likely that neural mechanisms, we have not explored can enhance accuracy relative to our baseline. The model suggests that fish are able to detect conspecifics at a distance of 75 cm, which is comparable to observations in laboratory and wild conditions (Henninger et al., 2018; Stamper et al., 2012; Yu et al., 2012).

Resolution accuracy is also estimated in the model and found to decrease rapidly beyond 30 cm. However, these ranges could be increased by relying on neural mechanisms that have been implicated in coding in this system. Information can be encoded in the pattern of spike rates across the receptor population, and some cases, the degree of synchrony in spike times can convey additional information, such as the presence of communication signals: such

as chirps (Benda et al., 2006). Future modeling efforts should consider population synchrony to better understand its impact on conspecific localization.

Receptors in the fish electrolocation system exhibit negative serial correlations in inter-spike intervals (ISIs), where long ISIs tend to be followed by short ISIs. This characteristic reduces noise at low frequencies and allows for more accurate encoding of information about prey items by the receptors. The mechanism underlying these correlations has been replicated in leaky integrate-and-fire (LIF) models (Chacron et al., 2000; Lindner et al., 2005) and it would be useful for future studies to consider this mechanism in the context of localization.

Jung et al. (Jung et al., 2016) recently identified a mechanism for detecting weak signals that relies on a finely balanced inhibition and excitation from feedforward inputs. Balanced inhibition and excitation are common features in many neural networks, including the cortex, and play a role in shaping sensory tuning in various systems (Anderson et al., 2000; Haider, 2006). Furthermore, studies in various sensory systems have demonstrated that nervous systems can effectively extract weak signals using two mechanisms: stochastic resonance and Bayesian inference. Stochastic resonance refers to the phenomenon where the addition of random noise to a weak signal can improve its detectability, while Bayesian inference suggests that prior knowledge about sensory input, facilitated by extensive feedback from higher brain areas, helps in interpreting ambiguous or weak sensory signals (Douglass et al., 1993; Linkenkaer-Hansen et al., 2004).

The analysis presented in Chapter 2 considered spatially fixed signals. However, in addition to sensory mechanisms, movement could play an important role in localizing

conspecifics. For instance, crickets exhibit a zig-zag pattern when approaching a calling song source, suggesting that they first use lateralization to determine the direction of the sound and then adjust their orientation accordingly. This behavior indicates that even though they can localize a fixed sound source precisely (Schöneich & Hedwig, 2010) crickets will need to rely on behavioral strategies to target a source while moving.

Elephantnose (mormyrid) electric fish also employ similar behavioral strategies to localize conspecifics. When moving toward another fish, they tend to follow electric field lines instead of moving directly toward the source. This behavior likely arises from the fish's attempt to balance the strength of the electric field current on each side of its body (Schluger & Hopkins, 1987). Many other animals also utilize active sampling strategies to enhance their sensory abilities (Schroeder et al., 2010). For example, knifefish utilize body movements to improve the localization of nearby objects, and tail bending can enhance the electric image or shadow cast on the fish's body (Heiligenberg, 1975; Stamper et al., 2012). Incorporating these movement-related components and realistic body bending into the analysis could provide further insights into how fish localize conspecifics.

Ethology: Integration of Computational Techniques and Naturalistic Settings for Behavior Analysis

In recent years, the field of neuroethology has witnessed significant progress due to the development of computational techniques for quantifying animal behavior. These methods leverage the power of machine learning and computer vision to track and analyze complex behavioral patterns with greater accuracy and efficiency (Mathis et al., 2018; Nath et al., 2019;

Pereira et al., 2019; Walter & Couzin, 2021). By automating the process of behavior tracking and annotation, these computational tools provide researchers with invaluable insights into the relationship between neural activity and behavior. Visual tracking systems have been successfully employed in various model organisms, such as C. elegans, Drosophila, zebrafish, and even unique animals like electric fish and bats (Branson et al., 2009; Graving et al., 2019; Henninger, 2015; Nath et al., 2019; Pereira et al., 2019; Walter & Couzin, 2021). These systems enable researchers to precisely track the position, movement, and communication of animals, enabling the establishment of causal relationships between neural circuits and behavioral responses. The use of automated analysis in neuroethology allows for large-scale experiments and provides quantitative measures for behavior that were previously challenging to obtain.

Automated analysis of electric fish behavior involves tracking the fish's position in space. While tracking movement and communication are crucial for understanding animal behavior, a comprehensive analysis requires annotation of actions, activities, and functions. Although automated systems can perform some of these annotations and behavior classifications, a significant portion of behavior classification still relies on human input. The field of Computational Ethology aims to develop frameworks and computational capabilities for identifying and quantifying behavior, but currently, there is a shortage of software that generalizes well across different setups. For the tracking system used in electric fish studies, manual identification and annotation of behavior are still necessary. In Chapter 3, a fast and reliable tracking system was developed specifically for tracking agonistic interactions among fish. This system can automatically track the fish and flag sequences where reliable tracking is challenging, allowing the user to guide the tracking for those specific sequences. We also

attempted to develop an automated behavior identification algorithm. We found that the behaviors we are interested in are particularly variable and hard to categorize with the algorithms we tested. Particularly, the challenge came from the fact that we were searching for algorithms that could delineate unknown movement patterns. The situation would have been different if we wanted an automated system to simply mark recordings with behaviors that we had already defined. In that case, a supervised deep-learning network would have probably been able to accomplish the task. Since we started without knowledge of the categories of behaviors to identify, we could not train a supervised network. Therefore, the only way to leverage machine learning in this context was to use unsupervised networks that exploit natural patterns in the data to create categories. Our attempts with such networks failed. We suggest that successful attempts will require further pre-processing of the data, such as the calculation of derived kinematic measures or time-wrapping. Exploration of this topic is left for future work.

Numerous laboratory studies have investigated various aspects of electric organ discharge (EOD) behavior in fish. Some studies have explored the relationship between chirping and various EOD mimic parameters (Dunlap & Larkins-Ford, 2003). Others have focused on the influence of hormones (Zakon & Dunlap, 1999), staged encounters (Hupe & Lewis, 2008; Triefenbach & Zakon, 2008), and courtship (Hagedorn & Heiligenberg, 1985). While a few studies have created elaborate naturalistic environments (Black-Cleworth, 1970), most experiments have been conducted in less than natural settings. In contrast, there are fewer cited field studies on natural behavior, primarily the works of Carl Hopkins (Hopkins, 1972, 1974; Hopkins & Heiligenberg, 1978), and Henninger (Henninger et al., 2018). These field

studies provide insights into the ecology, life history, and species-specific distributions of EOD in gymnotiform fish. However, due to the labor-intensive nature of these studies and limitations in monitoring freely roaming fish behavior, many observations remain anecdotal. Consequently, numerous natural electric signals and their functions have yet to be fully characterized and understood. While the controlled laboratory setting allows for a detailed characterization of the electrosensory system (Knudsen, 1974), the full range of its capabilities is best revealed in a natural environment. Therefore, future behavior studies should focus on more naturalistic settings.

Henninger et al. (Henninger et al., 2018) found that agonistic encounters sometimes occurred simultaneously with courtship, and these aggressive behaviors had very short durations compared to more restrictive lab settings where the fish cannot escape, leading to an increase in aggressive behaviors over minutes (Hagedorn & Heiligenberg, 1985; Hupe & Lewis, 2008; Triefenbach & Zakon, 2008). Similarly, in our larger and less restrictive tank, we observed a similar trend of short-lived aggressive behavior. Once the submissive and dominant hierarchy is established, and the submissive fish can escape, the interactions cease. This highlights the need for more natural settings to conduct behavioral experiments that can provide insights into the behavior of these fish.

Future Directions

Role of Chirps and Echo Responses

Numerous studies have provided evidence of changes in chirp frequency and patterns in fish during agonistic and exploratory behavior (Hofmann et al., 2014; Pedraja et al., 2016; Perrone et al., 2009). These studies also suggest that chirp characteristics can be analyzed in

interactions between fish. Research indicates that the dominant or more aggressive fish tends to increase its chirp rate, while the submissive fish decreases its chirp rate and frequency (Henninger et al., 2018; Hupe & Lewis, 2008; Triefenbach & Zakon, 2008). Submissive fish may also exhibit chirping in an echo pattern (Salgado & Zupanc, 2011; Zupanc & Maler, 1993). Intra-species agonistic interactions, both among males and females, often involve small chirps, whereas males emit high-frequency chirps during courtship (Bastian et al., 2001; Triefenbach & Zakon, 2008; Zakon et al., 2002).

In general, males of *Apteronotus leptorhynchus* chirp more often and at higher rates than females, although females can also produce chirps but do so less frequently (Dunlap et al., 1998). These chirps can be categorized as either small or big chirps. Both types involve a brief increase in frequency accompanied by a corresponding decrease in amplitude. The frequency rise and amplitude decrease are consistently linked in all species of Apteronotids. Specifically, in *A. leptorhynchus*, small chirps last 10-40 milliseconds and have a frequency increase of 50-150 Hz, while big chirps last 15-80 milliseconds and have a frequency increase of 150-900 Hz (Bastian et al., 2001; Dunlap et al., 1998; Hupe & Lewis, 2008; H. Zakon et al., 2002). The pattern of frequency modulation over time resembles a Gaussian curve. Male *A. leptorhynchus* emit chirps regularly when near other members of their species or when exposed to an artificial male-like electric discharge. When one fish chirps, another fish may respond within 500-1000 milliseconds, a behavior known as the echo response (Zupanc et al., 2006). This echo response seems to indicate submission during aggressive interactions. However, if chirping occurs in a non-echo pattern, it may indicate a motivation to escalate the aggressive interaction (Hupé et al., 2008).

Less is known about the use of chirps during courtship, but it is clear that they play a role in courtship behavior and spawning coordination. In this context, males chirp frequently, but females also respond (Henninger, 2015). The exact functions of different types of chirps are still unclear, partly because courtship behavior is rarely observed in captive settings.

Supporting this understanding, a neurophysiological study by Benda et al. (Benda et al., 2006) found that small chirps are distinct signals in the P-unit output when the difference in electric organ discharge frequency (EODf) is small (<30 Hz). On the other hand, high-frequency chirps are prominent signals when the EODf difference is large (~50-200 Hz). The echo response, previously observed in Apteronotus during fights between males (Hupé et al., 2008; Zupanc et al., 2006) and in a playback study (Salgado & Zupanc, 2011), still lacks a clear understanding of its functional significance during male-male interactions. However, in Chapter 3, I describe these behaviors in a spacious tank that allows the same freedom of movement as in natural settings. A better understanding of the use of chirps during naturalistic behavior could involve a study that follows our approach in Chapter 3 where we study movement. Taking into account both movement and communication signals in context that are as naturalistic as possible, we could categorize joint movement-chirping patterns and form ethograms of these behaviors. We believe that this project would be particularly successful if we first resolve the difficulties we encountered when trying to automatically delineate stereotyped behavior through quantitative algorithms (e.g., unsupervised machine learning).

Spatial coding during motion

In chapter 3 I define the range of behaviors and kinematics that the fish undergo during agonistic behaviors. In Chapter 2 I have the precise natural stimuli of the strength of the signal

reaching the fish's sensory surface. Similar to methods established in (Allen & Marsat, 2018; Marsat & Maler, 2010) we can perform neurophysiological recordings from various azimuth recordings from the behavior experiment. Using quantification methods established in (Marsat et al., 2023) we can estimate how reliably the stimuli location can be distinguished based on the population responses. By testing the response to different duration of stimuli we can also answer the question of how quickly the animal can reliably extract behaviors about change in stimuli location. We can also test how movement affects spatial coding by providing moving stimuli during electrophysiological recordings. This will provide a clear description of the spatial information present in the first stage of sensory processing and the way this information is represented.

Furthermore, we now have all the tools necessary to model the temporal dynamics of moving conspecific signals. We have a description of behavior; this data can be used to model the spatiotemporal dynamic of EI. These spatiotemporal signals can be used with our population of model receptors. We also have a full-scale model of the primary sensory area (Milam, unpublished data) that replicates the complex receptive field structure of pyramidal cells in that area. This comprehensive set of data and full-scale models, from behavior to the primary sensory area, can be used to dissect and better understand sensory processing during complex behaviors.

Localization strategies in weakly electric fish

Our modeling study considers how the signal is transformed from EI to the response of the array of electroreceptors. To evaluate how accurately spatial information is encoded uses a decoding algorithm that is conservative and makes few assumptions on the way the system

processes the signal. Nevertheless, a different decoding method could result in a different performance and we currently do not know how the system actually processes the signal. For example, we do not average together the response of the subpopulation of receptors before using it in our weighted Euclidean distance analysis. The sensory system could for example on a "lateralization" strategy and simply average all the inputs from one side, and all the input from the other side, and compared them to determine if the next turn should be left right, or straight. This possibility is worth considering since it is the general strategy of the auditory system and the electrosensory system is evolutionarily derived from the same source as the auditory system (Duncan & Fritzsch, 2012) . We could then assume that the output of the receptors is, at one point or another of the pathway, averaged together. This would change the structure of noise which could improve coding for some aspects of the stimulus (e.g., better detection) but deteriorate other aspects (e.g., precise angular resolution would be traded for lateralization paired with localization movements). The large-scale model framework we have created can serve as a key tool to investigate these possibilities. For example, coding-decoding mechanisms could be tested with the model, predictions of localization accuracy generated, and the results compared to moment-by-moment movement during behavior that involves moving relative to a target.

Conclusion

Localizing the source of a signal is key in guiding the behavior of the animal successfully. Localization mechanisms must cope with the challenges of representing the spatial information of weak, noisy signals. Comparing these strategies across modalities and model systems allows a broader understanding of the general principles shaping spatial processing. The

electrosensory system provides an advantageous comparison because it has a spatially mapped architecture right from the periphery -like the visual system- but it must also compute the location of conspecific -like the auditory system- since these signals activate the entire receptor array. In order to understand the neural mechanisms responsible for the localization of conspecific signals in the electrosensory system, we first aimed to have a quantitative understanding of the spatiotemporal structure of the sensory input during natural behaviors

This dissertation details the spatiotemporal dynamic of behaviorally relevant signals and how spatial information is represented in the electrosensory system. The significance of the contributions at each level of analysis is essential for uncovering how spatial information is coded in the early sensory system and how precise behavioral sensitivity is achieved. This research will serve as a foundation for a wide range of future studies on sensory processing in these systems. In particular, a major undertaking of this project was the development of a series of sophisticated tools that will be used in future studies: the tracking software, the EI modeling tool, and the full-scale receptor model. We also identified key features of spatial behavior and processing that will motivate future investigations: the limited range of sensory accuracy, the need to combine receptor responses in optimal ways to enhance accuracy, or the dynamics of cumulative assessment during agonistic encounters. In conclusion, we argue that this research not only clarified the way spatial dynamics is exploited by the early sensory system but also will serve as a stepping stone for a wide range of future studies in this system.

References

Allen, K. M., & Marsat, G. (2018). Task-specific sensory coding strategies are matched to detection and discrimination performance. *The Journal of Experimental Biology*, *221*(6), jeb170563. https://doi.org/10.1242/jeb.170563

Anderson, J. S., Carandini, M., & Ferster, D. (2000). Orientation Tuning of Input Conductance, Excitation, and Inhibition in Cat Primary Visual Cortex. *Journal of Neurophysiology*, *84*(2), 909–926. https://doi.org/10.1152/jn.2000.84.2.909

Bastian, J., Schniederjan, S., & Nguyenkim, J. (2001). Arginine vasotocin modulates a sexually dimorphic communication behavior in the weakly electric fish Apteronotus leptorhynchus. *Journal of Experimental Biology*, *204*(11), 1909–1924. http://www.ncbi.nlm.nih.gov/pubmed/11441033

Benda, J., Longtin, A., & Maler, L. (2006). A synchronization-desynchronization code for natural communication signals. *Neuron*, *52*(2), 347–358. https://doi.org/10.1016/j.neuron.2006.08.008

Black-Cleworth, P. (1970). The Role of Electrical Discharges in the Non-Reproductive Social Behaviour of Gymnotus carapo (Gymnotidae, Pisces). *Animal Behaviour Monographs*, *3*, 1-IN1. https://doi.org/10.1016/S0066-1856(70)80001-2

Branson, K., Robie, A. A., Bender, J., Perona, P., & Dickinson, M. H. (2009). High-throughput ethomics in large groups of Drosophila. *Nature Methods*, *6*(6), 451–457. https://doi.org/10.1038/nmeth.1328

Caputi, A. A., Aguilera, P. A., Carolina Pereira, A., & Rodríguez-Cattáneo, A. (2013). On the haptic nature of the active electric sense of fish. *Brain Research*, *1536*, 27–43.

https://doi.org/10.1016/j.brainres.2013.05.028

Chacron, M. J., Longtin, A., St-Hilaire, M., & Maler, L. (2000). Suprathreshold stochastic firing dynamics with memory in P-type electroreceptors. *Physical Review Letters*, *85*(7), 1576–1579. https://doi.org/10.1103/PhysRevLett.85.1576

Douglass, J. K., Wilkens, L., Pantazelou, E., & Moss, F. (1993). Noise enhancement of information transfer in crayfish mechanoreceptors by stochastic resonance. *Nature*, *365*(6444), 337–340. https://doi.org/10.1038/365337a0

Dunlap, K. D., & Larkins-Ford, J. (2003). Diversity in the structure of electrocommunication signals within a genus of electric fish, Apteronotus. *Journal of Comparative Physiology. A, Sensory, Neural, and Behavioral Physiology*, *189*(2), 153–161. https://doi.org/10.1007/S00359-003-0393-3

Dunlap, K. D., Thomas, P., & Zakon, H. H. (1998). Diversity of sexual dimorphism in electrocommunication signals and its androgen regulation in a genus of electric fish, Apteronotus. *Journal of Comparative Physiology. A, Sensory, Neural, and Behavioral Physiology*, *183*(1), 77–86.

Fotowat, H., Harrison, R. R., & Krahe, R. (2013). Statistics of the Electrosensory Input in the Freely Swimming Weakly Electric Fish Apteronotus leptorhynchus. *Journal of Neuroscience*. https://doi.org/10.1523/JNEUROSCI.0998-13.2013

Gama Salgado, J. A., & Zupanc, G. K. H. (2011). Echo response to chirping in the weakly electric brown ghost knifefish (*Apteronotus leptorhynchus*): role of frequency and amplitude modulations. *Canadian Journal of Zoology*, *89*(6), 498–508. https://doi.org/10.1139/z11-014

Graving, J. M., Chae, D., Naik, H., Li, L., Koger, B., Costelloe, B. R., & Couzin, I. D. (2019). DeepPoseKit, a software toolkit for fast and robust animal pose estimation using deep learning. *ELife*, *8*, e47994. https://doi.org/10.7554/eLife.47994

Hagedorn, M., & Heiligenberg, W. (1985). Court and spark - Electric signals in the courtship and mating of Gymnotoid Fish. *Animal Behaviour*, *33*(1), 254–265. https://doi.org/10.1016/S0003-3472(85)80139-1

Haider, B. (2006). Neocortical Network Activity In Vivo Is Generated through a Dynamic Balance of Excitation and Inhibition. *Journal of Neuroscience*, *26*(17), 4535–4545. https://doi.org/10.1523/JNEUROSCI.5297-05.2006

Heiligenberg, W. (1975). Theoretical and experimental approaches to spatial aspects of electrolocation. *Journal of Comparative Physiology A*, *103*(3), 247–272. https://doi.org/10.1007/BF00612021

Henninger, J. (2015). Social interactions in natural populations of weakly electric fish. *PhD Thesis, University of Tübingen*. https://doi.org/10.15496/PUBLIKATION-6731

Henninger, J., Krahe, R., Kirschbaum, F., Grewe, J., & Benda, J. (2018). Statistics of natural communication signals observed in the wild identify important yet neglected stimulus regimes in weakly electric fish. *The Journal of Neuroscience*. https://doi.org/10.1523/JNEUROSCI.0350-18.2018

Hofmann, V., Geurten, B. R. H., Sanguinetti-Scheck, J. I., GÃ³mez-Sena, L., & Engelmann, J. (2014). Motor patterns during active electrosensory acquisition. *Frontiers in Behavioral Neuroscience*, *8*, 186. https://doi.org/10.3389/fnbeh.2014.00186

Hopkins, C. D. (1972). Sex differences in electric signaling in an electric fish. *Science*, *176*(4038),

1035–1037. https://doi.org/10.1126/science.176.4038.1035

Hopkins, C. D. (1974). Electric Communication: Functions in the Social Behavior of Eigenmannia Virescens. *Behaviour*, *50*(3), 270–304. https://doi.org/10.1163/156853974X00499

Hopkins, C. D., & Heiligenberg, W. F. (1978). Evolutionary designs for electric signals and electroreceptors in gymnotoid fishes of Surinam. *Behavioral Ecology and Sociobiology*, *3*(2), 113–134. https://doi.org/10.1007/BF00294985

Hupe, G. J., & Lewis, J. E. (2008). Electrocommunication signals in free swimming brown ghost knifefish, Apteronotus leptorhynchus. *Journal of Experimental Biology*. https://doi.org/10.1242/jeb.013516

Hupé, G J, Lewis, J. E., & Benda, J. (2008). The effect of difference frequency on electrocommunication: Chirp production and encoding in a species of weakly electric fish, Apteronotus leptorhynchus. *Journal of Physiology Paris*, *102*(4–6), 164–172. https://doi.org/DOI 10.1016/j.jphysparis.2008.10.013

Hupé, Ginette J., Lewis, J. E., & Benda, J. (2008). The effect of difference frequency on electrocommunication: Chirp production and encoding in a species of weakly electric fish, Apteronotus leptorhynchus. *Journal of Physiology-Paris*, *102*(4–6), 164–172. https://doi.org/10.1016/J.JPHYSPARIS.2008.10.013

Jung, S. N., Longtin, A., & Maler, L. (2016). Weak signal amplification and detection by higher-order sensory neurons. *Journal of Neurophysiology*, *115*(4), 2158–2175. https://doi.org/10.1152/jn.00811.2015

Knudsen, E. (1974). Behavioral thresholds to electric signals in high frequency electric fish. *Journal of Comparative Physiology*, *91*(4), 333–353. https://doi.org/10.1007/bf00694465

Knudsen, E. I., & Konishi, M. (1979). Mechanisms of sound localization in the barn owl (Tyto alba). *Journal of Comparative Physiology A*, *133*(1), 13–21. https://doi.org/10.1007/BF00663106

Lindner, B., Chacron, M. J., & Longtin, A. (2005). Integrate-and-fire neurons with threshold noise: A tractable model of how interspike interval correlations affect neuronal signal transmission. *Physical Review E - Statistical, Nonlinear, and Soft Matter Physics*, *72*(2), 1–21. https://doi.org/10.1103/PhysRevE.72.021911

Linkenkaer-Hansen, K., Nikulin, V. V, Palva, S., Ilmoniemi, R. J., & Palva, J. M. (2004). Prestimulus oscillations enhance psychophysical performance in humans. *The Journal of Neuroscience : The Official Journal of the Society for Neuroscience*, *24*(45), 10186–10190. https://doi.org/10.1523/JNEUROSCI.2584-04.2004

Marsat, G, Daly, K. C., & Drew, J. A. (2023). Characterizing neural coding performance for populations of sensory neurons: comparing a weighted spike distance metrics to other analytical methods. *BioRxiv*, 778514. https://doi.org/10.1101/778514

Marsat, Gary, & Maler, L. (2010). Neural heterogeneity and efficient population codes for communication signals. *Journal of Neurophysiology*, *104*(5), 2543–2555. https://doi.org/jn.00256.2010 [pii]10.1152/jn.00256.2010

Marsat, Gary, & Maler, L. (2012). Preparing for the unpredictable: adaptive feedback enhances the response to unexpected communication signals. *Journal of Neurophysiology*, *107*(4), 1241–1246. https://doi.org/10.1152/jn.00982.2011

Mathis, A., Mamidanna, P., Cury, K. M., Abe, T., Murthy, V. N., Mathis, M. W., & Bethge, M. (2018). DeepLabCut: markerless pose estimation of user-defined body parts with deep

learning. *Nature Neuroscience*, *21*(9), 1281–1289. https://doi.org/10.1038/s41593-018-0209-y

Nath, T., Mathis, A., Chen, A. C., Patel, A., Bethge, M., & Mathis, M. W. (2019). Using DeepLabCut for 3D markerless pose estimation across species and behaviors. *Nature Protocols*, *14*(7), 2152–2176. https://doi.org/10.1038/s41596-019-0176-0

Pedraja, F., Perrone, R., Silva, A., & Budelli, R. (2016). Passive and active electroreception during agonistic encounters in the weakly electric fish Gymnotus omarorum. *Bioinspiration & Biomimetics*, *11*(6), 065002. https://doi.org/10.1088/1748-3190/11/6/065002

Pereira, T. D., Aldarondo, D. E., Willmore, L., Kislin, M., Wang, S. S.-H., Murthy, M., & Shaevitz, J. W. (2019). Fast animal pose estimation using deep neural networks. *Nature Methods*, *16*(1), 117–125. https://doi.org/10.1038/s41592-018-0234-5

Perrone, R., MacAdar, O., & Silva, A. (2009). Social electric signals in freely moving dyads of Brachyhypopomus pinnicaudatus. *Journal of Comparative Physiology A: Neuroethology, Sensory, Neural, and Behavioral Physiology*. https://doi.org/10.1007/s00359-009-0427-6

Rasnow, B., Assad, C., & Bower, J. M. (1993). Phase and amplitude maps of the electric organ discharge of the weakly electric fish, Apteronotus leptorhynchus. *Journal of Comparative Physiology A*, *172*(4), 481–491. https://doi.org/10.1007/BF00213530

Sas, E., & Maler, L. (1983). The nucleus praeeminentialis: a Golgi study of a feedback center in the electrosensory system of gymnotid fish. *The Journal of Comparative Neurology*, *221*(2), 127–144. https://doi.org/10.1002/cne.902210202

Sas, E., & Maler, L. (1987). The organization of afferent input to the caudal lobe of the cerebellum of the gymnotid fish Apteronotus leptorhynchus. *Anatomy and Embryology*,

177(1), 55–79.

Schluger, J. H., & Hopkins, C. D. (1987). Electric fish approach stationary signal sources by following electric current lines. *The Journal of Experimental Biology*, *130*(December), 359–367.

Schöneich, S., & Hedwig, B. (2010). Hyperacute directional hearing and phonotactic steering in the cricket (Gryllus bimaculatus deGeer). *PLoS ONE*, *5*(12). https://doi.org/10.1371/journal.pone.0015141

Schroeder, C. E., Wilson, D. A., Radman, T., Scharfman, H., & Lakatos, P. (2010). Dynamics of Active Sensing and perceptual selection. *Current Opinion in Neurobiology*, *20*(2), 172–176. https://doi.org/10.1016/J.CONB.2010.02.010

Stamper, S. A., Madhav, M. S., Cowan, N. J., & Fortune, E. S. (2012). Beyond the Jamming Avoidance Response: weakly electric fish respond to the envelope of social electrosensory signals. *Journal of Experimental Biology*, *215*(23), 4196–4207. https://doi.org/10.1038/bjc.2011.109

Takahashi, T., & Keller, C. (1992). Commissural connections mediate inhibition for the computation of interaural level difference in the barn owl. *Journal of Comparative Physiology A*, *170*(2), 161–169. https://doi.org/10.1007/BF00196898

Triefenbach, F. A., & Zakon, H. H. (2008). Changes in signalling during agonistic interactions between male weakly electric knifefish, Apteronotus leptorhynchus. *Animal Behaviour*, *75*(4), 1263–1272. https://doi.org/10.1016/j.anbehav.2007.09.027

Walter, T., & Couzin, I. D. (2021). TRex, a fast multi-animal tracking system with markerless identification, and 2D estimation of posture and visual fields. *ELife*, *10*, e64000.

https://doi.org/10.7554/eLife.64000

Yu, N., Hupé, G., Garfinkle, C., Lewis, J. E., Longtin, A., & Fortune, E. (2012). Coding Conspecific Identity and Motion in the Electric Sense. *PLoS Computational Biology*, *8*(7), e1002564. https://doi.org/10.1371/journal.pcbi.1002564

Zakon, H. H., & Dunlap, K. D. (1999). Sex steroids and communication signals in electric fish: A tale of two species. *Brain Behavior and Evolution*, *54*(1), 61–69. https://doi.org/6612

Zakon, H., Oestreich, J., Tallarovic, S., & Triefenbach, F. (2002). EOD modulations of brown ghost electric fish: JARs, chirps, rises, and dips. *Journal of Physiology, Paris*, *96*(5–6), 451–458. https://doi.org/10.1016/S0928-4257(03)00012-3

Zupanc, G. K. H., & Maler, L. (1993). Evoked chirping in the weakly electric fish Apteronotus leptorhynchus – a quantitative biophysical analysis. *Canadian Journal of Zoology*, *71*(11), 2301–2310. https://doi.org/10.1139/z93-323

Zupanc, G. K. H., Sîrbulescu, R. F., Nichols, A., & Ilies, I. (2006). Electric interactions through chirping behavior in the weakly electric fish, Apteronotus leptorhynchus. *Journal of Comparative Physiology A: Neuroethology, Sensory, Neural, and Behavioral Physiology*, *192*(2), 159–173. https://doi.org/10.1007/s00359-005-0058-5